STUDIES OF EXPERIMENTAL TECHNIQUES FOR SOUNDING THE IONOSPHERE AT LOW AND VERY LOW RADIO WAVE FREQUENCIES

Thesis by

Carl William Bergman

In Partial Fulfillment of the Requirements

for the Degree of

Electrical Engineer

California Institute of Technology

Pasadena, California

1954

TABLE OF CONTENTS (Cont'd.)

TABLE OF CONTENTS

ABSTRACT

Phase measurements of waves reflecting from the lower regions of the ionosphere using frequencies in the range 15 to 100 kc/s furnish a new method of investigating the effects of solar activity on radio communication. In an effort to explore this method of measurement the Ionospheric Research Project of the California Institute of Technology constructed a complete 50-kc/s station in the Mojave desert with the transmitter near Randsburg and the receiver near Victorville. This paper describes the equipment requirements of the station, and a paper by R. S. Macmillan (Cf. Ref. 1) will present the theoretical aspects of the data that were obtained.

A crystal-controlled transmitter was used to drive a half-wave resonant dipole, which at 50 kc/s was 8600 feet long. The antenna pattern was such that radiated power was directed upward to the ionosphere and thence back to the receiving site by means of reflection. The necessary reference signal was sent to the receiving site by means of a very-high-frequency, frequency-modulated transmitter.

A double superheterodyne receiver received the 50-kc/s signal and converted it to 1.61 kc/s. This output was then compared by means of a phase meter with a 1.61-kc/s reference, derived from the 50 kc/s reference signal. The output of the phase meter was filtered (bandwidth = 1 c/s) and then recorded. A commercial field-strength meter (bandwidth = 350 c/s) was used in conjunction with this receiver to obtain the amplitude of the reflected wave.

ACKNOWLEDGMENTS

I personally am indebted to many people who directly or indirectly made the completion of this thesis possible. With few exceptions these people had nothing to gain in extending a helping hand. I wish to thank Dr. W. H. Pickering especially for his guidance in this work. His encouragements together with the love of my wife Alice and the affection of my children Carl and Annette, to a large measure, are responsible for the successful completion of this thesis.

I. COMPREHENSIVE BACKGROUND

The basic research on the ionosphere which was done in England (Cf. Ref. 2) at low and very low frequencies indicated that the changes in effective height of the ionosphere over relatively short periods of time showed excellent correlation with occurrence of solar flares. Since radio fadeouts affecting communication links are also related to solar flares, more information is required to determine the exact relationships. The Ionospheric Research Project of the California Institute of Technology was formed to study and experiment with systems capable of continuously recording the changes in the effective height of the reflecting layers. The contents of this thesis are but the beginning of a long-range plan of research to investigate the phase changes and the reflection coefficient changes which take place over a period of the order of minutes for the frequency range 15 to 100 kc/s. The restriction in frequency limits the research to the D and E layers of the ionosphere, regarding which there is actually a dearth of knowledge. Lack of interest and of suitable equipment originally was the cause of the lethargy in this field; however, the newer types of navigational systems, together with increased interest in establishing communication links at frequencies below 100 kc/s, are remedying these faults. For example, it is expected that considerable information concerning propagation of radio waves at 14.5 to 35.0 kc/s will become available after the completion of the 1-megawatt transmitter near Arlington, Washington (Cf. Ref. 3).

The only satisfactory way of investigating the ionosphere is to use radio waves, and to this end the system to be described in the present paper was designed. The station in the first stage of develop-

ment will provide information concerning changes only of phase and amplitude. It is hoped, since communication radio fadeouts are due to the activities on the sun, that the results may be eventually used to predict when, where, and on what frequency radio-frequency communications will be reliable.

A station capable of making such measurements may be very worth while if it is located in Southern California. As of now the information concerning the propagation of radio wave at frequencies below 100 kc/s is coming largely from the Cavendish Laboratories in England (longitude 0° and latitude 52°). The longitude and latitude at the Southern California station are 118° and 35°, respectively; thus the time of observation of the solar effects is different because of the difference in longitude; the intensity of the solar effects will be greater since the minimum zenith distance of the sun is 17° smaller (Cf. Section I-D).

A. History of the Project

In the minds of many observers the history of this project was considered to be very unusual; it might be of interest to review its development. Originally I was interested in doing research at the California Institute of Technology involving the radiation of the sun at ultrahigh frequencies, and fortunately I was able to go to Cornell University to work with the radio astronomy group whose program it was to set up a solar radio observatory at Sacramento Peak, New Mexico. When the delays in the building program at Sacramento Peak made it impossible to do any immediate research, a meeting was arranged with Dr. W. H. Pickering at White Sands Proving Ground, New Mexico, in September, 1950, and it was decided that I should return to the California Institute of Technology. In discussing possible thesis

projects, Dr. Pickering suggested investigating the ionosphere at low frequencies in order to obtain further information about the sun. When I returned to the California Institute of Technology, R. S. Macmillan joined me in a project which would obviously need a good working group to accomplish the objectives set up.

A study of the literature indicated that there was a definite need of techniques for the successful measurement of phase as a continuous function of time at low frequencies. Power levels used in research projects were, in general, well above 50 kw, and commercially available receivers were conspicuously unsuitable as research tools. An unsuccessful attempt to obtain the use of a Navy transmitter forced us to consider the building of our own transmitting antenna. The discouraging part about this consideration was that the Navy customarily estimated the cost of antenna to be $1,000,000.00 for every 10 per cent efficiency in this frequency region.

While we were talking with the Navy concerning the use of its transmitting facilities, the Institute acquired a supersonic generator capable of putting out 750 watts of power. At the time, it was proposed that this generator would be used, first of all, as a transmitter; then, if more power was needed, it would serve as a driver for a more powerful transmitter. In March, 1951, much consideration was being given to stringing wire across a deep canyon to serve as an antenna, and a trip to Mount Palomar indicated that this type of radiator was a possible but not an easy solution to the antenna problem. Dr. Pickering suggested that we could possibly take advantage of the dryness of the desert and excite an antenna which would consist of two well pipes, the water table, and a wire between the two wells, thus forming a vertical loop. Consid-

eration of this idea led us to believe that we might put a horizontal loop on the ground such that it was a full wavelength in circumference. In April, 1951, such a loop was built 7 miles east of Palmdale where the parents of R. S. Macmillan owned a quarter section of land. It was expected that the radiation from such an antenna would have a maximum value for small angles above the horizon.

After performing several local tests on the loop, we went to Death Valley in May, 1951, to see whether or not we could receive any signal. Death Valley (125 miles from the loop) was chosen because the atmospheric noise level there is unusually low. The nearest town is many miles away, and transmission lines have not yet penetrated into the valley. We were able to detect our signal by using a Navy-owned, low-frequency receiver, the AN/URM-6, which was capable of being used as a field-strength meter. It had a field strength of approximately 10 μvolts/meter. In the presence of only 2 μvolts of noise, such a signal was easily detectable.

There were many disadvantages in using a loop antenna. Most important was the fact that using the loop required the receiver to be many miles away from the transmitter because of the field pattern. The field pattern of a horizontal half-wave dipole close to the earth, on the contrary, is a maximum directly above the antenna (Cf. Appendix A); thus the decision was made to use such a dipole in succeeding experiments.

For such an antenna to radiate, it is necessary that the dielectric constant of the earth be reasonably low. Also, if the water table is too near the surface, the dielectric constant approaches that of a perfect conductor, preventing any radiation whatever. With the help of Dr. J. P. Buwalda of the geology department at California Institute of Technology, an antenna site was chosen southwest of Randsburg (Cf.

map of Fig. 1). It was strongly believed that the water table at this location was down at least 1500 feet below the surface and possibly much farther, since the site was located over a huge granite block which could well have been impervious to water. In addition to being electrically satisfactory, the earth's surface did not vary more than 500 feet in altitude along the 5-mile length of the antenna.

In September, 1951, a dipole was built along the Mojave-Randsburg road just south of the permanent antenna site. The dipole was made of No. 20 wire strung from bush to bush for 1.3 miles in order to keep it off the ground (Cf. Appendix A). It resonated at 60 kc/s and had an input impedance of 125 ohms.

The receiving site was chosen at Shadow Mountain, a location on a line almost normal to the length of the transmitting antenna in order that the polarization of the incident wave would be normal to the plane of incidence (Cf. Fig. 1). Several early attempts were made to receive the 60-kc/s wave but with submarginal results. Finally, in November, 1950, the difficulties were eliminated, and a strong signal was received. It was then possible to make plans for a more permanent installation. By the time the transmitted signal was finally received, the California Institute of Technology had applied to the Office of Naval Research (ONR) for financial support of the project. Interest in low and very low frequencies was running high, and it appeared that a contract would be granted. The reception of the transmitted signal was very important in convincing the ONR that the project had a good chance of being successful.

Actual work on the project came to a standstill after December 15, 1951, as the California Institute of Technology did not wish to contribute

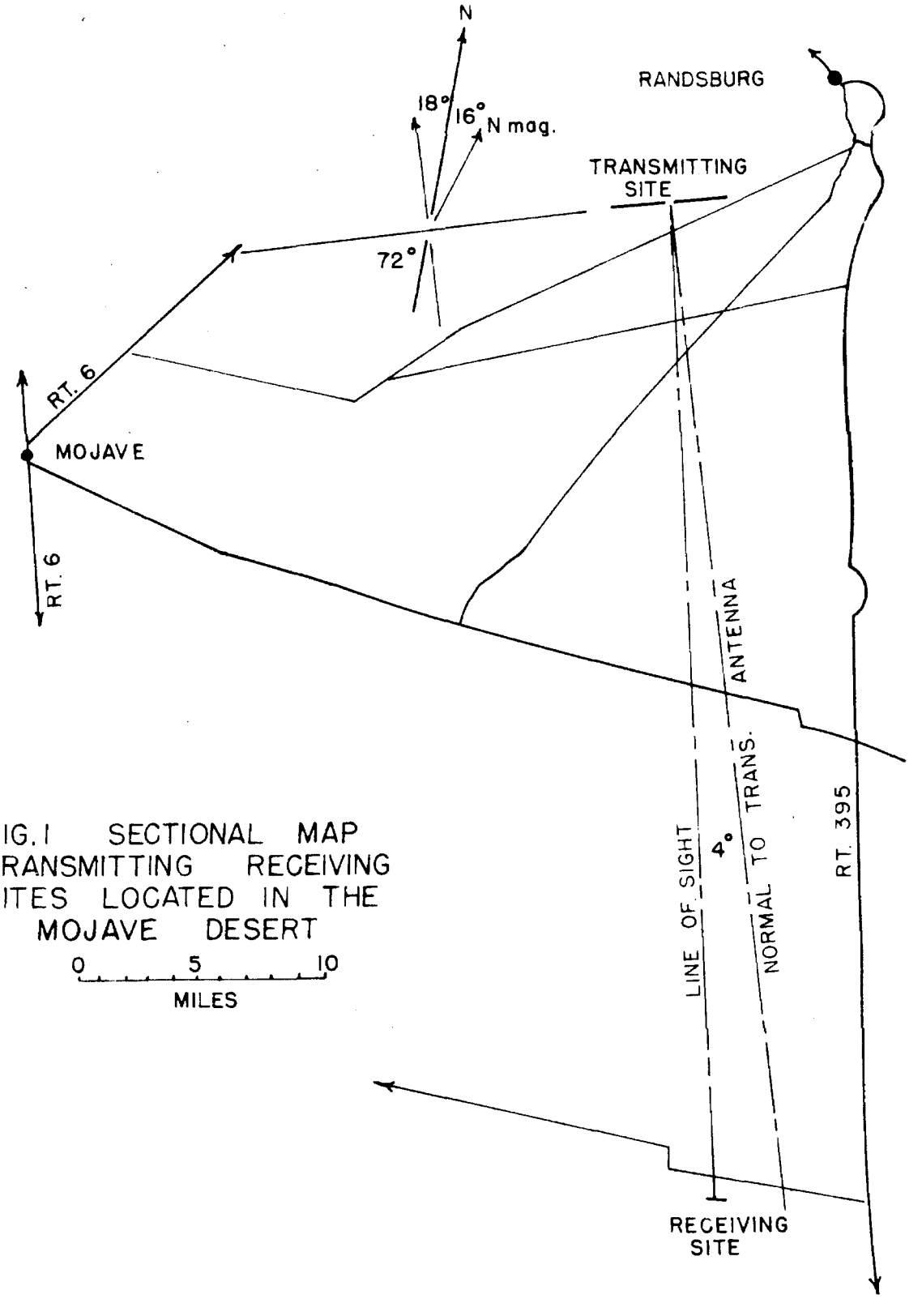

FIG. 1 SECTIONAL MAP TRANSMITTING RECEIVING SITES LOCATED IN THE MOJAVE DESERT

more funds until the money from the contract became available. Soon after April 1, 1952, when the contract went into effect, the construction of the permanent transmitting antenna was started. The line of the antenna was surveyed, and work was contracted to put in the poles and string the wire. The antenna was started in May, 1952, and finished after 3 weeks' work.

Concurrently with this activity the Office of Naval Research was obtaining on loan for us as much needed equipment as it could. Through the ONR we obtained the two AN/FRC-6 transmitter-receiver units, the AN/URM-6 low-frequency receiver, and two RAK receivers which unfortunately were not suitable for our use. A PE99 mobile 115-volt, 60-c/s generator, also on loan from the Navy, furnished the power for the transmitting site. A small Onan 1000-watt generator furnished power for the receiving site. The Office of Naval Research not only gave us the necessary funds to carry on this work but made it possible to obtain equipment which would have otherwise been virtually impossible for us to procure.

After several previous unsuccessful attempts, we obtained a good strong signal radiated from the permanent transmitting antenna during the first week in July, 1952. Receiving the signal at this time essentially gave us all the information needed to design and build the receiving and recording equipment. During this experiment it was also determined that the receiving site was almost in line of sight of the transmitter if not actually line of sight. Being line of sight assured us that a UHF or VHF link between the two sites would have a high signal-to-noise (S/N) ratio.

Activity for the next 4 months centered around building an entire system which would function in the field. Several trips to the desert

were made in order to test the equipment in its development. All of the work and planning required to put the project into shape was suddenly bringing results. Finally, during the last half of October, 1952, continuous measurement of the changing phase and amplitude of the reflected wave was taken successfully over the period of 2 days. The first stage of this research project was complete.

B. The Upper Atmosphere

One viewing the earth from a distance would see a disc whose radius is 6,368 km (or 3,960 miles). At a distance from the surface of 16 km (1/649 of the radius of the earth) there is the imaginary boundary between the troposphere below and the stratosphere above. At 20 km there is a boundary between the stratosphere and the upper atmosphere. The study of the upper atmosphere (Cf. Ref. 4) is as interesting as it is complex. It is divided into regions of study such as the study of meteor trails which appear at about 66 miles (106 km) and disappear at heights varying from 46 to 34 miles. The ozonosphere is the lower layer of the upper atmosphere and, as the name suggests, is characterized by the presence of ozone (O_3). The diffuse layer of ozone between 10 and 50 km with a maximum concentration in the vicinity of 25 to 30 km accounts for the sharp cutoff near 2900 Å of the solar spectrum which was observed many years ago.

Above the ozonosphere the ionized regions of the upper atmosphere begin. These regions which constitute the ionosphere are divided into layers which are characterized in general by points of maximum ionization. The source of energy for the ionization of the upper atmosphere comes from the sun; thus the characteristics of the various layers are very dependent upon the sun's position with respect to the earth and with respect to any given point on the earth. We might say that the charac-

teristics are also very dependent on the disposition of the sun since sun spots, solar flares, and other solar outbursts are strongly felt and reflected by the degree of ionization at a given time. There are at least four layers of ionization. The two outer layers, the F_1 and F_2, exist at heights of 200 and 275 km, respectively. At night these two regions merge as shown in Figure 2. The E layer maximum exists at 100 km in height; the D layer does not seem to have any maximum but is merely an ionized blob existing between 60 and 100 km. The D layer is directly dependent upon the presence of the sun; thus it does not exist at night and may not exist during the day during the winter-time at certain latitudes. Figure 3 gives a graphical representation of the ion density as a function of height as it might exist at noon on a summer day.

In the past there has been and still is a great deal of speculation as to the process of ionization of the various layers. For example, the E layer is possibly "formed by the ionization of molecular oxygen in the region where its concentration falls rapidly as a result of photo-dissociation," but "there is uncertainty regarding the process of ionization and the wavelength of the active radiation" (Cf. Ref. 5). It is accepted that the ionization of the D layer (Cf. Ref. 6) is produced by the ionization of molecular oxygen (O_2) at the first ionization potential. Further details about the composition of the upper atmosphere may be found in Reference 1.

C. Propagation in an Ionized Medium

Since an understanding of the basic principles of propagation in an ionized medium is necessary in the design of an ionospheric station, let us investigate in more detail what happens when an electromagnetic wave enters an ionized region. The electric-field component sets in

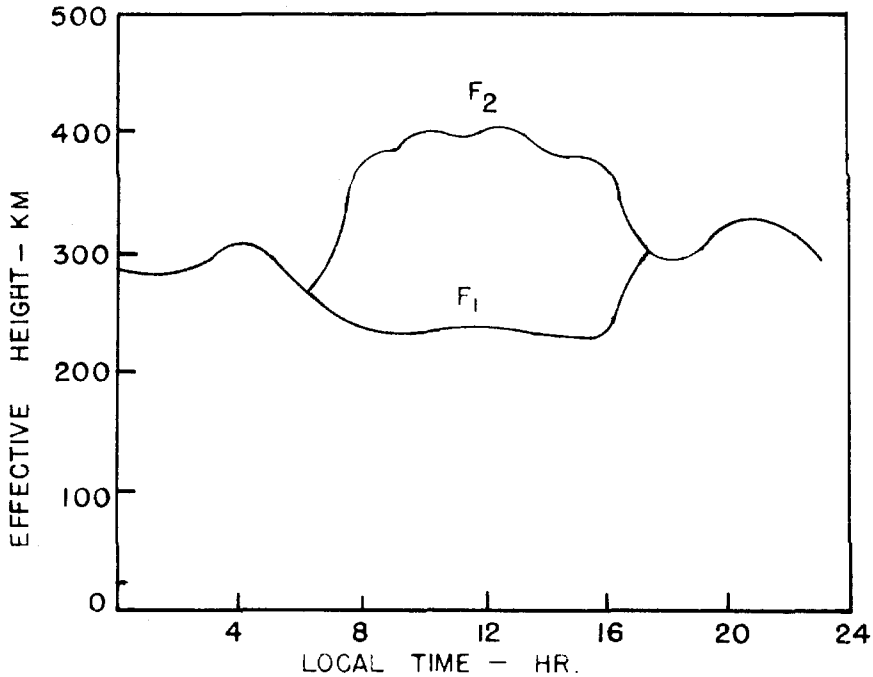

FIG. 2 EFFECTIVE HEIGHT OF THE F_1 AND F_2 LAYERS (Cf. Ref 4)

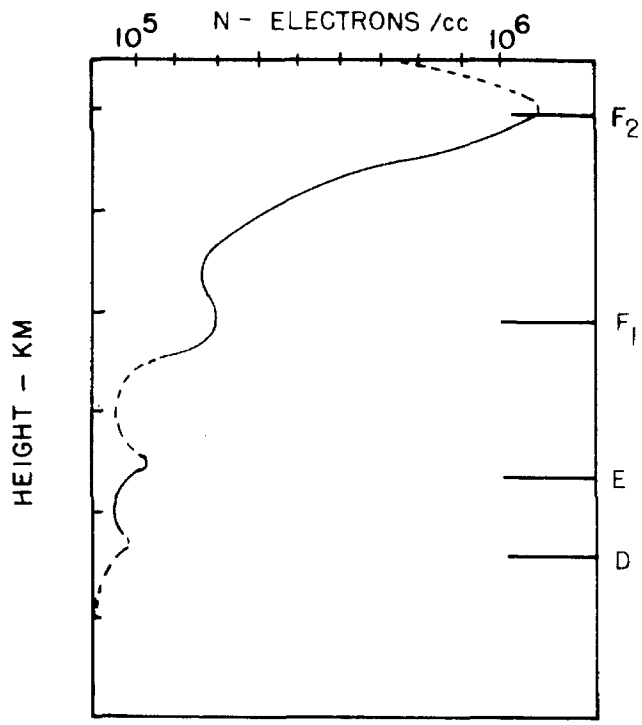

FIG. 3 AVERAGE ELECTRON DENSITIES

motion the ions and/or electrons, producing a current which opposes the displacement current. The result is that the refractive index changes from unity for free space to

$$\mu^2 = 1 - \frac{4\pi N e^2}{\epsilon_0 m \omega^2} \tag{1}$$

where N = number of electrons/cc, ϵ_0 = permittivity of free space, m = mass of the charged particle, ω = frequency of the electromagnetic wave, and e = the charge of the particle.

The condition necessary for propagation is that μ be greater than zero; therefore under no condition can the wave propagate if N $N > \epsilon_0 m\omega^2/4\pi e^2$. We note that it makes no difference whether the charge be positive or negative. If N is less than $\epsilon_0 m\omega^2/4\pi e^2$, then the wave can propagate but only under the constraint of a reduced μ. The phase velocity defined by

$$v_p = \frac{c}{\sqrt{1-(4\pi N e^2/m\omega^2)}} \tag{2}$$

then becomes greater than the velocity of light c, and the group velocity

$$v_g = \frac{v_p}{1 - \frac{\omega}{v}\frac{\partial v_p}{\partial \omega}} \tag{3}$$

becomes less. Thus if a wave enters an ionized region where the ion density increases as the wave progresses, the group velocity will reach zero and the wave will be reflected from the point in space where $N = \epsilon_0 m\omega^2/4\pi e^2$. If the ion density is not constant along the entire wave front of the electromagnetic wave, then continuous refraction or bending of the wave front takes place. As an example, Figure 4 shows an electromagnetic wave entering an ionized region where the ion density is an increasing function of height only. From Snell's law as applied

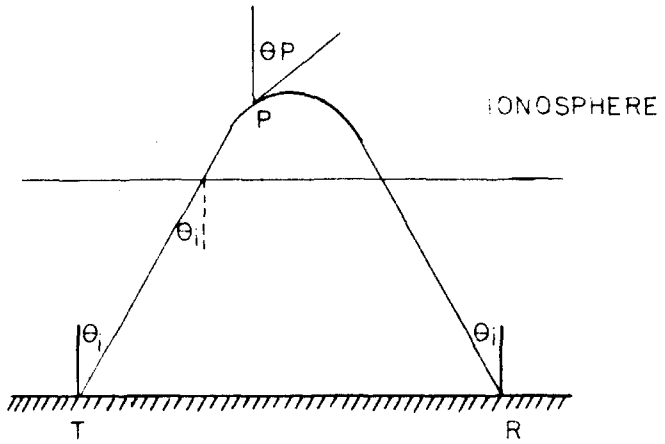

FIG. 4 REFLECTION OF A WAVE FROM THE IONOSPHERE

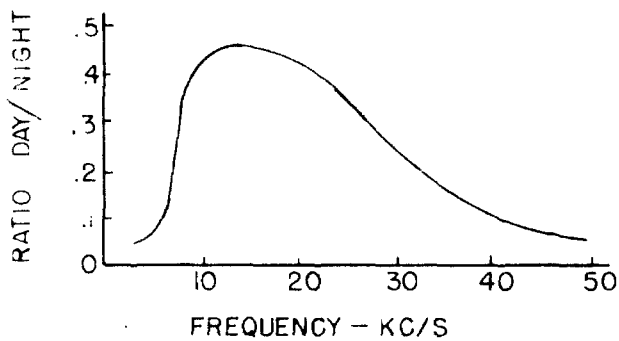

FIG. 5 RATIO OF DAY ATMOSPHERIC TO NIGHT ATMOSPHERICS (Cf Ref. 7)

in optics,

$$\sin \theta_i = \mu \sin \theta_p \tag{4}$$

where θ_i and θ_p are defined in Figure 4. The point where the wave has zero vertical component of velocity is defined by $\mu = \sin \theta_i$.

Most investigations of the ionosphere require the use of electromagnetic waves, and the determination of the height of the layer in turn requires a time measurement. From Equation (3) we see that the wave is slowed down in passing through the ionized region. The result is that the time interval measured is longer than the time that would have been required if the path of travel had been entirely in free space. Thus the definition of virtual height is as follows: Virtual height is that which would be calculated from the geometry of the system containing a receiver, a transmitter, and a definite plane of reflection wherein the retardation of the wave is not considered. A corollary is that the virtual height as measured is always greater than, or equal to, the actual height of reflection.

If the propagation takes place along the direction of a magnetic field line of the earth, the wave is split into two components which see two different indices of refraction, namely,

$$\mu^2 = 1 - \frac{4\pi N e^2}{\epsilon_0 m \omega(\omega + \omega_H)} \tag{5}$$

for the ordinary wave and

$$\mu^2 = 1 - \frac{4\pi N e^2}{\epsilon_0 m \omega(\omega - \omega_H)} \tag{6}$$

for the extraordinary wave where

$$\omega_H = \frac{He}{\epsilon_0 m c^2} \tag{7}$$

which is the natural frequency of gyration of an ionized particle in a magnetic field H.

Now we find that the ordinary wave may propagate as long as $4\pi Ne^2/\epsilon_0 m\omega(\omega+\omega_H) < 1$ and that the extraordinary wave may be propagated only if $\omega_H > \omega$ or if $\omega_H/\omega < 1 - (4\pi Ne^2/\epsilon_0 me^2)$. Therefore the ordinary wave and the extraordinary wave will be reflected from different points in a medium of changing ion density.

By referring to Figure 3 it is seen that an electromagnetic wave in arriving at the point of reflection and returning to the earth passes through ionized regions. In such regions energy may be removed from the wave and dissipated by means of collision of electrons or ions with other particles. These losses can be considered as equivalent to conduction losses in a dielectric whose complex dielectric constant is $\hat{\epsilon} = \epsilon - j(4\pi\sigma/\omega)$ where σ is defined as

$$\sigma = \mathrm{Re}\left|\frac{Ne^2(\nu - j\omega)}{m(\omega^2+\nu^2)}\right| \qquad (8)$$

and where ν is the collision frequency. This absorption accounts for the loss of power in a wave in being reflected from the ionosphere.

D. Properties of the Ionosphere at 15 to 100 kc/s

In setting up an experimental station one needs to know approximately what type of results may be expected and how much radio interference will be encountered. Let us set forth the characteristics of the ionosphere as they affect the propagation of waves in the frequency range 15 to 100 kc/s. First of all, there will be atmospheric noise, which will vary from day to night. This variation at a given frequency is a direct function of the relative reflection coefficient variation. For example, Figure 5 shows the ratio of daytime noise to nighttime noise when there are no storms in the vicinity of the receiver. Figure

5 shows that atmospherics will be much less noisy at 50 kc/s during the day than at night, whereas at 15 kc/s there will be a reduction of only one-half (Cf. Ref. 7).

If a plane-polarized wave reflects from the ionosphere, it will, in general, come away elliptically polarized (Cf. Ref. 7). In general, any incident wave may be split into two components (considering the electric vectors for reference purpose), one parallel to the plane of incidence and the other perpendicular. The ratio R of either component after reflection to the same component before reflection will be termed the reflection coefficient. The ratio $_{\parallel}R_{\perp}$ and $_{\perp}R_{\parallel}$ will be termed the conversion coefficients. All these coefficients are about equal in magnitude. Figure 6 shows how $_{\parallel}R_{\perp}$ varies as a function of frequency; Figure 7, how $_{\parallel}R_{\perp}$ varies through the year; and Figure 8, how $_{\parallel}R_{\perp}$ varies over the period of a day. This information has been extremely useful to us since we were able to pick times for experimentation when a maximum return signal could be expected. The variation of $_{\parallel}R_{\perp}$ suggests the fluctuations in field strength that may be expected.

Reflection-height data given in Reference 2 indicate a phase change of the order of 600° for a normal summer day at 16 kc/s (1800° at 50 kc/s). These phase changes are directly related to the changes in height. The height of the ionized layer is a function of the sun's zenith angle χ and is given by

$$h_{\chi} = h_{\chi=0} + A(t) \ln(\sec \chi) \qquad (9)$$

where A(t) is a function of the time of the year and $h_{\chi=0}$ is the height when $\chi=0$, or the sun is directly overhead.

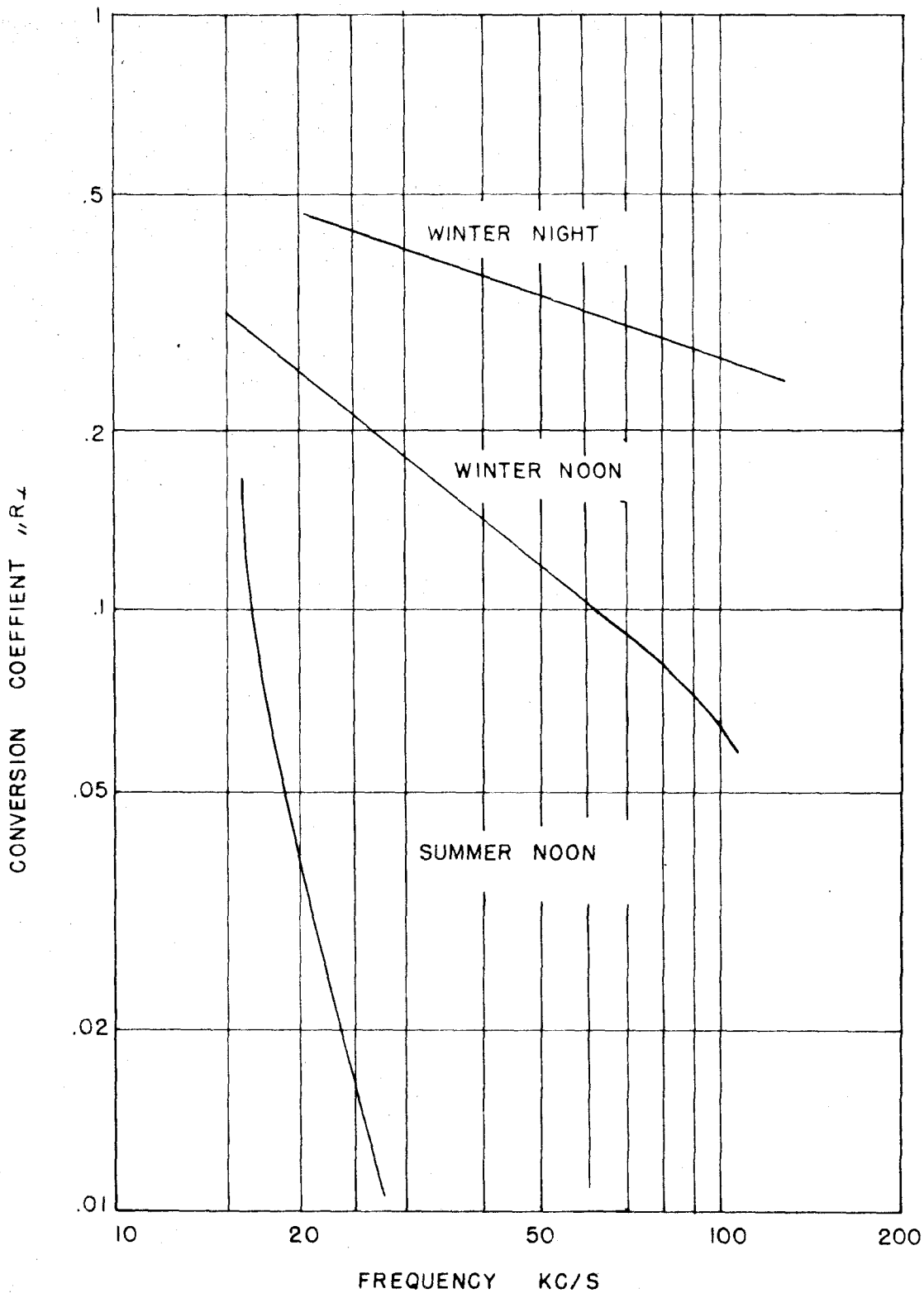

FIG. 6 THE VARIATION OF CONVERSION COEFFICIENT „$R_{\perp}$ WITH FREQUENCY (AFTER BRACEWELL)

(Cf Ref. 2)

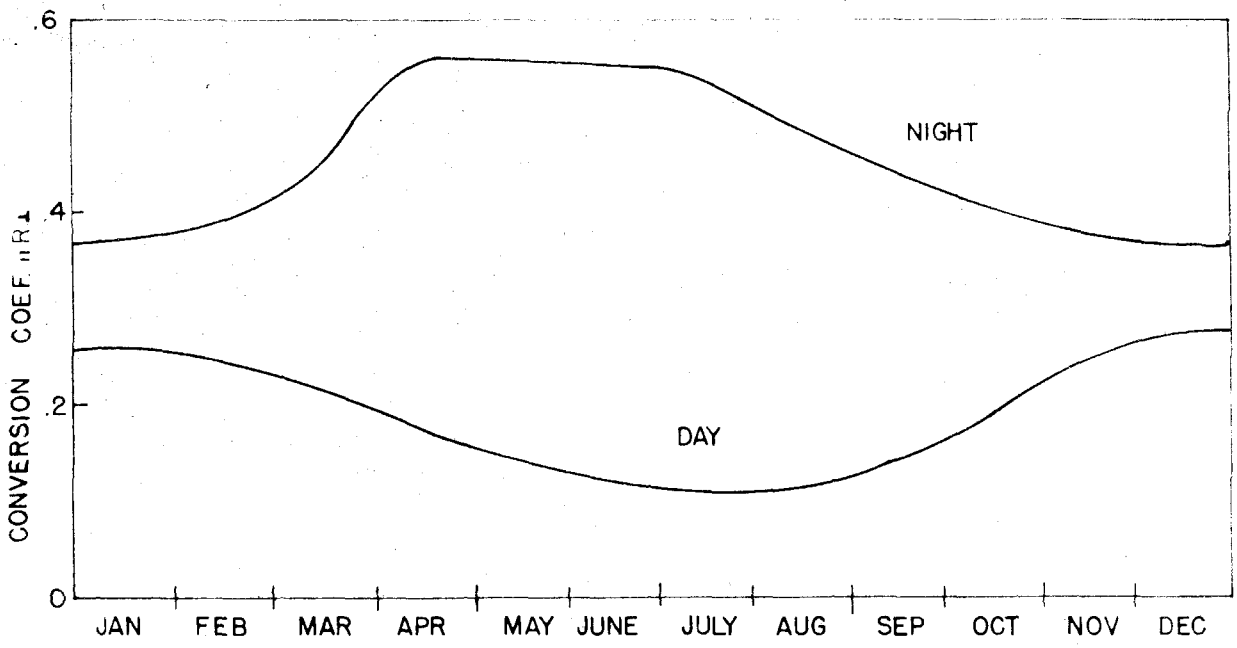

FIG. 7a SEASONAL VARIATION OF ||R⊥ AT 16 KC/S

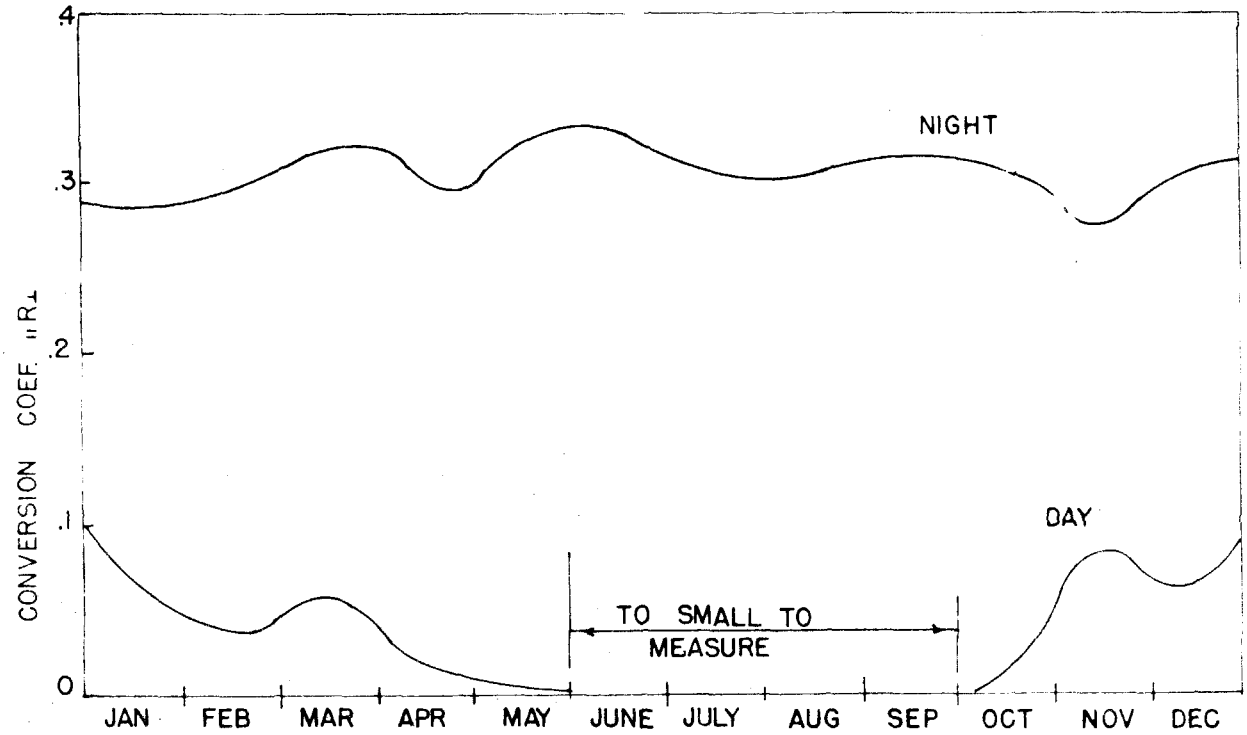

FIG. 7b SEASONAL VARIATION OF ||R⊥ AT 70 KC/S
(Cf. Ref. 2)

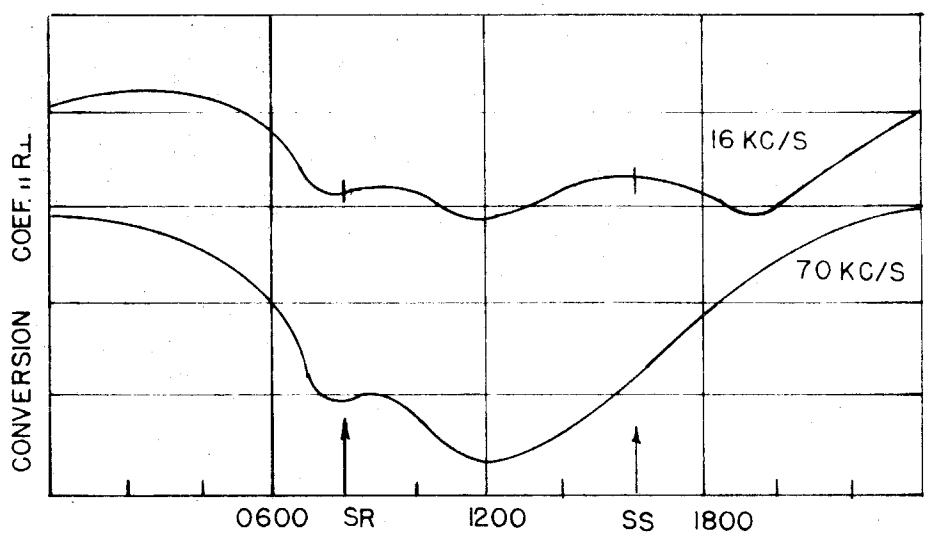

FIG. 8a DAILY VARIATION OF ∥R⊥ IN WINTER

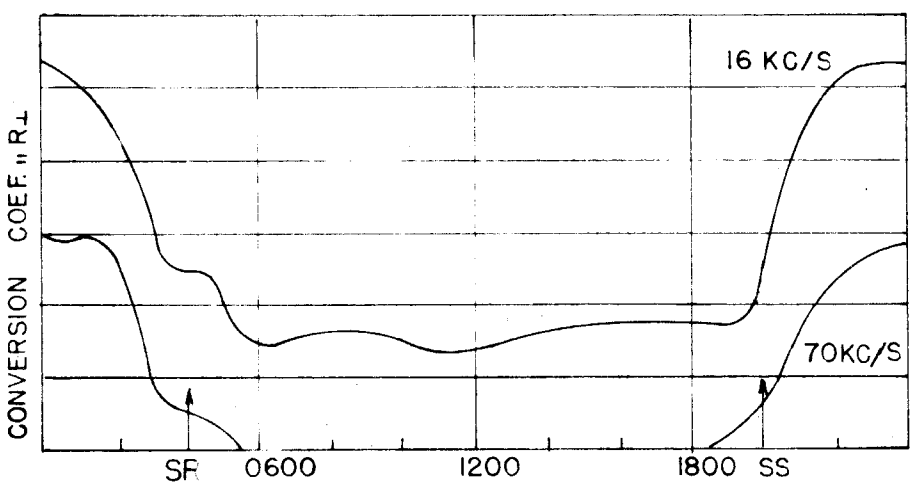

FIG. 8b DAILY VARIATION OF ∥R⊥ IN SUMMER
(Cf. Ref. 2)

E. Transient Behavior of the Ionosphere

The foregoing discussion has given what one might call the steady-state behavior of the ionosphere. The ionosphere also has a transient behavior due to disturbing elements. The disturbance may be caused by ionospheric clouds or holes passing over the point of reflection; as a result there is a change in the phase and the amplitude of the reflected wave. The disturbance may also be caused by increasing ionization due to increased radiation from the sun. During periods of sun spots, solar prominences, and solar flares the radiation over certain frequency ranges may increase a thousand fold or more. Flares, in particular, are believed to cause increased ionization which may last only a few minutes before returning to normal. In this time the variation in height has been known to be as high as 5 km. The radio wave reflecting from the ionosphere during such a period experiences a change in phase dependent on the change of height. This type of occurrence, which is now known as a phase anomaly, is described in Reference 8 as follows:

> "The anomaly which often accompanies reports of flares is the fall of the effective height of reflection through, say, three kilometers over a time of several minutes followed by a slower recovery taking about three times as long."

These changes in phase are generally accompanied by changes in reflection coefficient. Phase anomalies, as observed, show much more than chance correlation with sudden ionospheric disturbances of short waves and the sudden enhancements of atmospherics. Thus it is hoped that measurement of the phase changes in a reflected wave will allow us to study more completely the sun and how it affects us on earth. Figure 9 shows a plot of a phase anomaly, together with a plot of a flare. There certainly is little doubt that the two occurrences are related in time. The phase anomaly is a plot of phase change versus time, whereas the

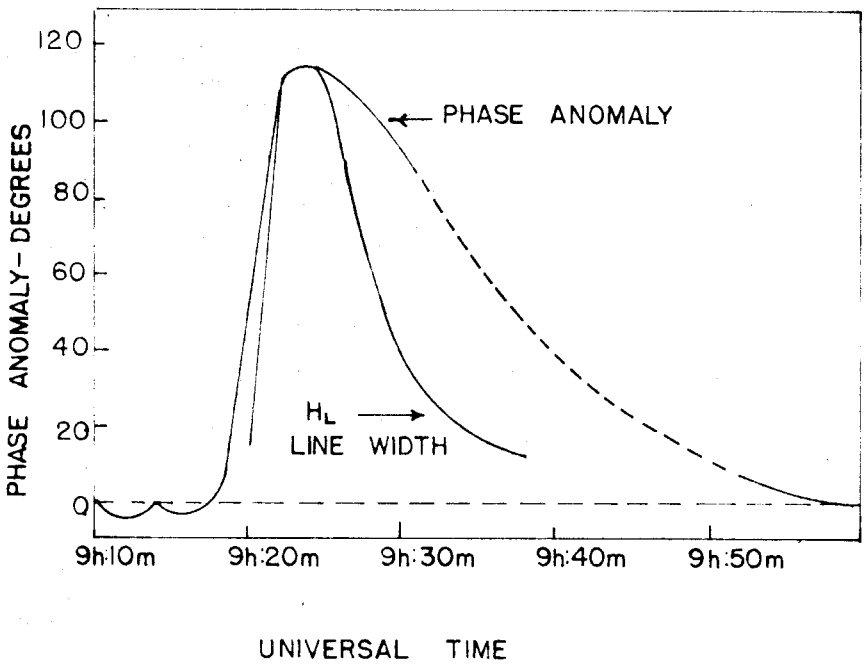

FIG. 9 A PHASE ANOMALY COMPARED WITH LINE WIDTH OF H_L EMITTED FROM ASSOCIATED PLACE (Cf. Ref. 8)

flare plot is the observed width of the H_α line in time. It is believed that the Lyman α ultraviolet line of hydrogen at 1215 Å is the ionizing agent, and certainly the enhancement of the H_α line (hydrogen Balmer α) coincident with the occurrence of the phase anomaly supports this argument.

F. Techniques of Measurement Being Used

The Naval Electronics Laboratory in San Diego, California, is doing work in low-frequency and very-low-frequency atmospherics through its station in Gila Bend, Arizona. Stanford University is carrying on research using a 100-kc/s wave with pulsing techniques. Central Radio Propagation Laboratory (Washington, D.C.), Pennsylvania State College (State College, Pennsylvania), Syracuse University (Syracuse, New York), and Dartmouth University (Hanover, New Hampshire) are doing work in this field, but each institution is more or less limiting itself to one or two chosen frequencies usually well above 50 kc/s. It is hoped that, because of the versatility of the equipment, we will be able to switch to any frequency in the range 15 to 100 kc/s without a great deal of effort.

The British are using continuous wave (CW) in their investigation of phase anomalies, reflection coefficients, and general characteristics of the ionosphere. It is known that the ionosphere is stratified at times into distinct layers in such a way that a wave will be reflected from two or more layers. Using the CW technique makes it impossible to detect such multiple reflections; therefore, in addition to giving faulty information concerning the height because of slowing down of the wave as it enters the ionized regions, it gives erroneous information if the wave returning to the receivers has been made up of two or more reflected waves. The pulse method as used at Stanford University and

Pennsylvania State College directly measures the times of reception of reflected waves; therefore if the reflections occur at several heights, the return pulses will be separated by measurable times which may be recorded. The pulse technique is thus seen to be excellent for investigating the fine structure of the ionosphere.

Figure 10 is an idealized record that might be taken of an automatic ionospheric sounder if there were no sporadic D or E layer present or if there were no splitting due to the magnetic field of the earth. This instrument surveys the frequency range 1 to 20 mc/s and records time required for a transmitted wave to return versus the frequency transmitted. We note that the boundaries of the various layers are well defined and that near the critical frequencies appreciable time lag due to the slowing down of the electromagnetic wave is observed.

Assuming that an ionized layer is made up entirely of electrons, a theoretical curve can be plotted (Cf. Fig. 11) which shows the number of electrons per cubic meter needed to turn back a frequency of f kc/s. The curve is not directly applicable for the D layer since this layer is composed of both electrons and negative ions. At 70 km the electron density is roughly 2.5×10^3/cc, whereas the ion density is about 2.5×10^5/cc.

G. Related Work in Other Fields

It is perhaps interesting that the information that we would eventually like to obtain on phase anomalies in the frequency range 15 to 100 kc/s, as related to the sun's activities, is being obtained in a more direct manner at frequencies of 50 to 3000 mc/s and higher. The radiation from the sun at these frequencies varies according to

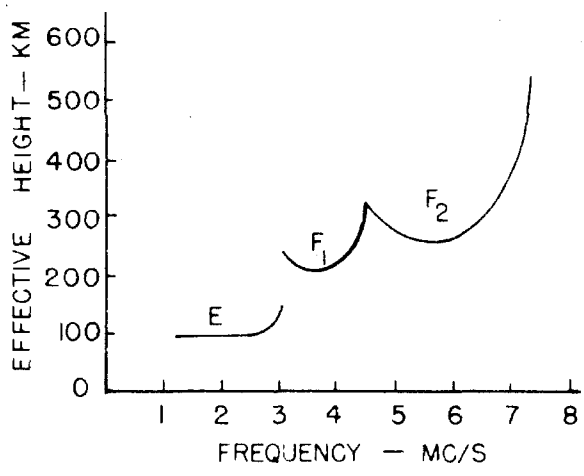

FIG. 10 h vs f

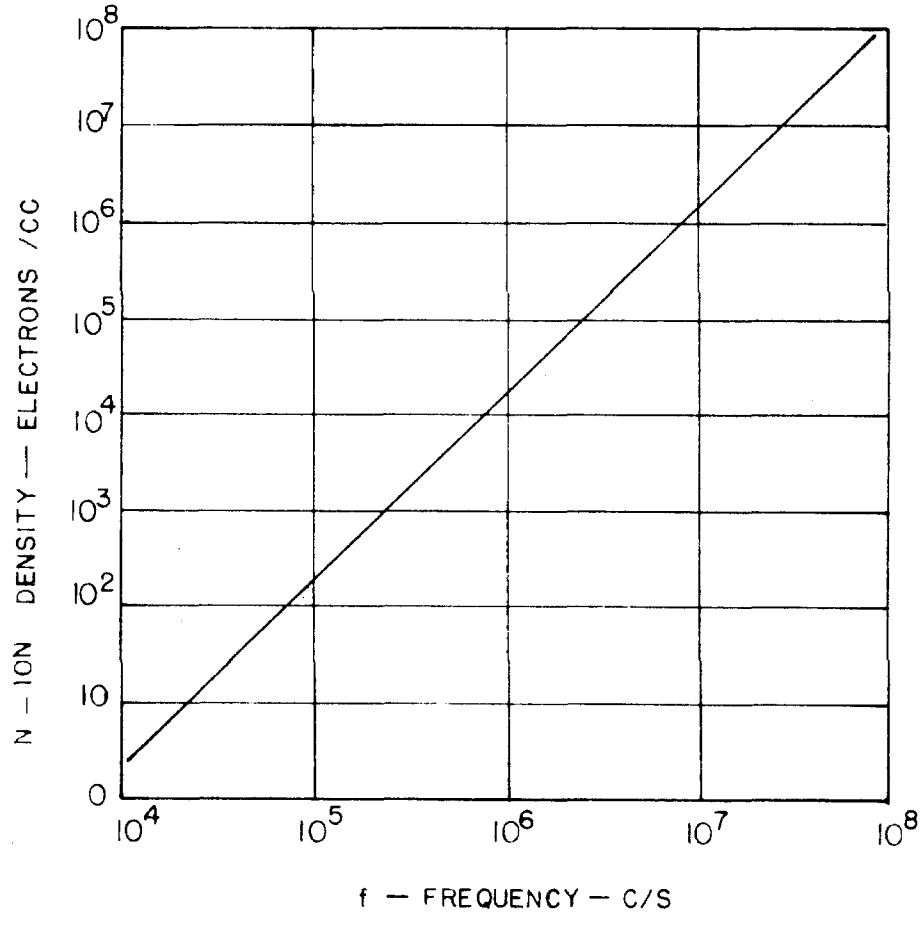

FIG. 11 ION DENSITY NECESSARY TO PROHIBIT PROPAGATION OF FREQ. f

the activity on the sun. If the quiet sun is ideally considered, one can determine at what distance from the center of the sun a given frequency starts to propagate. The sun is more densely ionized closer to the center; thus for the reasons discussed in Section I-C the depth that a given frequency can propagate is limited. The frequency of the receiver determines approximately what distance from the center of the sun is being surveyed; hence the advantage in using many receivers all at different frequencies. This plan allows the fine structure of the radio sun to be examined. The sun's signal is thermal noise which varies by many orders of magnitude when flares, sun spots, and prominences of any kind exist. Very good correlation between solar noise outburst and solar visual observation of sun spots, flares, and prominences is obtained.

The Naval Research Laboratory (Washington, D. C.) and Cornell University (Ithaca, New York) are doing most of the work in the United States in this field. England, Norway, Canada, and Australia are doing extensive work also. An interesting parallel to visual measurements is the behavior of the atomic hydrogen line at approximately 1420 mc/s. The line was first observed in a laboratory and then, after a great deal of effort, was found in the radiation from the sun. The width of the hydrogen line determines the degree of activity of the sun.

Radio astronomy data rely on the visual data taken by the various observatories throughout the world to obtain correlation of observed effects with probable stellar causes. In particular, field stations at Climax, Colorado, and Sacramento Peak, New Mexico, work together to obtain data exclusively on the sun. We are very fortunate in Southern California to have both Mount Wilson and Mount Palomar to

advise us of the sun's daily activities as affecting local conditions.

The list of the fields of study which are related to the study of solar disturbances and their effects does not end here. Cosmic-ray research being done in the field at Climax, in the course of time, obtained as a by-product correlation of cosmic-ray activity with solar outburst, thus giving clues to the origin of these cosmic rays. Thus are the activities of man carried on with a certain craving for knowledge of his environment: his place on earth, the earth's place in the solar system, the solar system's place in the galaxy, and our galaxy's place in all the infinities of space and time.

II. IONOSPHERIC SOUNDING METHODS

Three methods, all of which were feasible for sounding the ionosphere, were considered in the early phases of the project. The basic requirement was to transmit a signal from the transmitter to the receiver by way of the ionosphere. Each of the methods relies on the measurement of the time necessary for the radio wave to arrive at the receiving site from the transmitter.

A. The Pulse Method

One means of obtaining the height and the reflection coefficient of the ionosphere is to pulse-modulate the carrier so that it consists of n full cycles of a given frequency f_o. The time required for the electromagnetic wave to go from the transmitter to the receiver can be obtained directly by comparing the leading edge of the returned pulse with the leading edge of the transmitted pulse. There is, however, a physical limitation in making this comparison. If the time occurrence

of the leading edge of a pulse is to be defined exactly, the receiver used must have infinite bandwidth. Any finite bandwidth definitely limits one's ability to determine a measure of time. In order to determine what is an acceptable bandwidth (BW), consider a pulse consisting of n cycles of frequency f_o. It has a frequency distribution function $G(\omega)$ given by

$$|G(\omega)| = \left|\frac{2\omega_o}{\omega_o^2 - \omega^2} \sin\frac{\omega\tau}{2}\right| \tag{10}$$

where ω is $2\pi f$ and

$$\tau = n/f_o = 2\pi n/\omega_o \tag{11}$$

is the length of the pulse. $G(\omega)$ is plotted in Figure 12 (Cf. Appendix B) for $n = 4$, and from this plot it can be seen that a good portion of the total power is contained within the first zero on either side of ω_o. A circuit designed to accept only this portion of the band would have a bandwidth

$$BW = 2f_o/n = 2/\tau \tag{12}$$

where n is the number of full cycles in the pulse. This assumption agrees with Goldman (Cf. Ref. 9), who states (1) the detail of the pulse is good if $BW = 1/2\tau$, (2) the detail is lost if $BW = 1/4\tau$, (3) the detail of the leading edge is good if $BW = 7/4\tau$, and (4) the S/N ratio for the reception of the pulse in the presence of noise is best for $BW = 3/4\tau$:

$$BW = 1/4\tau \qquad \text{no detail} \tag{13}$$

$$BW = 1/2\tau \qquad \text{good detail} \tag{14}$$

$$BW = 7/4\tau \qquad \text{good detail in leading edge} \tag{15}$$

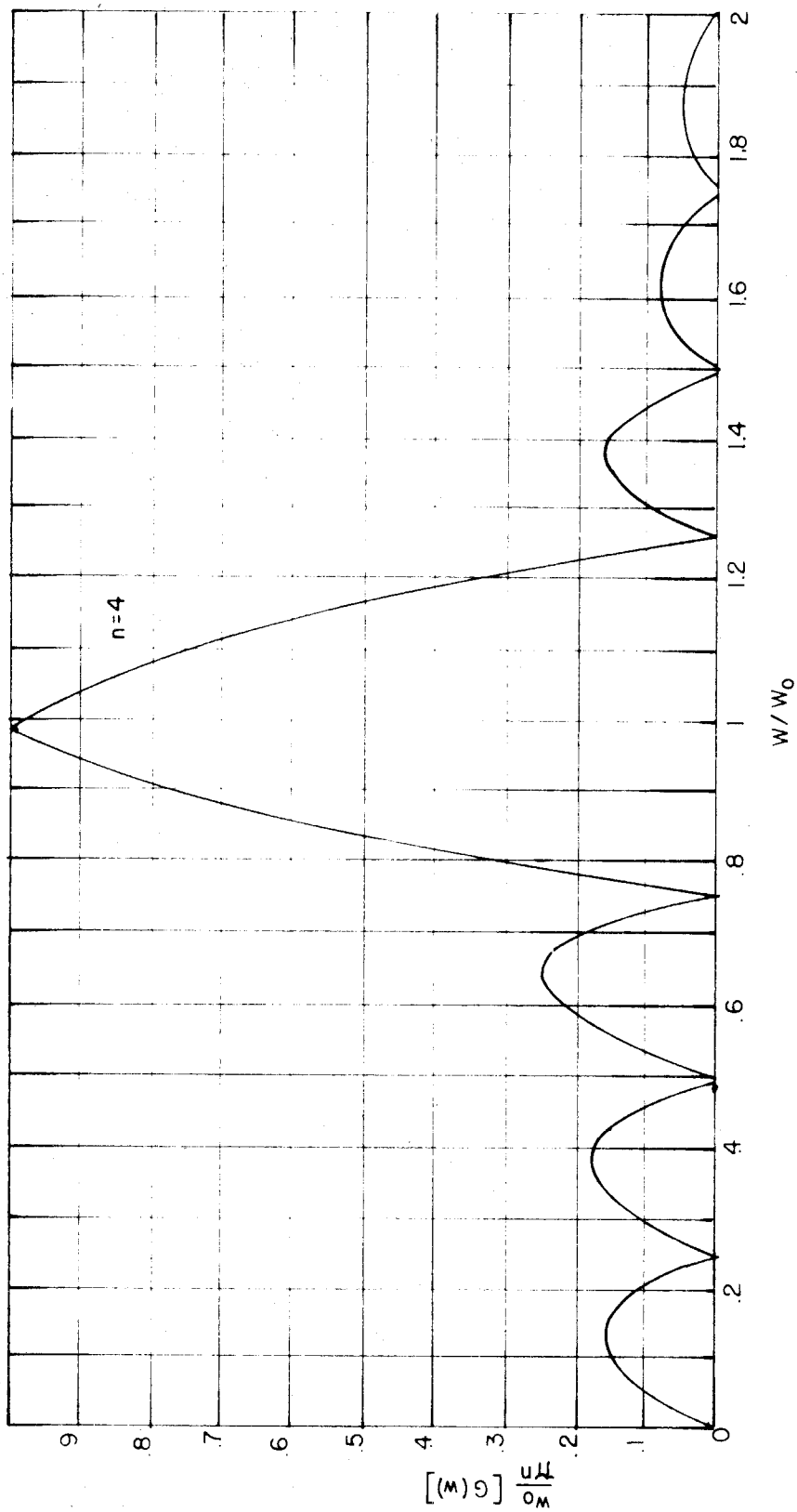

FIG. 12 NORMALIZED SPECTRAL DISTRIBUTION

$$BW = 3/4\tau \qquad \text{best S/N ratio} \qquad (16)$$

The response of a tuned circuit to a pulse takes Q/π cycles (Cf. Appendix C) to reach a value 1-(1/e) of the maximum amplitude of the pulse. Thus, if it be specified that the response reach a value 1-(1/e) at the end of the time and that the BW be $2/\tau$, the Q of the circuit is defined to be n/2 from

$$Q = f_o/BW \qquad (17)$$

As an example, assume that a 50-kc/s receiver has a BW of 1 kc/s, and determine what n must be to satisfy this condition. The number of cycles n must be equal to 2Q (or 100) for the pulse to be very well defined.

However, the pulse is going to be used as a time-measuring device, and it is not sufficient to have the pulse clearly defined if the length of the pulse needed is much greater than the time resolution desired. For a criterion, let us assume that, as long as the receiver can adequately define the pulse (i.e., BW = $1/2\tau$), the time at which the pulse takes place can be determined to the nearest $\tau/10$ second.

Figure 13 shows the geometry involved in sending a transmitted wave to the ionosphere for sounding purposes: 2d is the distance from transmitter to receiver via line of sight; 2ℓ is corresponding distance via the ionosphere; h is the height of the ionosphere; and θ is the angle of incidence. Since the effective height of the ionosphere for frequencies ranging from 15 to 100 kc/s is found to vary from 60 to 100 km, let a standard height h_o be 80 km. The time required for the wave to reach the receiver would be t_o (or $534/\cos\theta$ μsec). Let it be necessary to resolve the measurement in h to the nearest 1.0 km; it would be necessary to determine time to the nearest 6 μsec. This

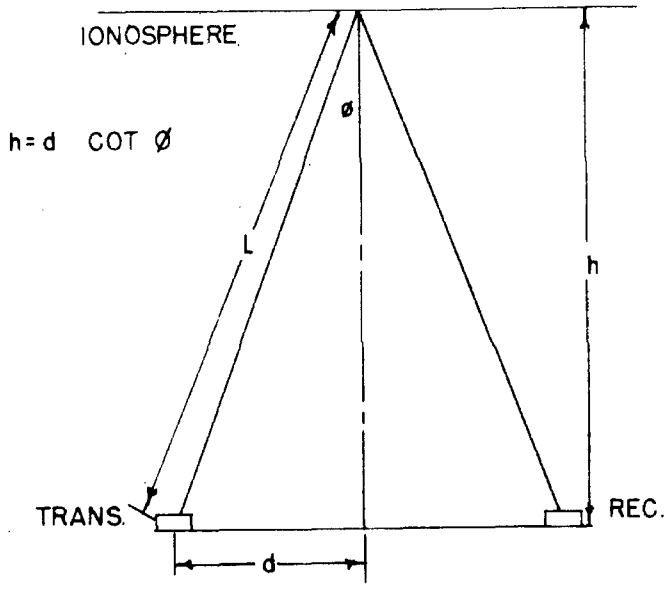

FIG. 13 GEOMETRIC CONFIGURATION OF REFLECTION

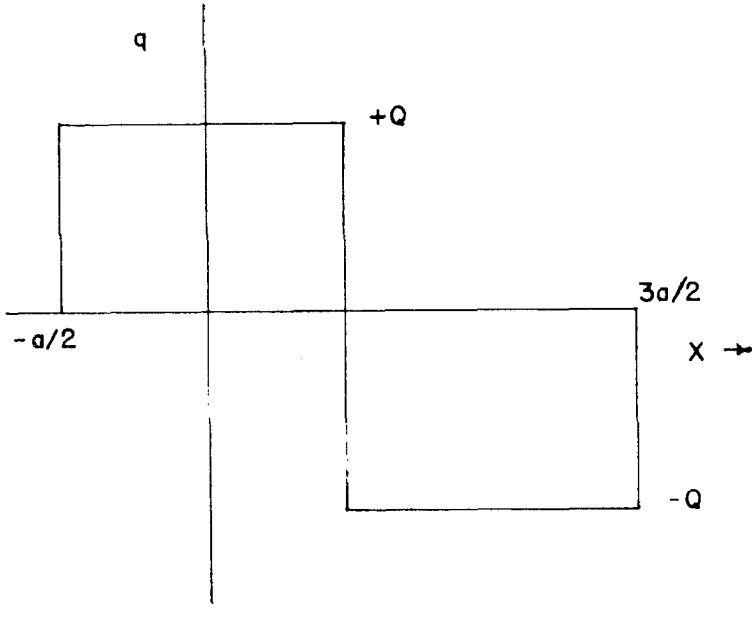

FIG. 14 DISTRIBUTION OF CHARGE ON HALF WAVE DIPOLE

requirement in turn, specifies that the pulse length should be 60 μsec. It should be pointed out once more that to make the pulse longer would not allow one to measure any more accurately the time of occurrence of the pulse, nor would a longer pulse allow the BW to be decreased. A pulse length of 60 μsec automatically calls for a BW of about 8.5 kc/s.

The transmitting antenna, to be described in Section III-A-2, is suitable for use with the pulse techniques in many ways. Briefly the antenna is a half-wave dipole of length 2a fed at the center. It can be charged to the point where -Q is on one half, and +Q is on the other. The charge distribution q is as shown in Figure 14 and can be expanded by Fourier series to

$$q = \frac{4Q}{\pi}\left(\cos\frac{\pi x}{a} - \frac{1}{3}\cos\frac{3\pi x}{a} + \frac{1}{5}\cos\frac{5\pi x}{a} - \cdots\right) \qquad (18)$$

where x is as defined in Figure 15 (Cf. Appendix D). When the antenna is fully charged, the boundary conditions are exactly those which are required to excite the first, third, fifth, seventh, etc. natural modes. Of the total power put into the antenna, 18.8 per cent will be distributed in the harmonics, leaving 81.2 per cent in the fundamental. Therefore the efficiency which is normally determined by copper losses and dielectric losses is further reduced.

The disadvantage in using a pulse technique is the large bandwidth required. Stanford University (Cf. Ref. 10) found it necessary to use a BW of 50 kc/s with a 100-kc/s pulse. This wide bandwidth, in the presence of atmospheric noise, requires many times more power, but since the pulses can be separated, the average power required is small. For example, a 60-μsec pulse with peak power of 1 megawatt repeated

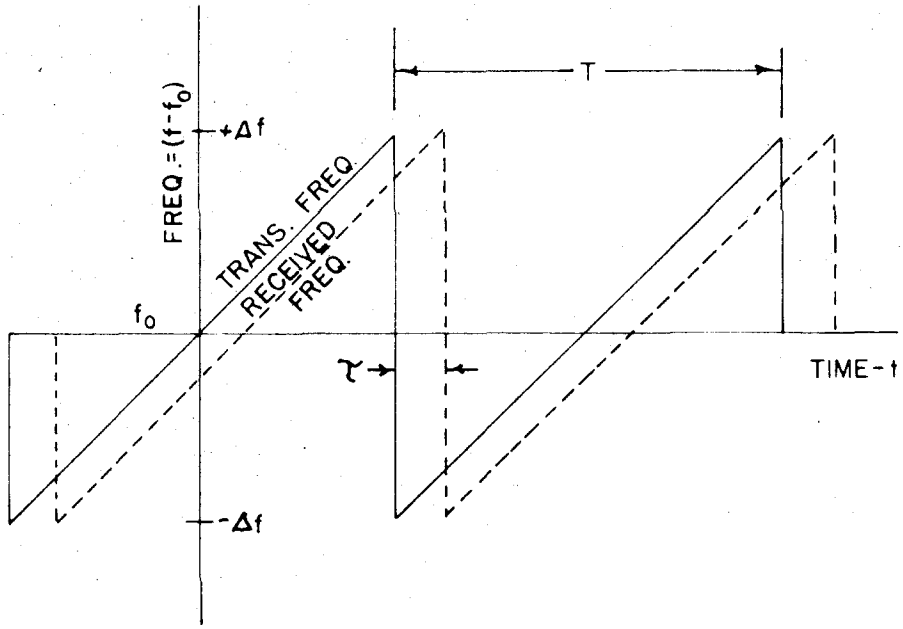

FIG. 15 FREQUENCY VARIATION OF TRANSMITTED AND REFLECTED SIGNAL.

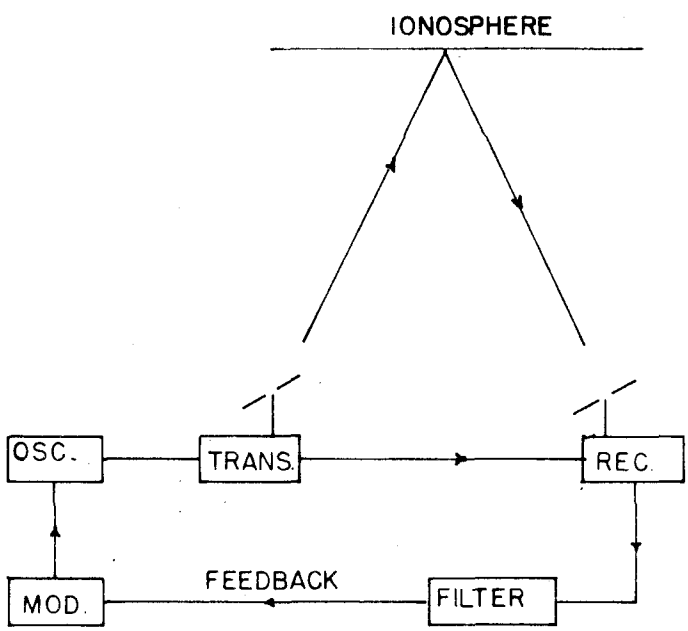

FIG. 16 BLOCK DIAGRAM OF F.M. SOUNDING STATION

every 60 millisec requires only 1000 watts, a value which is readily available.

The Q of the antenna determines how many cycles of a wave it will support. In the case of the Randsburg antenna where the Q was measured to be about 12 at 50 kc/s, the antenna would support Q/π (or about 4 cycles), before the exponential decay reaches 1/e or 0.368 of the initial value. This fact means that the pulse length to the 0.368 point would be 80 μsec at 50 kc/s, a value which is close to the specification required of the pulse length. It should be pointed out that, as the frequency of the pulse is increased (and hence the length of the pulse is decreased), the BW must be increased to keep the same time resolution.

The pulse technique was not used in the experimental setup for two reasons: First, the equipment which was available to the project could have not been used; second, the time required to build up all the equipment would have been prohibitive. A fact which is more important is that the peak power required to obtain the necessary S/N ratio would have been of the order of 5 megawatts, which in itself was impossible in view of the finances available.

B. The Frequency-Modulation Method

A second type of modulation can be used to obtain the information required in determining the height of the ionosphere for frequencies in the range 15 to 100 kc/s. This is frequency modulation of the carrier. The approach to this problem is not as straightforward as the approach to pulse modulation in that several means are available in picking out the desired information. One method is now discussed.

Let it be assumed that it is possible to use a sawtooth voltage

of variable period T to modulate the frequency f by an amount $\pm\Delta f$. The rate of change of frequency $\dot{f}$ is then

$$\dot{f} = \frac{T}{2\Delta f} \tag{19}$$

This is the waveform to be transmitted.

In this system as in each system discussed, the modulated wave must be piped directly to the receiving site for comparison with the received wave. Let τ be the time lag of the received wave with respect to the transmitted wave so that, when the two are mixed, the beat frequencies are related to τ, as can be seen in Figure 15. In the interval $T-\tau$ the beat frequency will be

$$f_1 = \dot{f}\tau \tag{20}$$

Similarly in the interval τ the beat frequency will be

$$f_2 = \dot{f}(T-\tau) \tag{21}$$

Note that the sum of f_1 and f_2 is $\dot{f}T$, which is independent of τ.

The optimum system for using this technique would require that the beat frequency be D.C. ($f_2 = 0$). From Equation (21) it is seen that this condition can be met by continuously controlling T to be equal to τ. The block diagram of Figure 16 shows how this technique could be applied by employing the use of a feedback network containing a narrow-band D.C. filter and a frequency discriminator, which in turn would control the period T of the modulation sawtooth. The stable system would be constrained to having T equal to τ. The measurement of T within 6 μsec would then provide a value of the height h with the specified resolution of 1 km.

This method was not used since it also would have required that many new pieces of equipment be designed and built in the allowed time.

Aside from this fact the system would have been acceptable, especially since the over-all S/N ratio would be limited only by the BW obtainable in the D.C. filter.

C. Continuous-Wave Method

The third means of measuring the height of the ionosphere to be discussed is that of using the unmodulated-wave technique. The information desired is now contained in the phase of the received wave.

Given a fixed transmitting station and a fixed receiver site, one can see that the time required for the wave to reach the receiver is a function of the effective height of the reflecting layer (Cf. Fig. 13). Inasmuch as the only measurement possible is that of phase, the relationship between the phase Φ and the height h must be determined. The phase of the received wave can be established only with respect to some stable reference signal of the same frequency. Thus the transmitted signal is sent directly to the receiver, requiring a time of 2d/c seconds, where c is the velocity of propagation. The time for the reflected wave to reach the receiver is $2\ell/c$. Thus the total phase lag of the received signal compared with the reference signal is

$$\Phi = \left(\frac{2\ell}{\lambda} - \frac{2d}{\lambda} \right) 360^\circ = \varphi + n\,360^\circ \qquad (22)$$

where φ is the function actually measured and is the phase in excess of a multiple of 360°. ℓ and d are as defined in Figure 13, and n = 1, 2, 3, ... By using the relationship

$$h = d \cot \theta \qquad (23)$$

and rewriting Equation (22),

$$\Phi = \frac{2d}{\lambda} \frac{1 - \sin\theta}{\sin\theta} 360^\circ \qquad (22a)$$

h can be calculated. As this method is not very convenient, a graphic method was derived from Equations (22a) and (23).

Let $\Theta = \Theta_0 + \delta\Theta$. If $\delta\Theta$ is kept less than 0.1 radian, Equations (22a) and (23) can be rewritten

$$\Phi = \frac{2d}{\lambda} \frac{\frac{1-\sin\Theta_0}{\cos\Theta_0} - \delta\Theta}{\tan\Theta_0 - \delta\Theta} 360^\circ \qquad (24)$$

$$h = \frac{1 + \delta\Theta \tan\Theta_0}{\tan\Theta_0 - \delta\Theta} \qquad (25)$$

Assume a standard $\Theta_0 = 21.925^\circ$ which corresponds to a height h of 80.00 km and a distance d of 32.20 km. For a frequency f_0 of 50 kc/s, Equations (24) and (25) are plotted as a function of $\delta\Theta$ in Figure 17. Now if Φ is determined from the phase measurement, then h can be picked off the curve as shown in the example.

It may have been noted by now that there is an ambiguity in h since there is an ambiguity in φ of 360° or multiples thereof. Table I, calculated from Equation (22a)and (23), shows all the possible values

Table I

$\Phi/360^\circ$	d	Θ	h
15	32.20	24° 39.1'	70.16
16	↓	23 40.3	73.45
17		22 46.1	76.72
18		21 9.7	79.96
19		21 56.1	83.18
20		20 26.4	86.40
21		19 46.2	89.59
22		19 8.5	92.77
23		18 33.2	95.94
24		18 0.0	999.10
25		17 28.8	102.51

of h for $\varphi = 0^\circ$ (f_0 is 50 kc/s). Similar tables can be made for other frequencies if desired. If a rough approximation for the ambiguity at any given frequency is needed, then

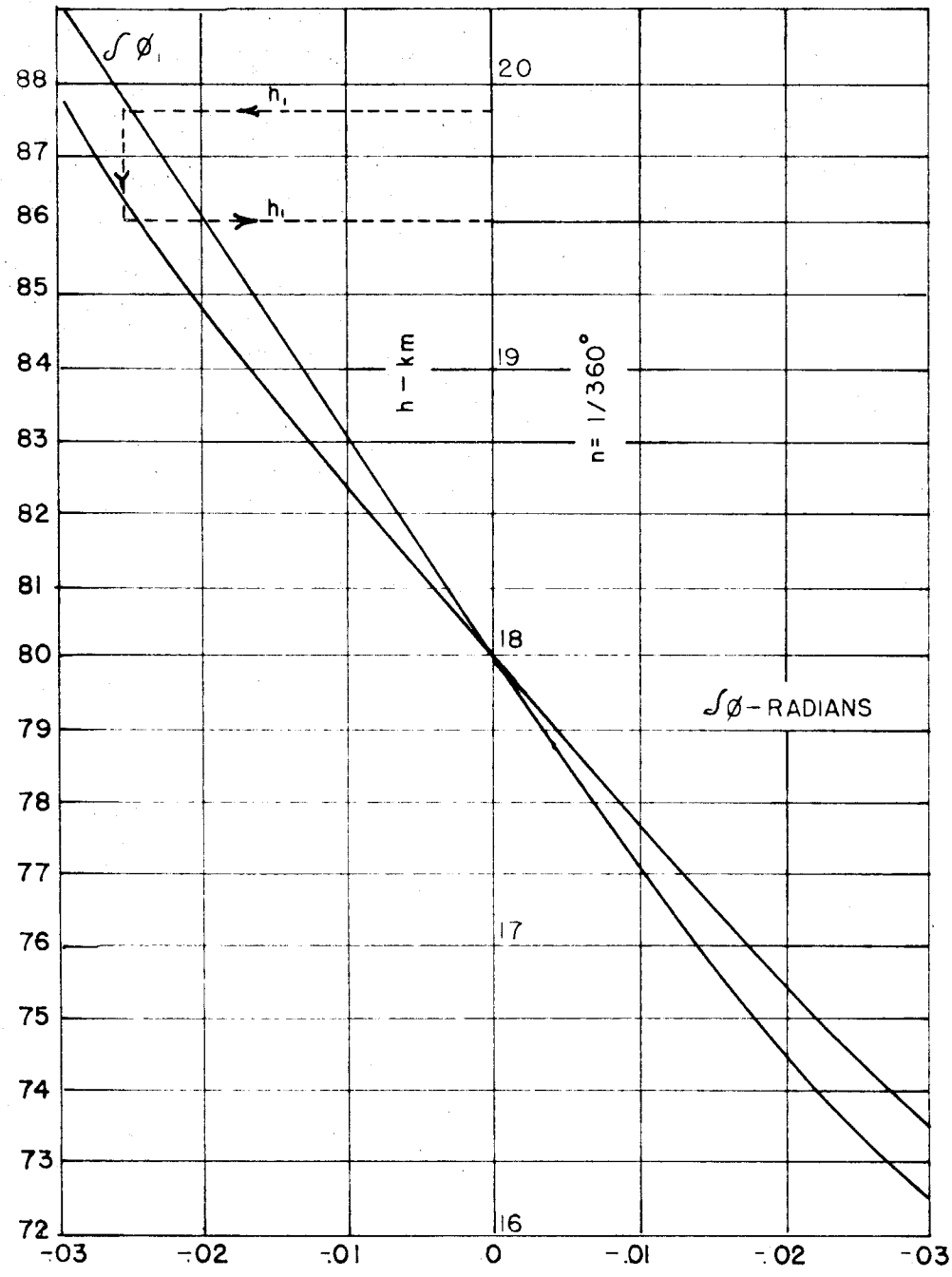

FIG. 17 CONVERSION OF PHASE TO HEIGHT

$$\delta h_{\Delta\varphi=360^\circ} = \lambda_0/2\cos\theta' \qquad (26)$$

where θ is the approximated value of Θ, and λ_0 is the wavelength of the frequency f_0. It now remains for this ambiguity to be resolved in the experimental setup. A somewhat impractical way to resolve the ambiguity is to set up a temporary station at a distance away from the permanent station but still on the line through the transmitting and receiving sites. From a table for this station similar to Table I one can observe that, for a given set of measurements of Φ at each of the two stations, there will be only one value of h that will satisfy all conditions. Two independent measurements of phase must be obtained in order to resolved the ambiguity. A more practical method is to use another frequency. Again a table like Table I can be computed, and again the ambiguity can be resolved. The practical limitation of the resolving power of the equipment in phase determines how much an offset in the distance d or frequency f is needed. If an uncertainty in φ of 15° is allowed, the difference in the distance d should be about 7.5 km, and the change in frequency f should be about 4 kc/s, assuming that the initial conditions were set up for f_0 of 50 kc/s and for d of 32.2 km.

Up to this point an effort has been made to keep the discussion general so that the results can be applied anywhere in the frequency range 15 to 100 kc/s. Having the system so flexible that the operating frequency can be changed in the matter of minutes was an objective, and it is hoped, for example, that the ion-density distribution can be determined. However, it was found that system difficulties increased too rapidly with decreasing frequency, and it was necessary to be

satisfied with setting up a station on one frequency, namely, 50 kc/s. One should constantly keep in mind the fact that it is the ultimate goal to extend the function of the equipment down to 15 kc/s. There is no problem in extending it to the higher frequencies.

III. IONOSPHERIC SOUNDING STATION AT 50 kc/s

We have determined how to find the effective height of the ionosphere by means of a phase measurement. The components of the 50-kc/s system that was actually put into operation are discussed in this section. The block diagram of Figure 18 shows the basic components of the system. The transmitting site (longitude 117° 45.53', latitude 35° 16.60') is located near Randsburg in the Mojave desert. The transmitting antenna is a dipole whose bearing is 72° and which extends for 13,000 feet on each side of the center where a trailer van housing the transmitting equipment was placed. The receiving site is located in the Shadow Mountains to the south. The exact location was chosen so that the transmitter was line of sight. The fact that it was line of sight was actually determined on several occasions by signaling elementary messages with powerful flashlights. The bearing of the receiver site from the transmitter was 166°; the distance was 40 miles. It is not a permanent location since there are no installations or equipment there.

The ionosphere station was designed so that the phase and amplitude of the reflected wave would be continuously recorded. To this end the transmitter was to furnish a stable frequency of 50 kc/s and the means wherewith to transmit both the test signal and the reference signal. On the other hand, it was the function of the receiver to receive the

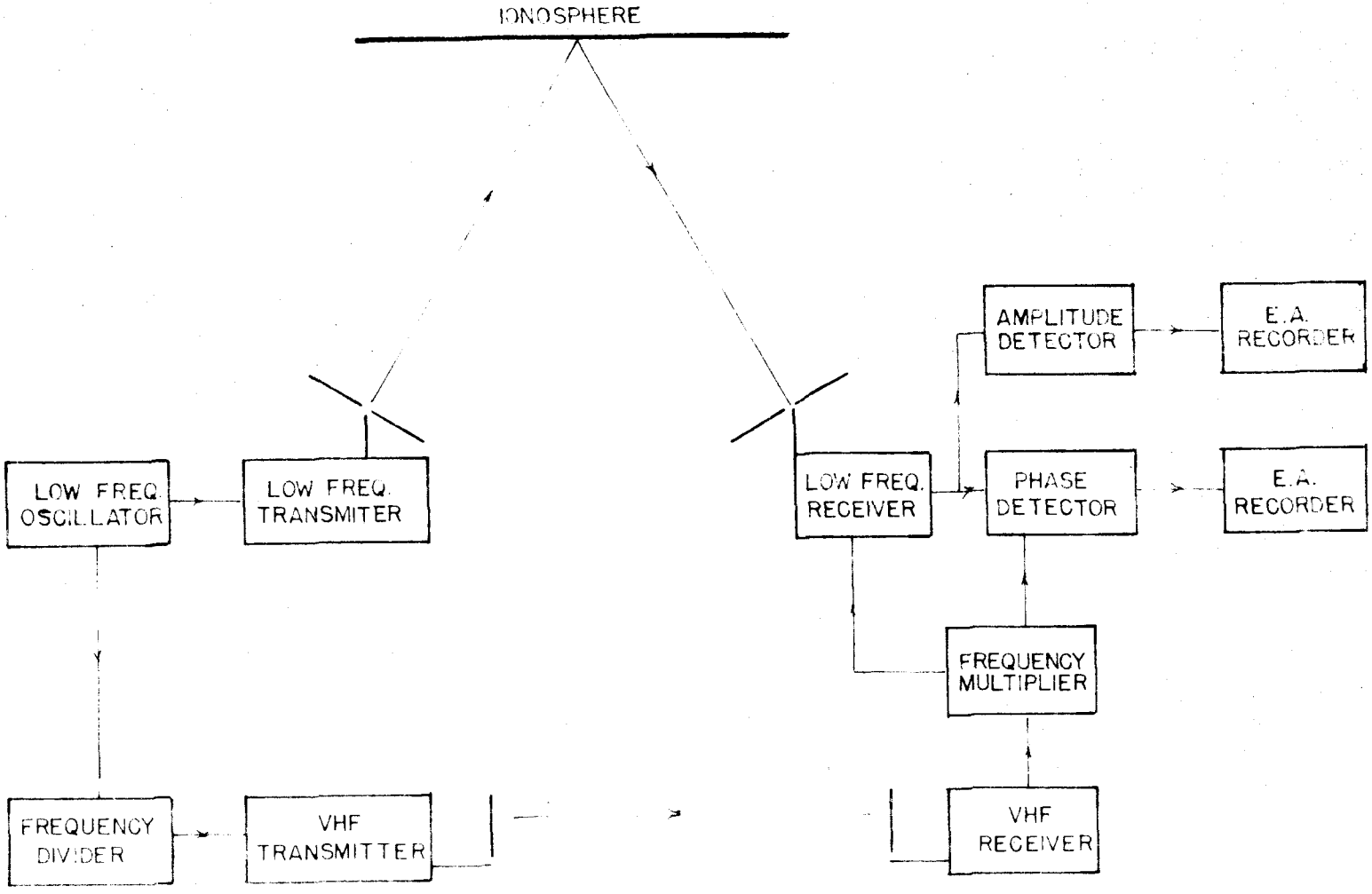

FIGURE 18 BLOCK DIAGRAM OF THE TRANSMITTING AND RECEIVING SYSTEM

reflected test signal and compare it with the reference signal. It must also present the resulting information in recordable form.

A. Transmitting System

The transmitting equipment is shown in the block diagram of Figure 19. A 100-kc/s crystal controls the frequencies of the entire system. The 100 kc/s is divided first by 2 in order to obtain the standard 50 kc/s of the transmitted wave. The 50 kc/s in turn is divided by a factor of 31 in order to obtain a frequency which can be used to modulate the VHF (30.54-mc/s) line-of-sight communication link. The VHF transmitter, an AN/FRC-6, is capable of putting out over 50 watts, whereas the low-frequency transmitter puts out over 600 watts.

An appreciable amount of power was required to operate the equipment at the transmitting site. This power was furnished by a trailer-mounted, motor-generator set with a rating of 7.5 kw which was ample.

1. Low-frequency power output and driver stages. The combined unit including the high-voltage power supply was built by the Herrnfeld Engineering Company (Los Angeles) under specifications for a supersonic power oscillator. The California Institute of Technology purchased the unit second hand especially for the ionospheric project. The unit has been modified slightly to conform to the circuit diagram of Figures 20 and 21. The maximum continuous power output is a little over 600 watts, and it is possible over short periods of time to increase the power output to about 800 watts. The output impedance was approximately 100 ohms and could be changed to 400 or 1600 ohms by making proper changes at the terminals of the output transformer. As seen in the circuit diagrams the power output stage consists of two 250TH Eimac tubes operating in push-pull and driven by two 6L6 tubes also in push-

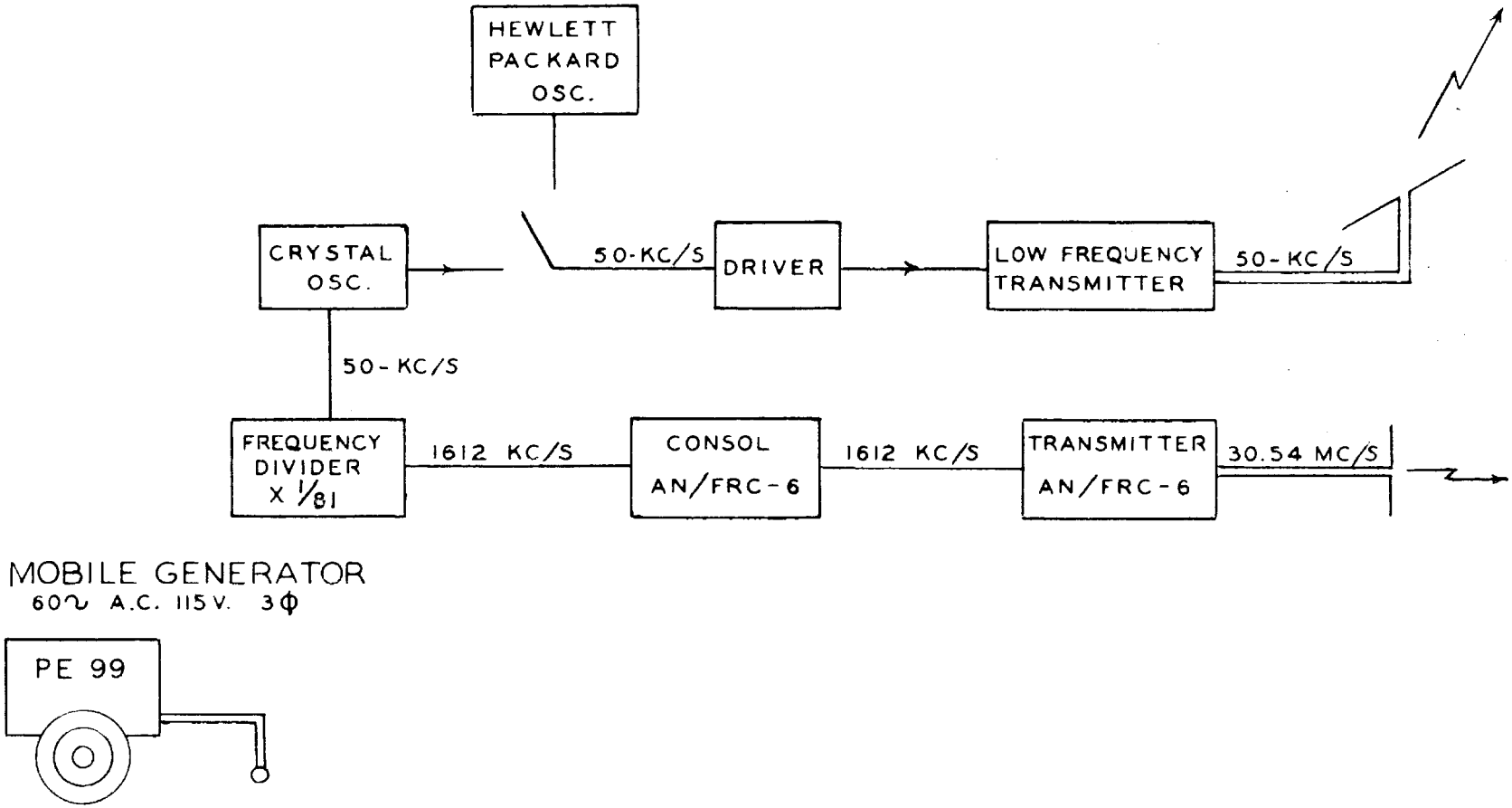

FIGURE 19.

BLOCK DIAGRAM OF TRANSMITTING STATION.

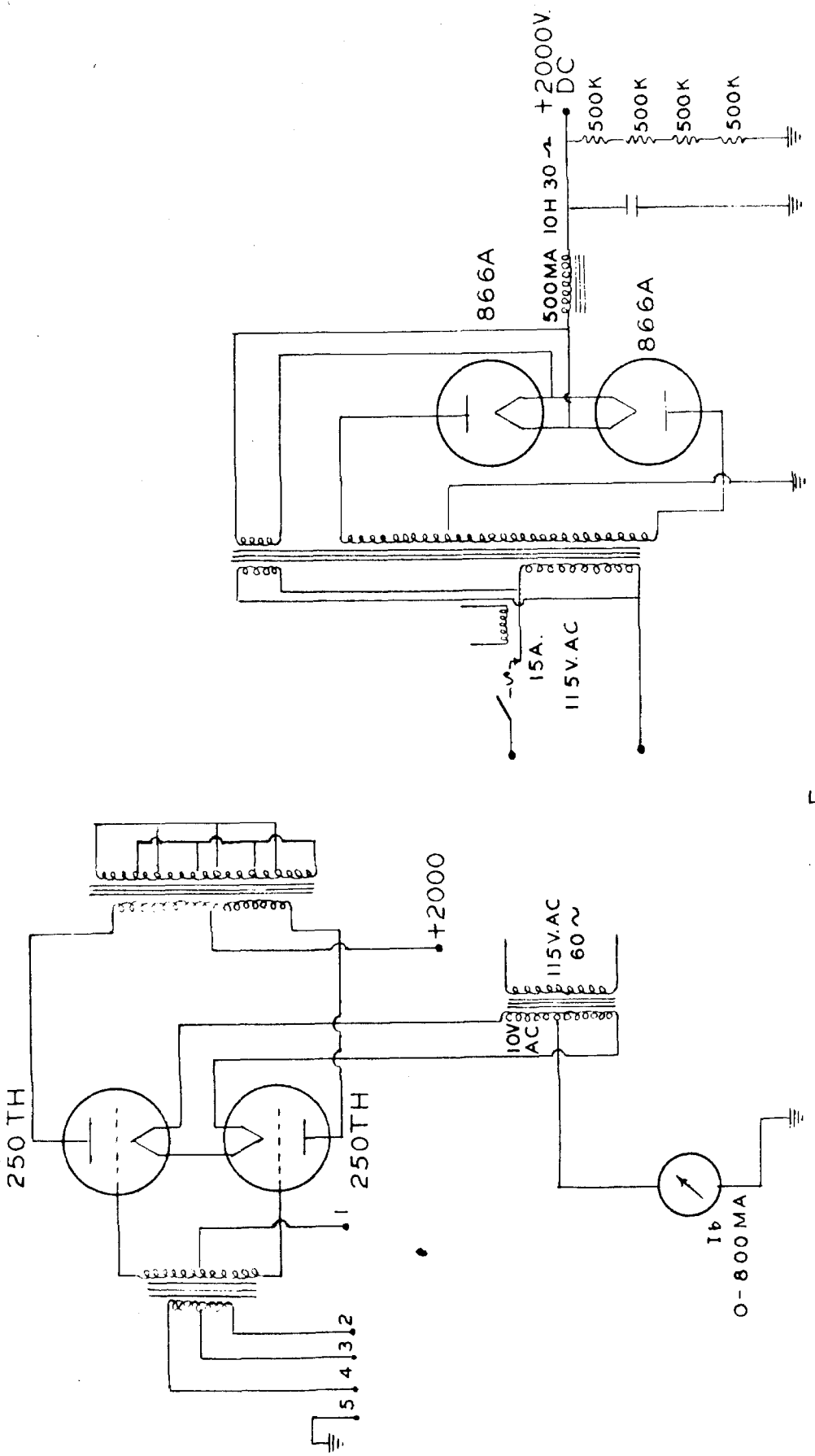

FIGURE 20

50-KC/S TRANSMITTER OUTPUT STAGE AND HIGH VOLTAGE POWER SUPPLY.

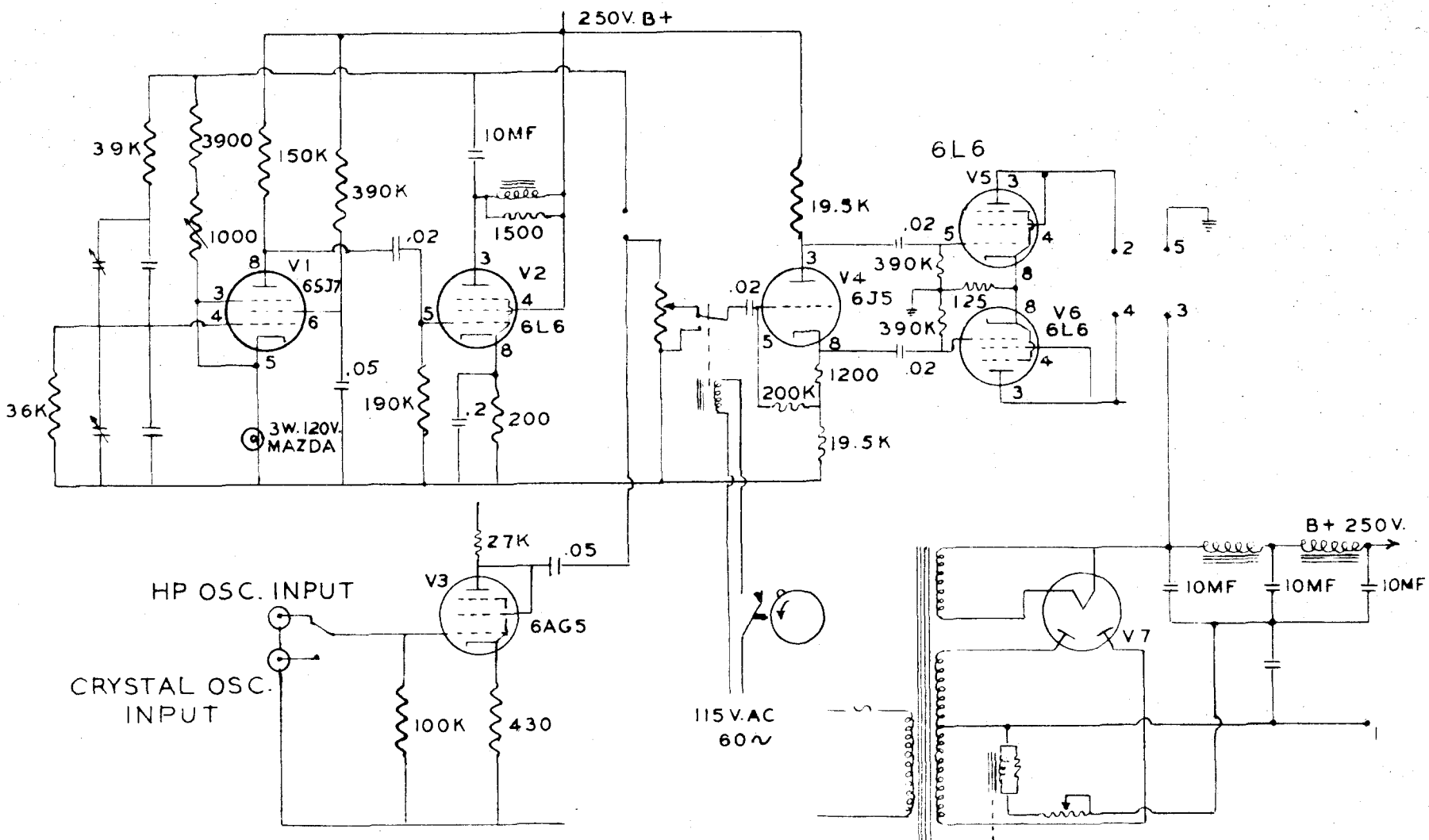

FIGURE 21

TRANSMITTER OSCILLATOR DRIVE.

pull. The oscillator stage incorporated in the original transmitter was not suitable for our purposes and changes were made to allow either a Hewlett-Packard oscillator or the crystal oscillator to control the frequency from 15 to 100 kc/s. One of the outstanding features of the transmitter was the relay operated by a timing motor which automatically removed the signal about 45 seconds out of every 5 minutes. Many times when signal level was low, this type of modulation was the only thing that assured the experimenters that the signal they were listening to was theirs.

A great deal of trouble was experienced with this transmitter in the early stages of the experiment. The original transmitting tubes (two 8000 tubes) would not withstand continuous full load. The Eimac transmitting tubes were more suitable. There was also great difficulty with the original oscillator circuit. Using the external oscillators effectively by-passed this trouble.

2. Transmitting antenna. The theory of the transmitting antenna appears as Appendix A. The antenna was constructed southwest of Randsburg as shown on the map (Cf. Fig. 1). The altitude at the center of the antenna is 3500 feet above sea level. The east end is at 3700 feet, whereas the west end is at 3200 feet. The terrain upon which the antenna is built is, on the whole, quite level.

The first transmitting dipole was constructed along the Randsburg-Mojave road merely by stringing No. 20 wire for 1.3 miles on the greasewood brush. When a signal was received at the Shadow Mountain receiving site in November, 1951, the antenna theory was confirmed, and plans were made to construct the permanent antenna. This antenna consisted of No. 10, No. 6, and No. 4 wire strung on poles placed 200 feet apart.

The line was broken every 1000 feet, or every fifth pole, and a switch was inserted in order to allow the antenna to be used at almost any frequency from 16 to 250 kc/s. Every fifth pole was also independently guyed in four directions to protect the whole antenna from collapsing in case one section should fail. The poles were 4 x 6's of select structural and No. 1 common lumber 16 feet long. The average depth of the pole holes was 3 to 3½ feet; thus the antenna wire everywhere was 10 to 11 feet above the ground. Light loading conditions (Cf. Ref. 11) were assumed in the structural design of the antenna, and since the altitude was slightly higher than 3,000 feet, additional safety factors were used.

The actual construction of the antenna was quite a task. The Building and Grounds Department of the California Institute of Technology undertook the job of putting the 131 poles into ground consisting of decomposed granite and rocks; 240 holes had to be drilled either by hand or with the pneumatic posthole digger. Putting the poles in the holes and stringing the wire were relatively easy. A five-man crew worked 3 weeks to complete the job.

The original object in building the dipole was to provide a low-cost transmitting antenna which would require no tuning inductances but would, instead, present a resistive load to the transmitter. In this way the design of the transmitter was greatly simplified. As a half-wave dipole at low and very low frequencies, this antenna presented a resistive load. The current distribution in the dipole is sinusoidal with a wavelength λ_{eff}, which was approximately 94 per cent of the free-space wavelength λ. The current distribution in the antenna (Cf. Fig. 22) is given by

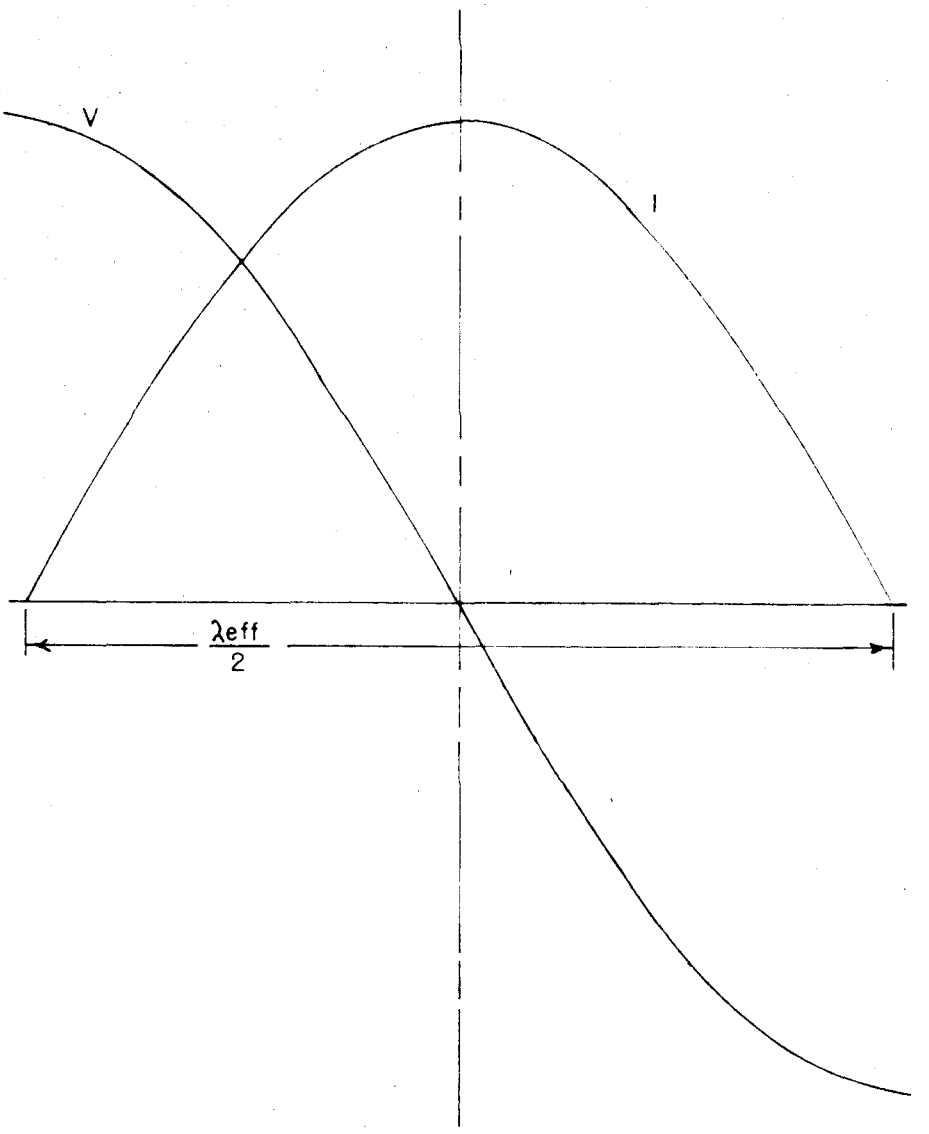

FIG. 22 CURRENT AND VOLTAGE DISTRIBUTION OF HALF WAVE DIPOLE

$$i = I\sqrt{2}\ \cos\frac{2\pi ct}{\lambda}\ \cos\frac{2\pi x}{\lambda_{eff}} \qquad (27)$$

where x is measured from the center. Similarly the voltage distribution is given by

$$v = V\sqrt{2}\ \cos\frac{2\pi ct}{\lambda}\ \cos\frac{2\pi x}{\lambda_{eff}} \qquad (28)$$

The losses of the dipole are attributed to copper losses R_c, distributed ground losses R_g, and radiation losses R_r. The efficiency of the antenna is given by $R_r(R_g + R_c + R_r)$, or R_r/R_o; therefore R_g and R_c should be made as small as possible. Unfortunately not much can be done about R_g; R_c can be reduced by using more copper in the antenna, especially if it is concentrated near the center. One finds that at a given frequency the ratio of the A.C. resistance to the D.C. resistance increases as the wire size increases. The ratio also increases for a given wire size with increasing frequency. In Figure 23 is plotted the ratio of the A.C. resistance to the D.C. resistance of No. 14 wire as a function of wire size for both 60 and 20 kc/s. It can be seen that there is a practical limit to increasing wire size effectively in order to decrease losses. The antenna consists mostly of No. 10 hard-drawn copper wire which was the smallest available. By using Equation (27) the copper losses are found to be $(I^2R_{ac}/4)\lambda_{eff}$ where I is the rms current at the center of the dipole. Therefore

$$R_c = R_{ac}\,\lambda_{eff}/4 \qquad (29)$$

R_c is found to be 21 ohms at 50 kc/s and 40 ohms at 16 kc/s, whereas the measured value of R_o was 65 ohms at 50 kc/s and 82 ohms at 16 kc/s. Note that the difference in the input resistances at the two frequencies

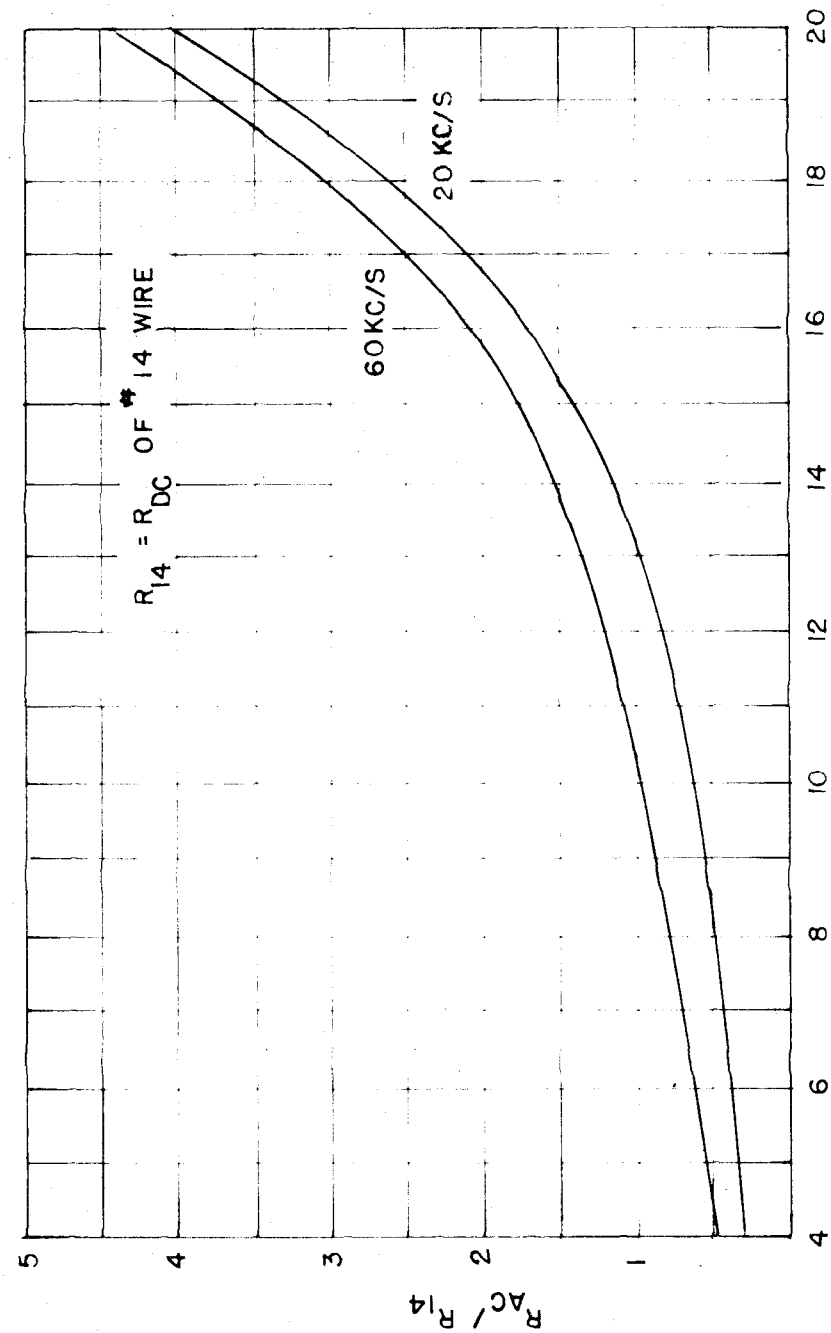

FIG. 23 VARIATION OF A.C. RESISTANCE AS A FUNCTION OF WIRE SIZE

is just the difference in copper losses. It can be inferred that $R_g + R_r$ is not a function of frequency; this inference agrees with the theory.

The dipole can be used as an impedance transformer under limited conditions. From Equations (27) and (28) one sees that the current and voltage are everywhere in phase. Thus if the dipole is fed at some point other than the center of the antenna, the input impedance remains resistive and increases to the value given by the empirical formula

$$R_{in_x} = R_o / \cos^2 \frac{2\pi x}{\lambda_{eff}} \qquad (30)$$

Here λ_{eff} turns out to be a function of x because of the effect of the transmitter and the lead-in wires. As the feed point moves away from the center of the antenna, λ_{eff} decreases.

At the experimental frequency 50 kc/s, the 65-ohm impedance of the dipole was transformed to 100 ohms to match the output impedance of the transmitter. This transformation was accomplished by feeding the 8600-foot dipole at a distance of 1700 feet from the center.

The Q of the antenna was found to be about 12 by determining the two frequencies f_1 and f_2 where the input impedance had a phase angle of 45° and by using the equation

$$Q = f_o / (f_2 - f_1) \qquad (31)$$

where f_o is the resonant frequency.

At this time reference might be made to the antenna paper in Appendix A in order to point out several important features concerning the radiation of the dipole. The radiation pattern has a maximum value

directly over the antenna, a fact which makes it especially suitable for vertical-incidence ionospheric sounding. It was calculated that, for a current of 1 ampere in the antenna, a dielectric constant of 6 for the ground, and a reflection coefficient of 0.5, the field strength at the receiver would be 75 μvolts/meter. From the experimental results the author estimates the actual value to be more like 20 μvolts/meter. Another important fact concerning the antenna is that, although it radiates a reasonably strong ground wave off the end of the antenna, it has a null at a right angle to the length of the dipole. Based on experimental results, it seems that the ratio of the field strength above the antenna to that off the end is about 10/1 at a distance of 15 miles.

3. Stable frequency source. The Federal Communications Commission in granting the project a license to operate the station specified that the frequency must be held to a tolerance of 0.01 per cent. The requirements of the phase-measuring system are a little more stringent in that the frequency must be held to 1 part in 500,000. The over-all system has a BW of about 1 c/s; thus any slight change in frequency results in an indication of phase change. These phase changes must be kept below about 5° since this is the estimated accuracy of the phase-measuring equipment. Since crystals operating below 80 kc/s were not readily available, it was necessary to take the output of a 100-kc/s crystal oscillator and divide it by 2 in order to supply a stable 50-kc/s signal. The circuit diagram of the oscillator and scalar is shown in Figure 24. The output of the oscillator stage is a sawtooth wave with more than enough amplitude to trigger the scalar, which is a bistable multivibrator. The multivibrator triggers only on receiving a negative pulse

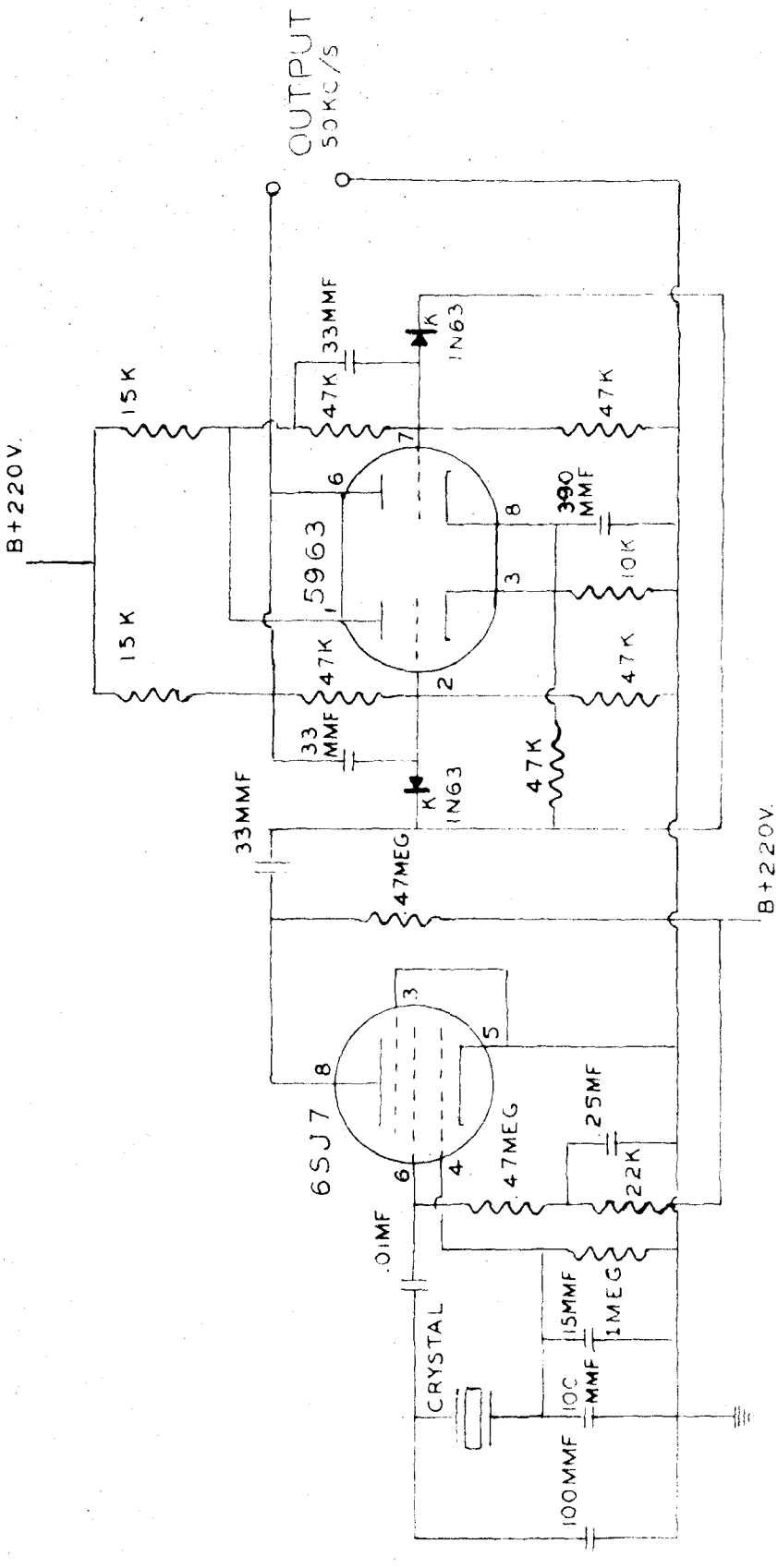

FIGURE 24

100-KC'S CRYSTAL OSCILLATOR AND SCALER CIRCUIT

from the preceding stage; therefore it goes through only 1 cycle for every two of the crystal oscillator.

The output of the frequency divider is a square wave with a period of 20 μsec. The transmitter (Cf. Fig. 22) on the other hand, requires a 50-kc/s sine wave and a voltage level up to about 30 volts. The 50-kc/s filter-amplifier (Cf. Fig. 25) filters out all but the fundamental of the square wave and is capable of putting out 50 volts undistorted. The filter section is of interest in that it (or a slight variation) is used many times in the system. The cathode followers are used to isolate the filter from the rest of the circuit. L_1 is a 5-mh toroid with a Q of about 100 at 50 kc/s. The tuned circuit consisting of L_1 and C_1, therefore, has a resonant impedance of 0.15 megohm. R_1 and the tuned circuit form a voltage divider network which gives a maximum output at the resonant frequency. If R_p be designated as the impedance and Q_p, the Q of the tuned circuit at resonance, then the Q of the filter is given by

$$Q = Q_p R_1 / (R_1 + R_p) \qquad (32)$$

If it is necessary to have a high Q, then R_1 must be made much larger than R_p, but then a sacrifice must be made in voltage output since there will be a loss in gain of $R_1/(R_1 + R_p)$. In the case of the 50-kc/s filter it was not necessary to have a high Q; therefor R_1 was put equal to R_p, giving a Q of $Q_p/2$.

The amplifier stage is operated from a high B+ voltage in order to obtain the 50-volt output. The cathode resistor is left unbypassed to help keep the distortion down.

4. Frequency divider of 50 kc/s to 1612 c/s. It is necessary to derive a frequency in the range 400 to 3000 c/s which is directly

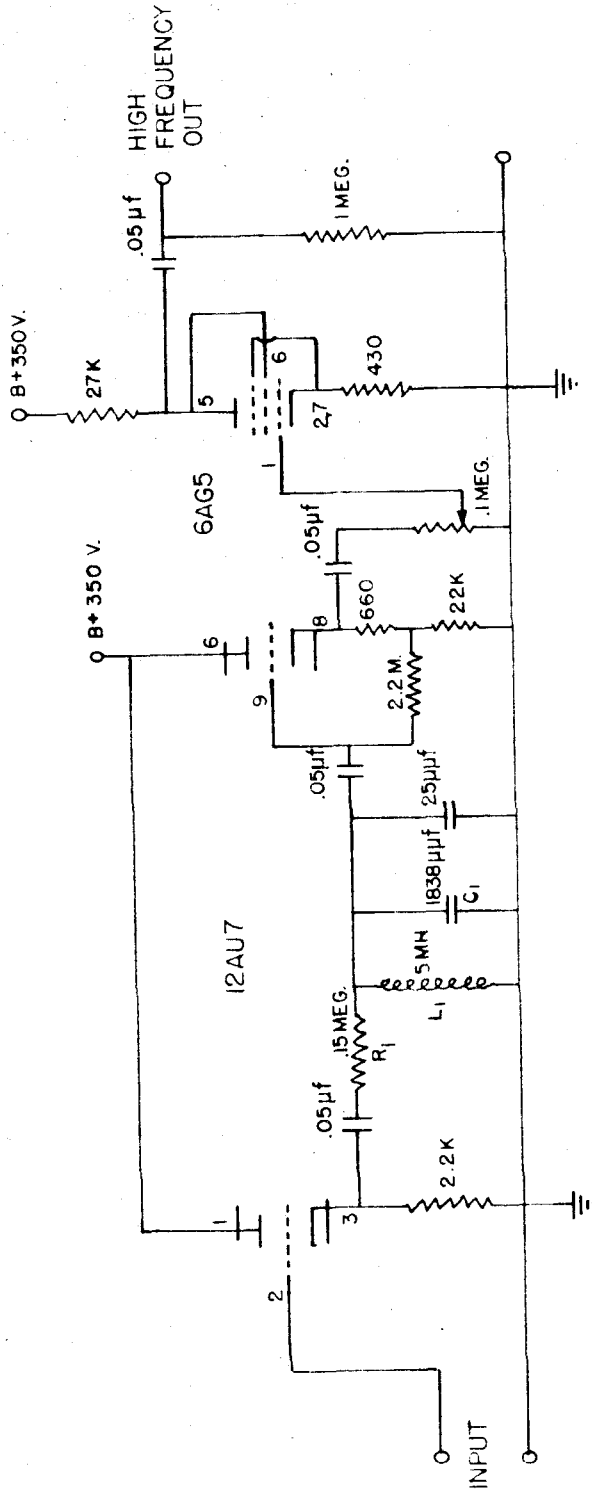

FIGURE 25, 50KC/S FILTER

related in phase to the 50 kc/s. This signal will be used to modulate the FM transmitter in the line-of-sight communication link. If 50 kc/s is divided by 31, the resulting frequency is 1612 c/s. The factor 31 is chosen because (1) it is an odd number, (2) it is simple to realize, and (3) it falls in this frequency range. The odd number is necessary since the square wave which will eventually be formed must contain the thirty-first harmonic. The General Electric Company makes a binary scalar (Cf. Fig. 26) which will operate at 50 kc/s; these scalars are used in the dividing circuit. They function exactly as the scalar shown in Figure 24 but cannot be operated at as high a frequency. The scalar by nature divides frequency by 2; thus one unit divides by 2, two units divide by 4, three by 8, four by 16, five by 32, etc. Feedback properly employed in the scalar circuits can produce division by any number required. In determining how to divide by a given number, each scalar is given a number in the binary system as shown in Figure 27a. One cycle of this system is defined as complete when the last scalar has been cleared, i.e., when it has put out a negative pulse. This negative pulse can be fed back to any one scalar or to all of the preceding scalars. Thus when the following cycle starts, a number which has been determined by the feedback is already set into the system. In Figure 27a the input frequency would be divided by 32 without feedback, but with the feedback the number 12 is set in at the end of each cycle, and the circuit divides by 20. Inasmuch as $1 + 2 + 4 + 8 = 15$, it is possible to count down by 17 to 32 with five scalars. To divide by a factor of 9 to 16, only four scalars are needed, etc.

For any division other than by a power of 2, the output of the scalar network is not a symmetrical square wave. The positive part remains

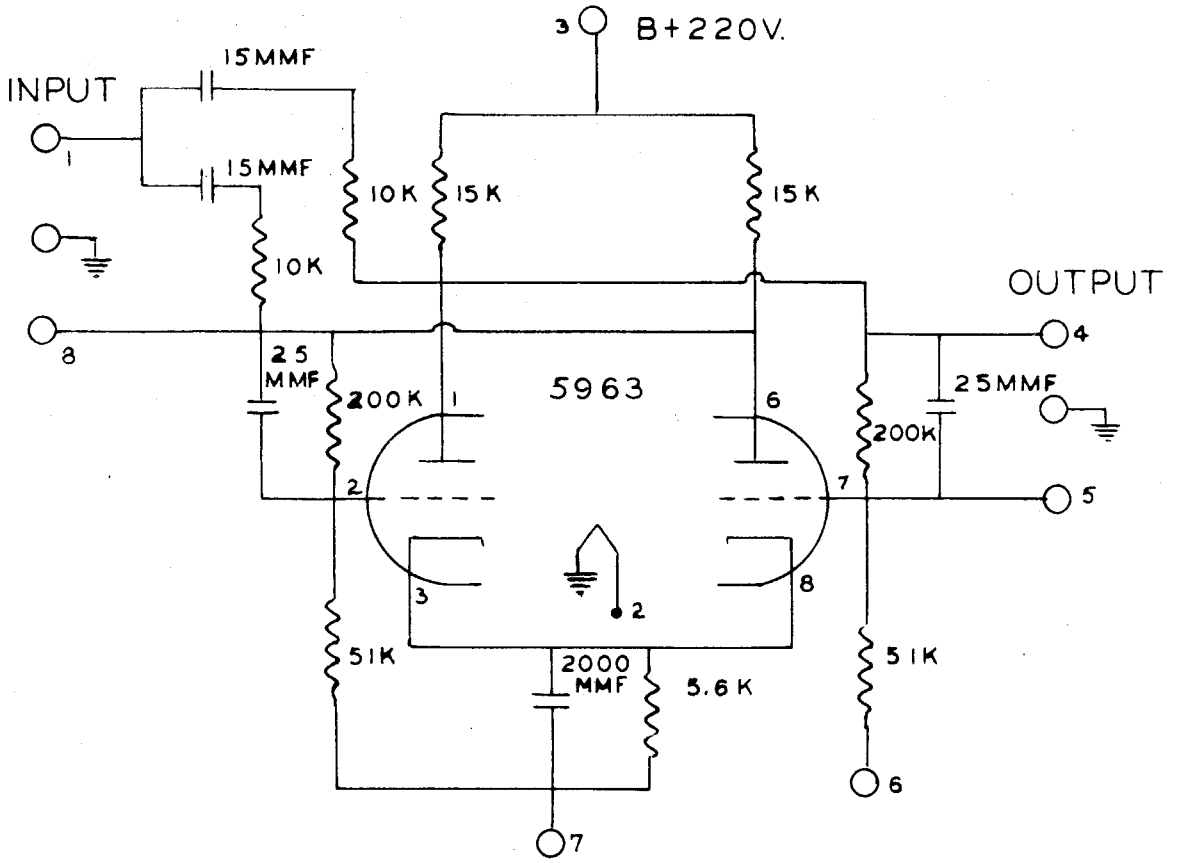

FIGURE 26

G.E. BINARY SCALER.

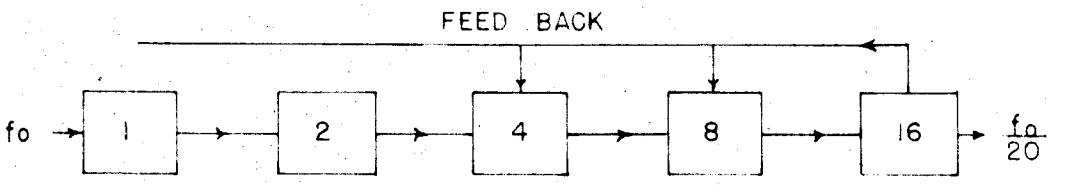

FIGURE 27a BLOCK DIAGRAM FOR DIVISION BY 20

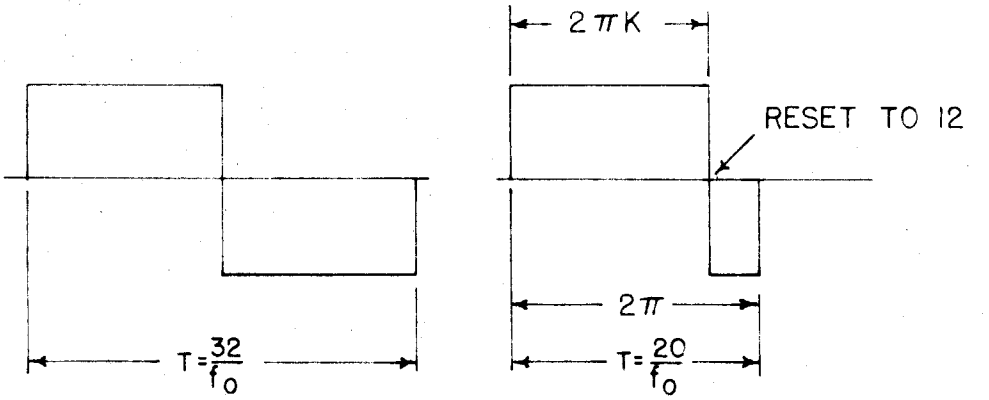

FIGURE 27b WAVE FORM FOR DIVISION BY 20

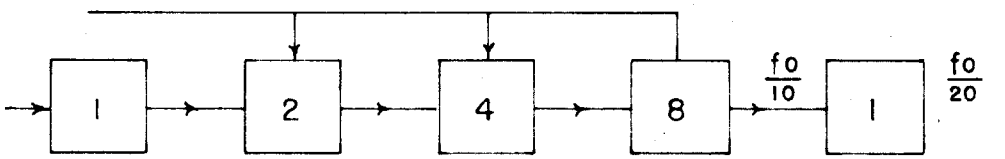

FIGURE 27c ALTERNATE DIAGRAM FOR DIVISION BY 20

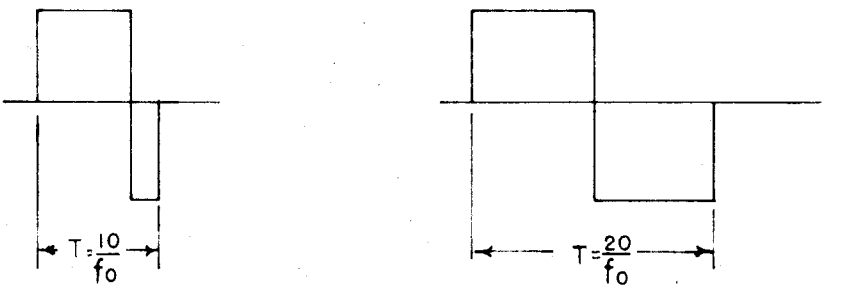

FIGURE 27d WAVE FORM OF ALTERNATE METHOD

the same length for all divisions between 32 and 17, for example, and the negative part diminishes in length. Assuming that the negative part can be divided into 16 parts for division by 32, it is found that the number of one-sixteenths subtracted from the length of the negative part is exactly equal to the number fed back (Cf. Fig. 27b). It may not be suitable to have the waveform shown in Figure 27 b for division by 20. Nothing can be done about the waveform unless the divisor is even, as it is in this case. Then the division can be done in two steps in order to obtain a symmetrical square wave (Cf. Figs. 27c and d).

In dividing by 31 (Cf. Fig. 28) the output of the five scalars will not be quite symmetrical. It will not matter, however, since only the first harmonic will be filtered out. The 1612-c/s filter is designed exactly as the 50-kc/s filter with the appropriate changes in the L_1 and C_1 (Cf. Fig. 25).

5. VHF frequency-modulated transmitter. The location of the receiving site was chosen so that it was line of sight from the transmitter. Fortunately such a choice was possible. From the very start of the project it was realized that a reliable means of communication was imperative for the success of the program. The U. S. Navy under the authority of the Office of Naval Research assigned to the project two AN/FRC-6 FM transmitter-receiver units as requested by the author. These units were designed to operate in the frequency range 30 to 40 mc/s with a power output of not less than 50 watts.

In an FM system the frequency changes according to the amplitude of the modulating signal. If Δf is the maximum frequency deviation of the transmitter, the instantaneous frequency for the signal $A \sin 2\pi f t$ is

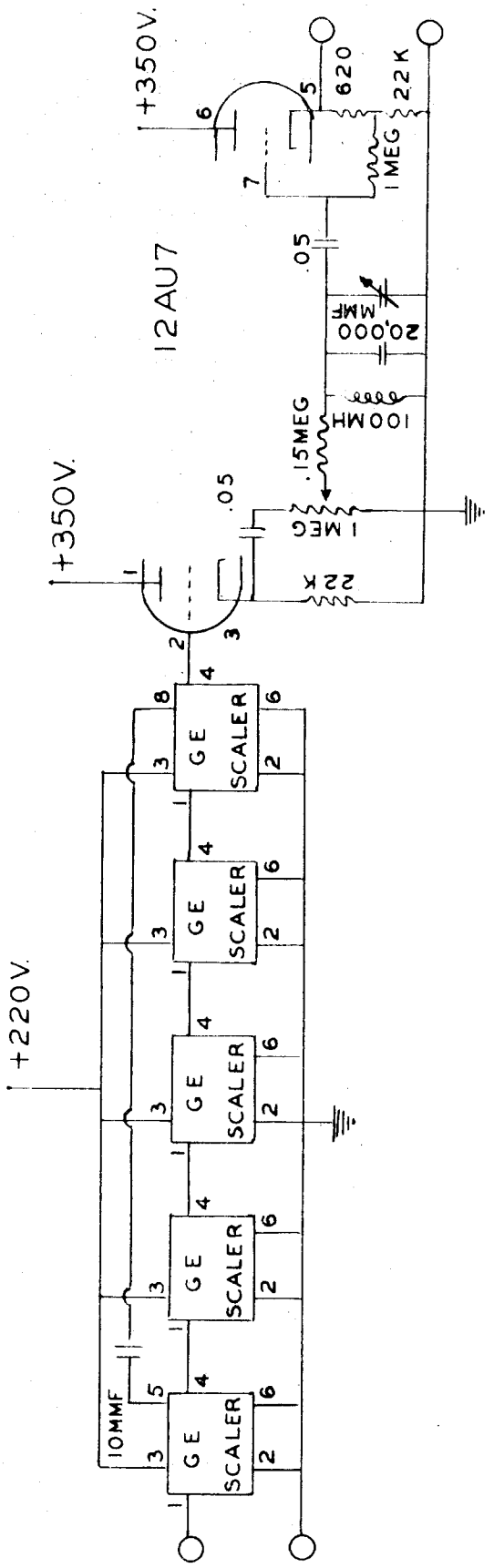

FIGURE 28

FREQUENCY DIVIDING CIRCUIT.

$$f = f_h + \Delta f \sin(2\pi f_L t) \tag{33}$$

where f_h is the unmodulated carrier. The instantaneous phase is related to the frequency by the relationship

$$f = \frac{1}{2\pi}\frac{d\theta}{dt} \tag{34}$$

which can be solved for θ

$$\theta = 2\pi f_h t + m_f \sin 2\pi f_L t + \theta_0 \tag{35}$$

where $m_f = \Delta f/f$ and θ_0 = constant. The output voltage v of the transmitter

$$v = V\sin(2\pi f_h t + m_f \sin 2\pi f_L t + \theta_0) \tag{36}$$

can be expressed in the form of the infinite series

$$\begin{aligned} v = V\{ & J_0(m_f)\sin[2\pi f_h t + \theta_0] + J_1(m_f)\sin[2\pi(f_h + f_L)t + \theta_0] - \\ & J_1(m_f)\sin[2\pi(f_h - f_L)t + \theta_0] + J_2(m_f)\sin[2\pi(f_h + f_L 2)t + \theta_0] + \\ & J_2(m_f)\sin[2\pi(f_h - 2f_L)t + \theta_0] + \cdots \} \end{aligned} \tag{37}$$

Each term of Equation (37) represents a side band on either side of the carrier frequency f_h. After a value of m_f has been chosen, a curve of $J_n(m_f)$ vs n can be plotted in order to determine how many side bands must be included in the bandwidth of the receiver. In general it can be said that $J_n(m)$ decreases rapidly for $n > m$ (Cf. Ref. 9). $J_n(1)$ and $J_n(5)$ are plotted in Figure 29. A plot showing the required BW as a function of m_f is given in Figure 30 (Cf. Ref. 12). It is seen that the needed BW is approximately twice the maximum frequency deviation

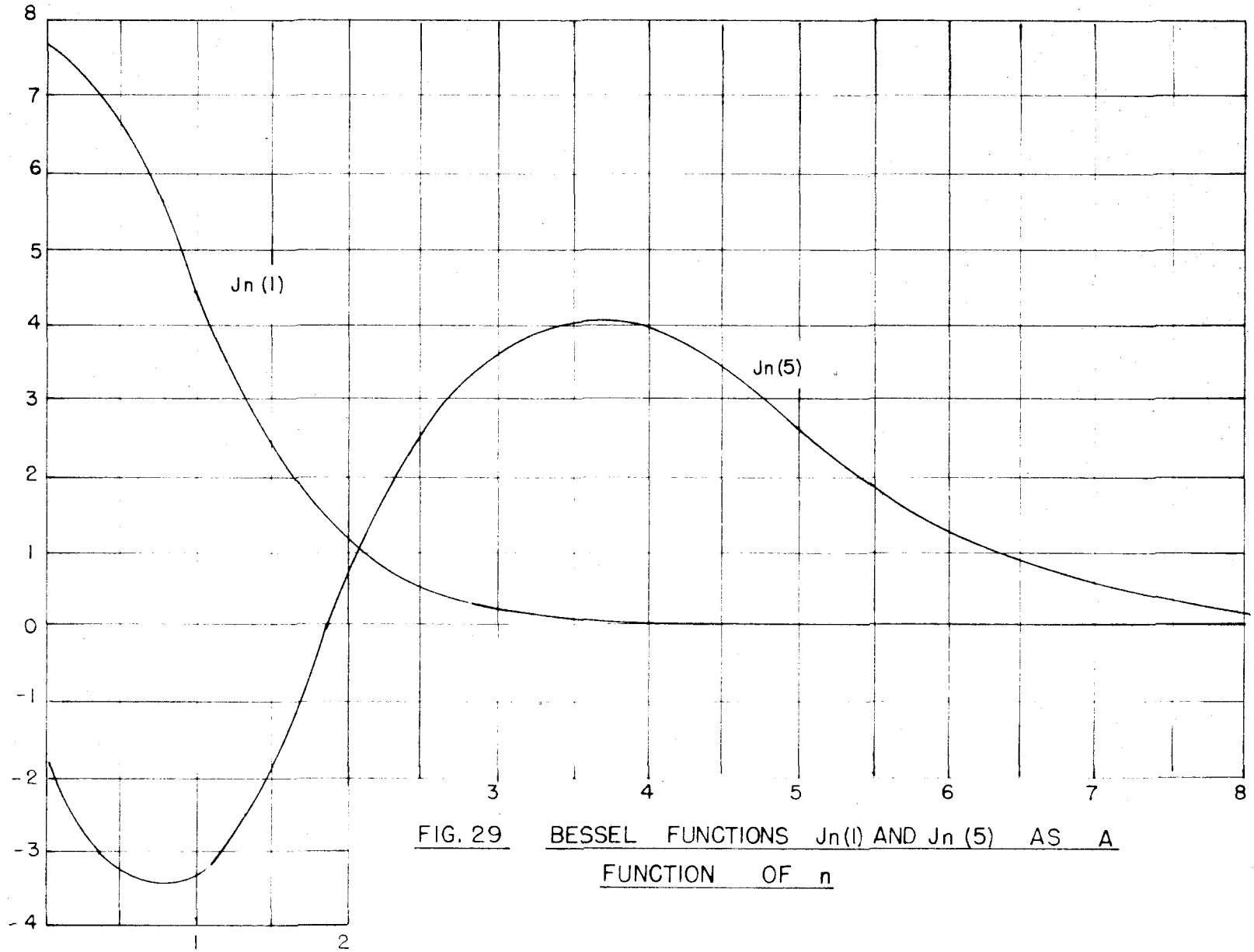

FIG. 29 BESSEL FUNCTIONS Jn(1) AND Jn (5) AS A FUNCTION OF n

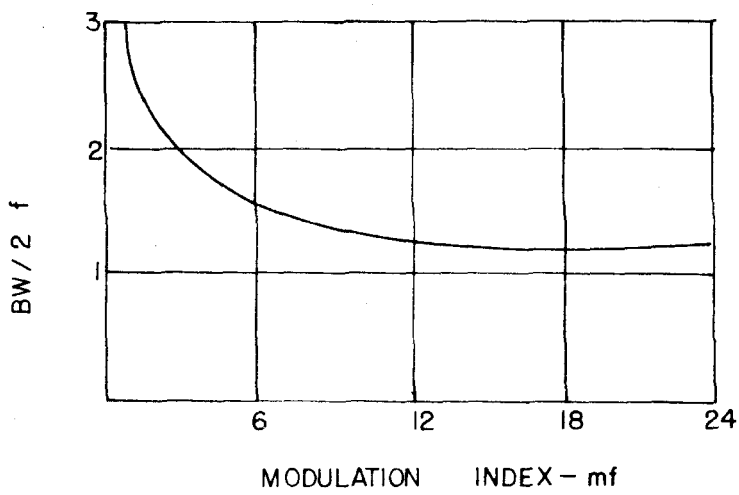

FIG. 30 VARIATION OF BW WITH mf

for large values of m_f, whereas for small values the BW becomes several times $2\Delta f$.

Having to reduce the transmitted frequency to the range 400 to 3000 c/s rather limits the functioning of the station. In the future it undoubtedly will be necessary to transmit frequencies as high as 50 kc/s. In practice the modulation index m_f is fixed at about 5; therefore from Figure 30 a BW of 800 kc/s would be required. If m_f was made equal to 1, the BW need be only 400 kc/s. The design problems would decide which modulation index to use.

The AN/FRC-6 operates with an m_f of about 5. Filters in the receiving circuit limit the response to 3000 c/s. This fact, of course, puts a limit on the frequency which is sent to the receiver for reference signal. A block diagram of the transmitter is shown in Figure 31. The actual type of modulation is phase, but proper filtering, together with the two quadruplers and the one doubler, convert phase modulation to frequency modulation. A console is a part of the AN/FRC-6 which can be used to control both the transmitter and the receiver. It was in the console that the modulating frequency was inserted (Cf. Ref. 13).

B. Receiving System

The block diagram of Figure 32 shows the function of the receiving station. The 50-kc/s signal is received by two receivers, one of which provides the phase measurement, and the other, the amplitude measurement. The AN/URM-6 Stoddart receiver on loan from the Navy Electronic Laboratory (San Diego) was designed to be a field-strength meter; thus except for the recorder it was complete in itself. On the other hand, the phase-measuring equipment had to be completely designed and built, except for VHF frequency-modulated receiver and the phase meter. By means of the

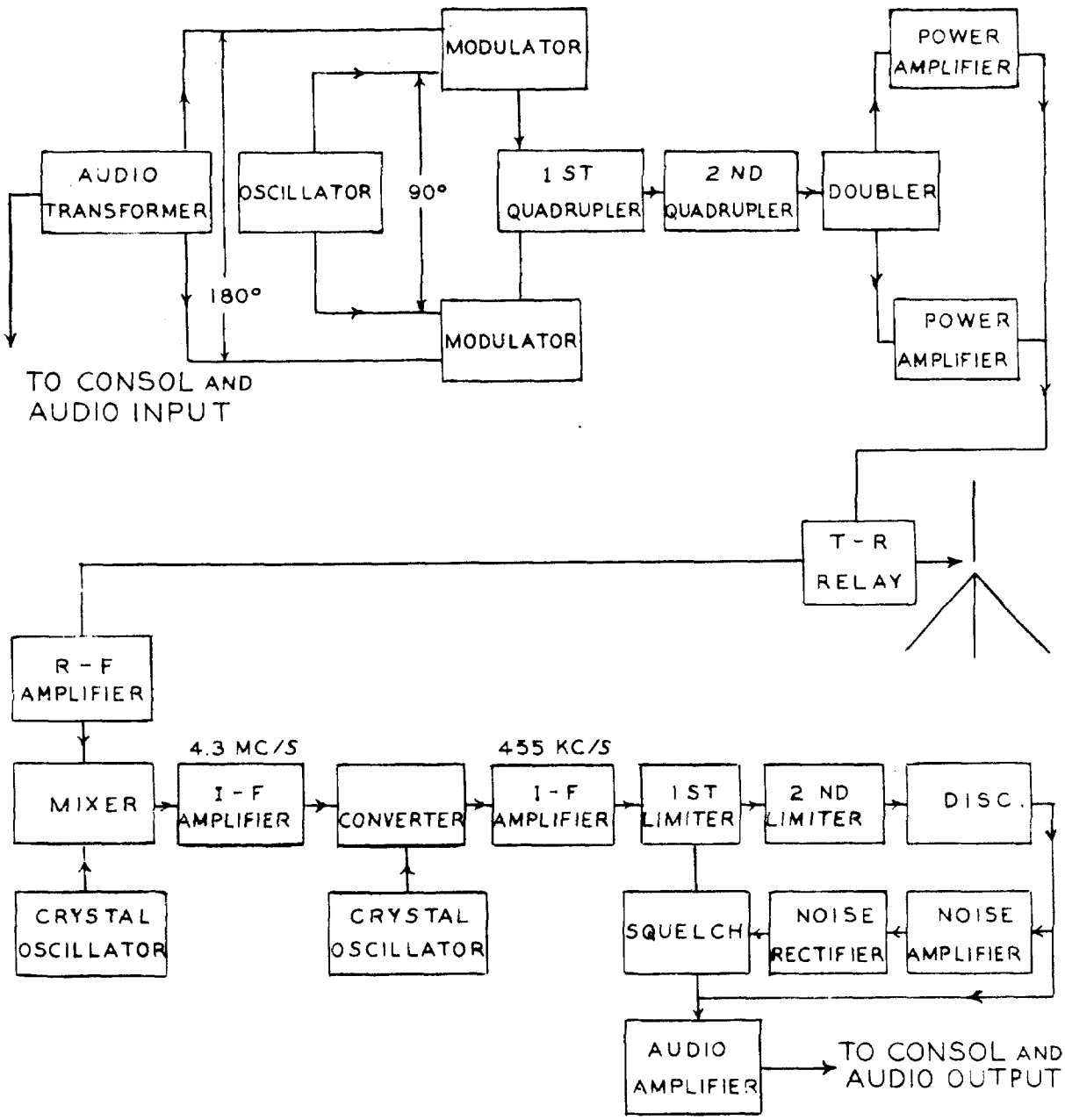

FIGURE 31 .

BLOCK DIAGRAM OF AN/FRC-6
30-Mc/s FM TRANSMITTER.

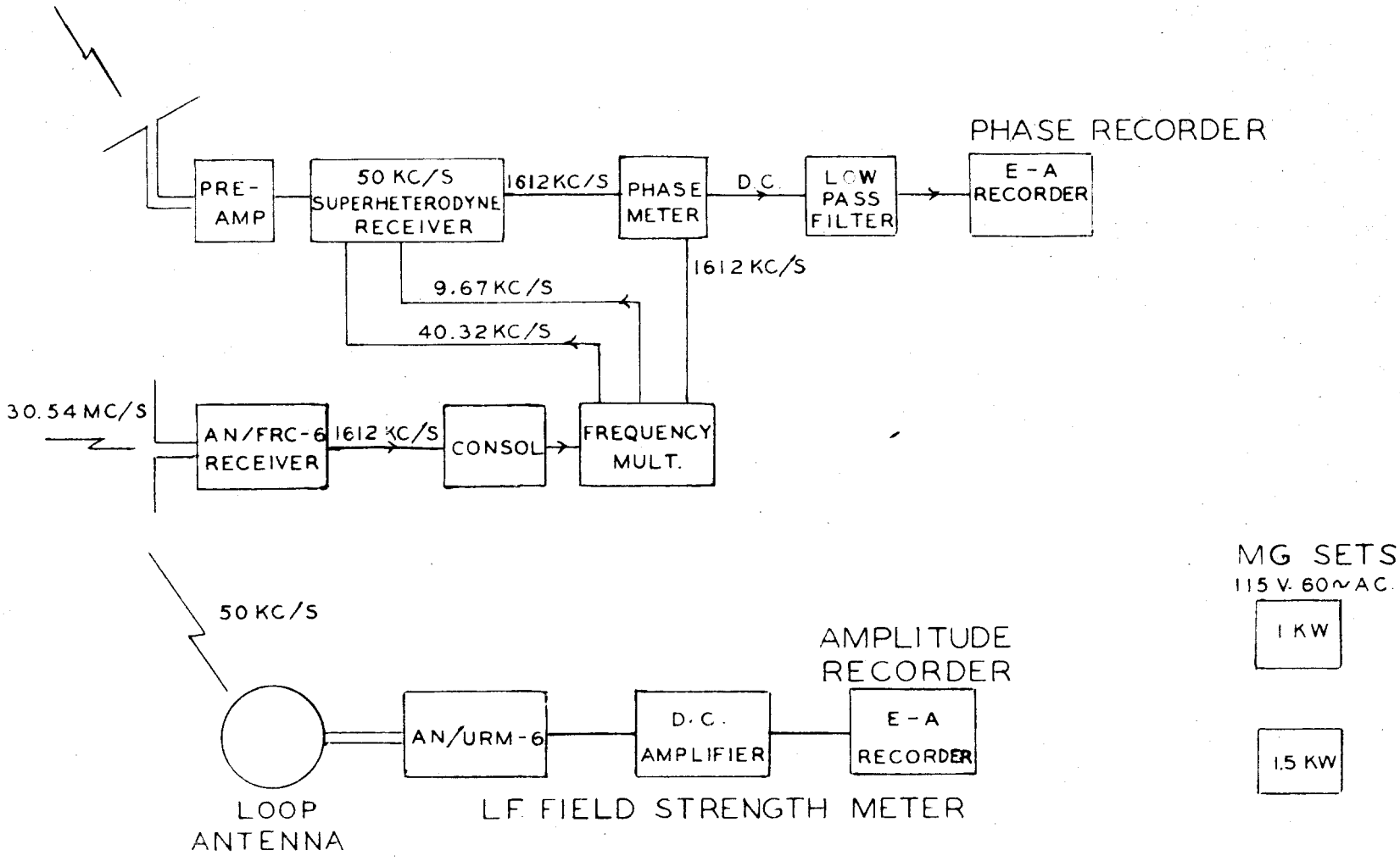

FIGURE 32

BLOCK DIAGRAM OF RECEIVING STATION

superheterodyning principle the 50-kc/s signal was reduced in frequency twice. The output of the receiver was then compared with the reference signal in the phase meter. In turn the output of the phase meter was recorded.

1. VHF frequency-modulated receiver. The AN/FRC-6 was used as a means of communication when the measurements were not being taken. The antenna used is described (Cf. Ref. 14) as an elevated, modified, ground-plane, wide-band antenna. The ground plane is at an angle of 143° with respect to the vertical. This feature helps to make the antenna match a greater range of frequencies and also "squashes" the radiation pattern down. It is estimated that the field strength at the receiver 40 miles away from, but line of sight to, the transmitting site was 1500 μvolts/meter. With this field strength the S/N ratio should have been, and was, excellent; it was measured at one time to be 30/1. As long as the S/N ratio is larger than 1, there is no doubt concerning the desirability of the FM system over the AM.

Goldman (Cf. Ref. 9) derives the equation for the noise reduction of an FM system over that of an AM system. The reduction factor r is given by

$$r_1 = \sqrt{3}\,\Delta f / BW_a \qquad (38)$$

for random noise and by

$$r_2 = 2.8\,\Delta f / BW_a \qquad (39)$$

for impulse noise. Here BW_a is the audio passband, and Δf is the maximum frequency deviation. For the case where m_f is 5, the noise-reduction factor is at least 8.

If there had been a choice for the frequency of the line-of-sight communication link, 30 mc/s would not have been chosen. Frequencies up to 100 mc/s propagate over long distances with the help of the F layer, and it is preferable that a frequency be chosen which is definitely limited to line-of-sight transmission. Although the work was being done in the desert, there was a great deal of interference at 30 mc/s which might have spoiled the measurement but fortunately did not.

The block diagram of the FM receiver is shown in Figure 31. It is a double-conversion receiver with a first IF frequency of 4.3 mc/s and a second IF frequency of 455 kc/s. The local oscillators are crystal-controlled. This factor is just as important as having the initial carrier frequency crystal-controlled, since drift in the local oscillator would appear as a drift in the carrier frequency. The output of the receiver during the experimental test is the 1612 c/s originating at the transmitter. This frequency is fed into the console control unit and thence into the frequency-multiplying circuit.

2. Frequency multiplier. The function of the frequency multiplier (circuit diagram in Fig. 33) is to generate from the 1612 c/s the 50 kc/s and the two local oscillator frequencies which are the twenty-fifth and the seventh harmonics of 1612 c/s. This function is accomplished by clipping the input sine wave and obtaining a square wave whose voltage can be described by

$$v = \frac{4}{\pi} E\left(\cos x - \frac{1}{3}\cos 3x + \frac{1}{5}\cos 5x - \frac{1}{7}\cos 7x + \cdots\right) \qquad (40)$$

which is seen to contain all the wanted odd harmonics of the fundamental frequency. Some care must be taken in designing the squaring circuit to make sure that the resulting waveform is symmetrical. Such an

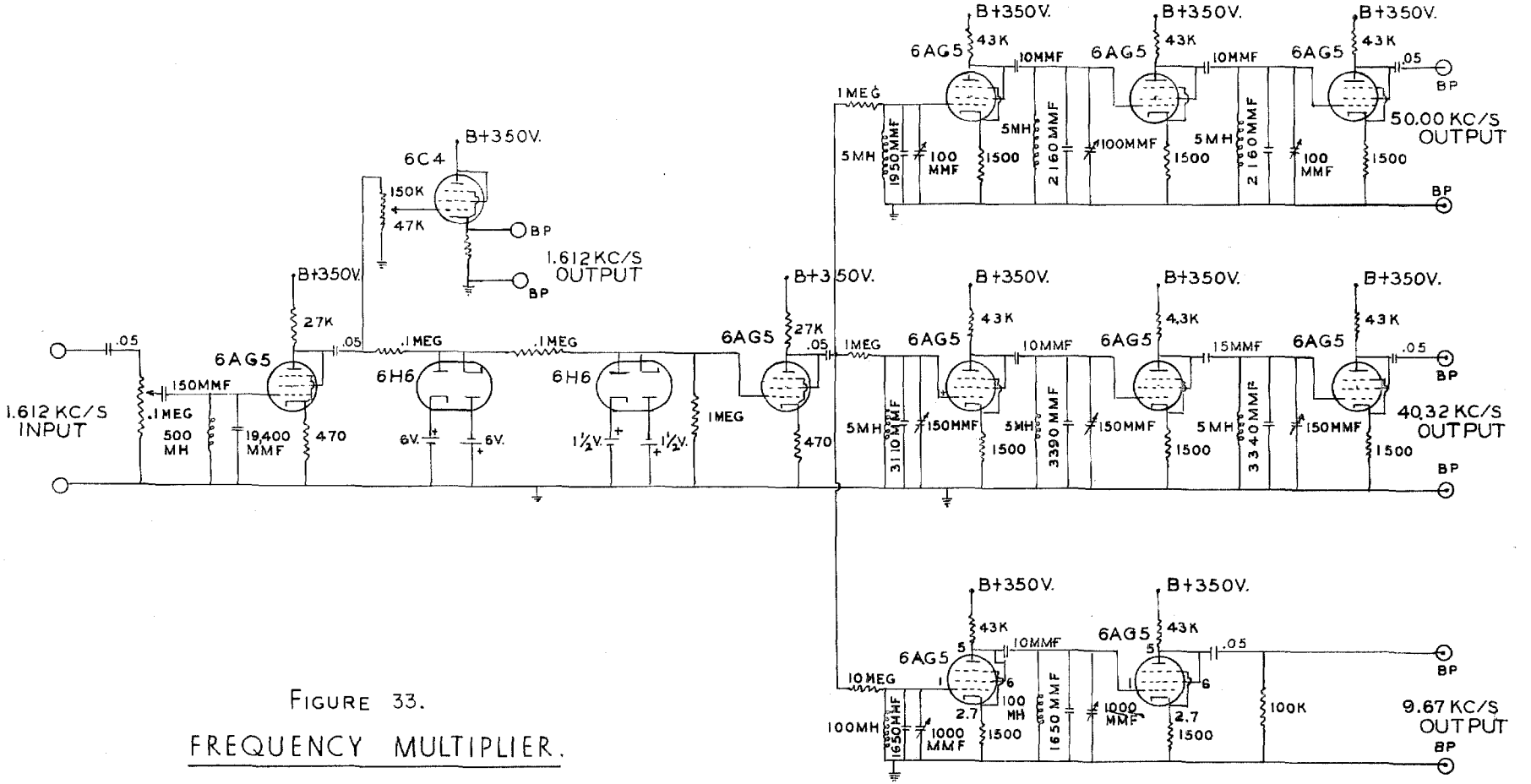

FIGURE 33.

FREQUENCY MULTIPLIER.

unsymmetrical waveform is shown in Figure 27b. The voltage v' of this waveform can be expanded into

$$v' = \frac{4}{\pi} E\left(\frac{2k-1}{4}\pi + \sin k\pi \cos x + \frac{1}{2}\sin 2\pi k \cos 2x + \cdots\right) \qquad (41)$$

which reverts to Equation (40) when k = $\frac{1}{2}$. In many squaring circuits the k of Equation (41) is actually a function of the voltage input. As k changes, one finds that the harmonic content changes. For example, if one wishes to extract the thirty-first harmonic of Equation (41) but k has a value of 15/31 or 16/32, there will be no thirty-first harmonic present to extract. Thus for a change in k of only 3.2 per cent the harmonic content goes from a maximum to zero. A circuit was actually built such that k was so sensitive to the changes of input voltage that it had to be discarded.

The block diagram of the multiplier is shown in Figure 34. Even with the very good S/N ratio obtained from the FM receiver, there remained with the reference signal sufficient noise to upset the desired operation of the multiplier. Whereas the BW of the receiver was about 3000 c/s, the bandwidth of the filter was about 30 c/s; therefore the S/N ratio was increased by a factor of 10 to a value of 300. The filter was followed by an amplifier whose function was to increase the voltage to above 50 volts rms. A clipping reference voltage of $1\frac{1}{2}$ volts working against the 50-volt input produces a well-shaped square wave. The cathode follower output makes available an isolated 1612-c/s source for the reference signal to be used with the phase meter. The voltage output is monitored in order to assure the operators that the linear limits of the amplifier are not exceeded. The clipping takes place in two stages. It was found that, if clipping was done in one

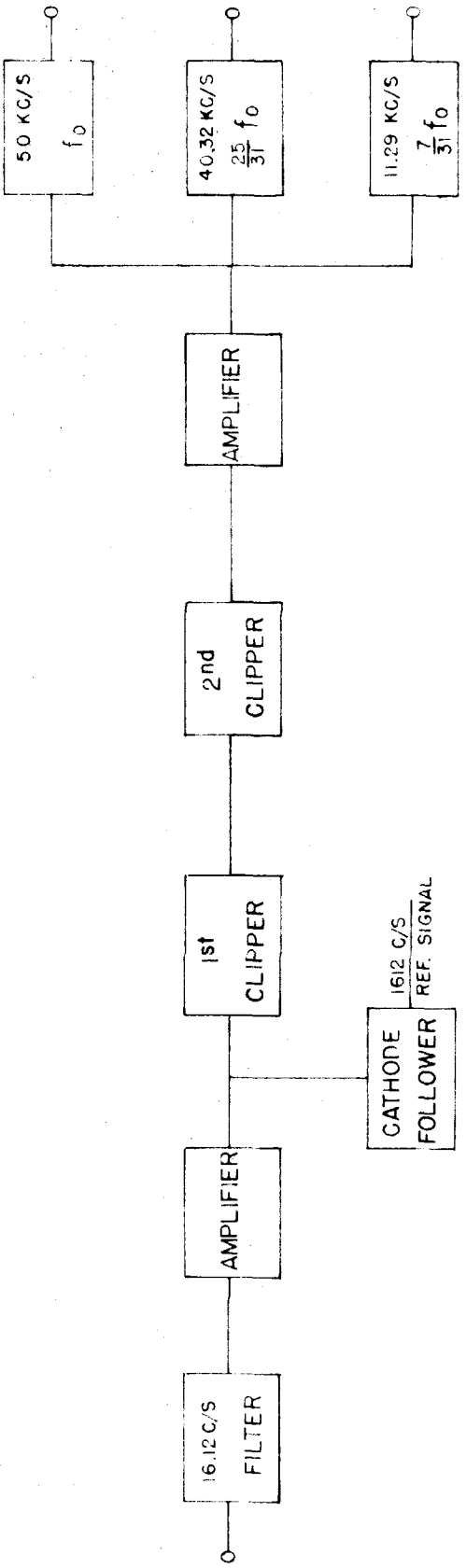

FIGURE 34 BLOCK DIAGRAM OF MULTIPLIER

stage, the resultant waveform was not suitable. Therefore the clipping was done first at the 6-volt level and then at the 1½-volt level.

It is of interest to discuss the filtering necessary to obtain, for example, the thirty-first harmonic. There are three filtering sections similar to the one described in Section III-A-3. The envelope of the waveform at the output of the first filter section is shown in Figure 35. One would expect this waveform if a tuned circuit received a burst of energy every 1/3,200 second. The Q of the tuned circuit determines the rate of decay. This waveform can also be regarded as an amplitude-modulated wave where the carrier is the 50 kc/s and the side bands are frequencies separated from the carrier by all the harmonics of 1612 c/s. The remaining filtering in the network must be sufficient to eliminate all the side bands. The specifications for complete filtering are thus no different from those requiring that the filter separate the thirty-first harmonic from the twenty-ninth and thirty-third harmonics. However, this discussion gives an insight into the type of waveform to be expected from incomplete filtering.

It was necessary to use three stages of filtering for the twenty-fifth and the thirty-first harmonics, but only two stages were needed to extract the seventh harmonic. The voltage output of the seventh and twenty-fifth harmonics was fed directly into the superheterodyne receiver. The 50-kc/s output was used to tune up the superheterodyne receiver. The author would like to point out how vitally important this was. The superheterodyne receiver has such an extremely narrow band that lining it up would have been virtually impossible without having the exact input frequency available. The 50-kc/s filtering section must be entirely incapacitated to avoid feeding this signal

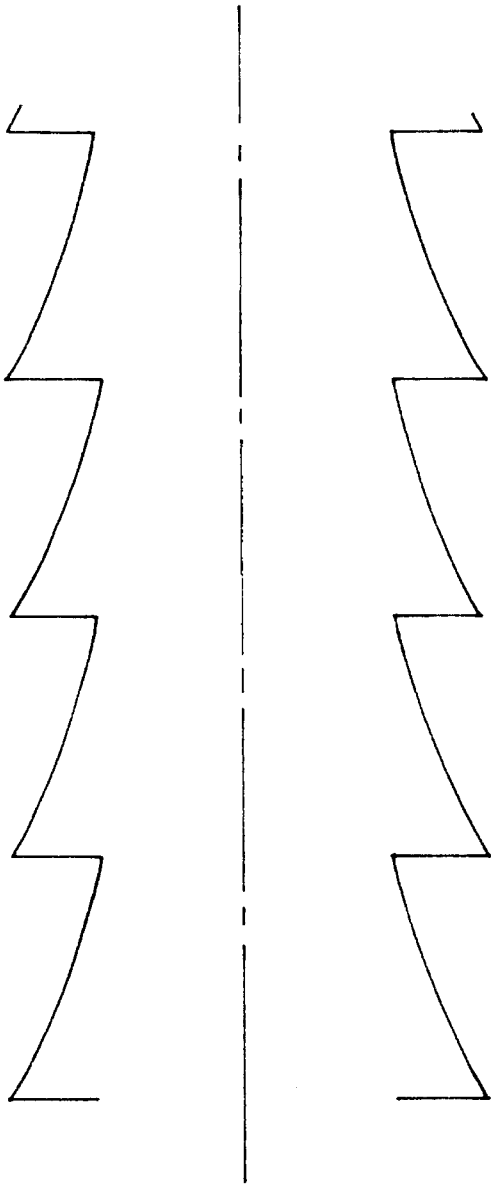

FIGURE 35

ENVELOPE OF FILTERED SQUARE-WAVE

back into the antenna during periods of operation.

3. Receiving antenna at 50 kc/s. The receiving-antenna system was a problem in itself, but through the process of elimination a suitable one was developed. The two types having the desired characteristics are the loop and the dipole since each can be used to discriminate between polarizations of a down-coming wave. The field pattern of the loop is well known, and the theory of the dipole is discussed in Appendix A. The loop antenna was used with the Stoddart receiver for field-strength measurements, and the dipole antenna was used with the phase-measuring receiver. The following discussion is directly applied to the dipole antenna but with a few obvious differences is directly applicable to the loop antenna.

Consider the dipole of Figure 36a lying on the plane earth. For all practical purposes it has two separate fields (Cf. Appendix A). One is that which can be calculated by merely considering reflection from the plane earth; the other is that which gives rise to the ground wave. The field pattern in the yz plane is shown in Figure 37, and the pattern in Figure 38, in the xy plane.

The pattern of Figure 37 has maximum sensitivity in the vertical direction and is responsible for receiving the reflected wave. The pattern of Figure 38 has the shape of a quadrupole field and is responsible for picking up the vertically polarized atmospheric noise which comes in as a ground wave or at large angles of incidence. Noise actually comes in from all directions but is more concentrated near the horizon. The over-all effect of the dipole field pattern is very similar to that of the loop antenna field. However, the dipole tends to emphasize the directivity toward the vertical and is somewhat superior

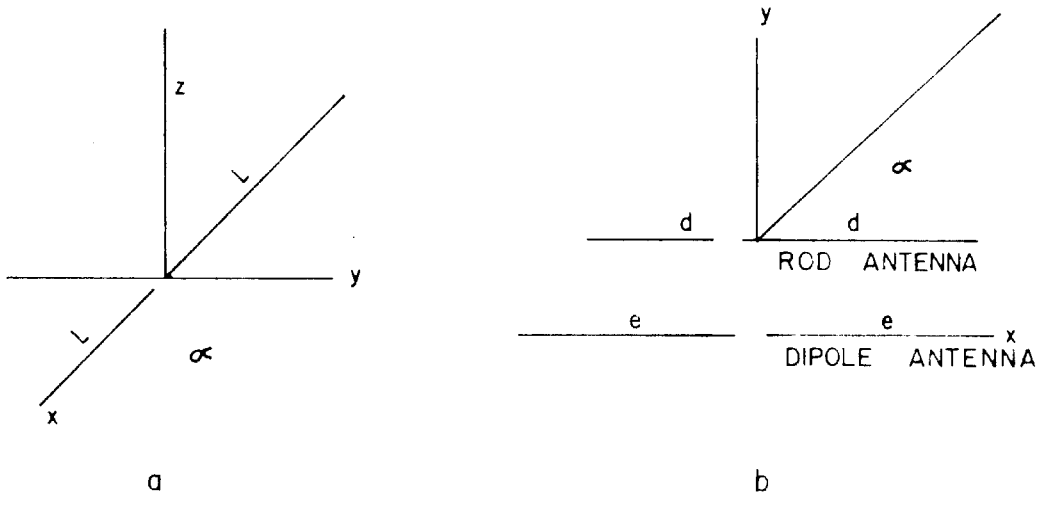

FIG 36 DIPOLE ANTENNA COORDINATE SYSTEM

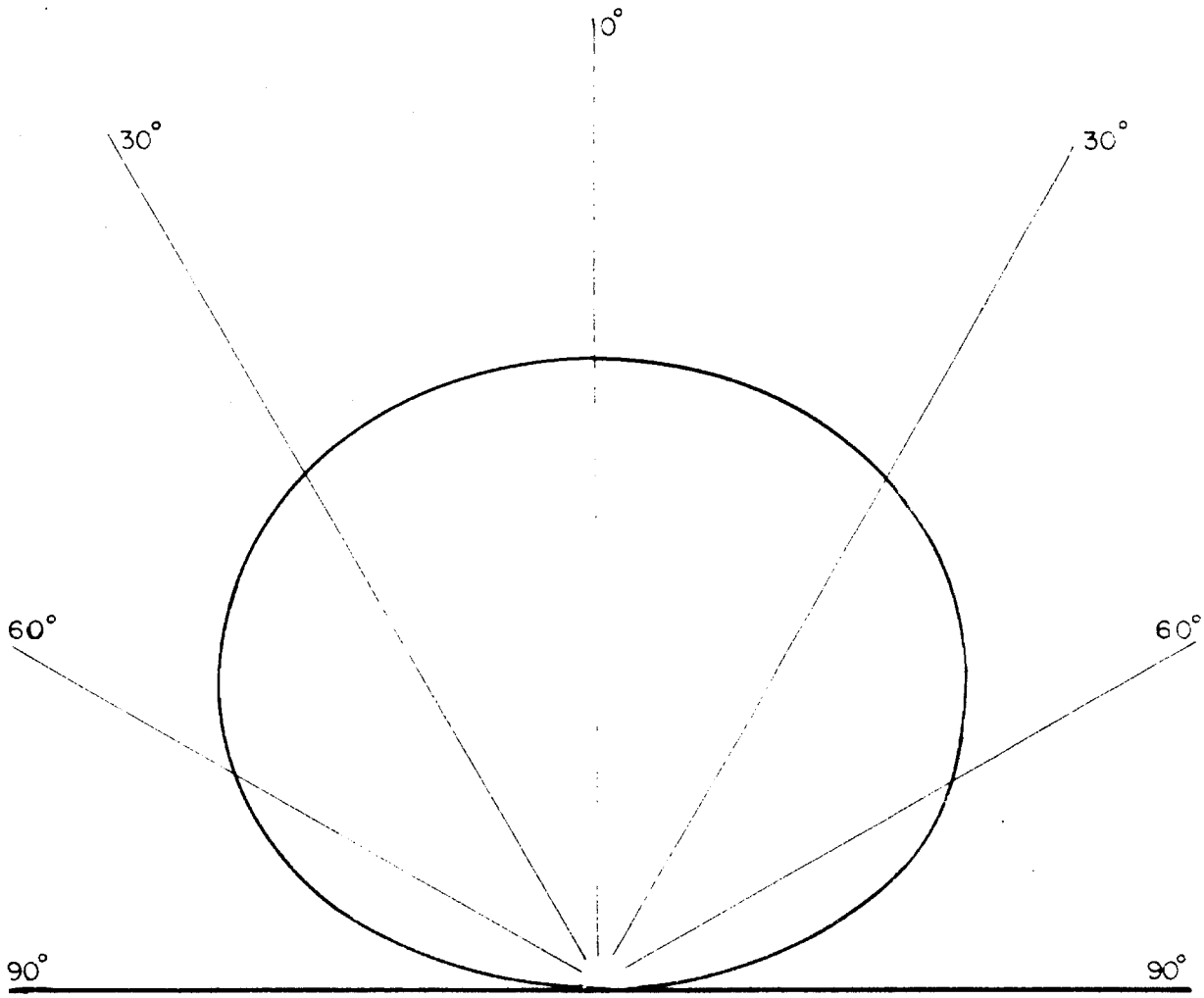

FIGURE 37 FIELD PATTERN IN THE PLANE NORMAL TO THE LENGTH OF THE DIPOLE

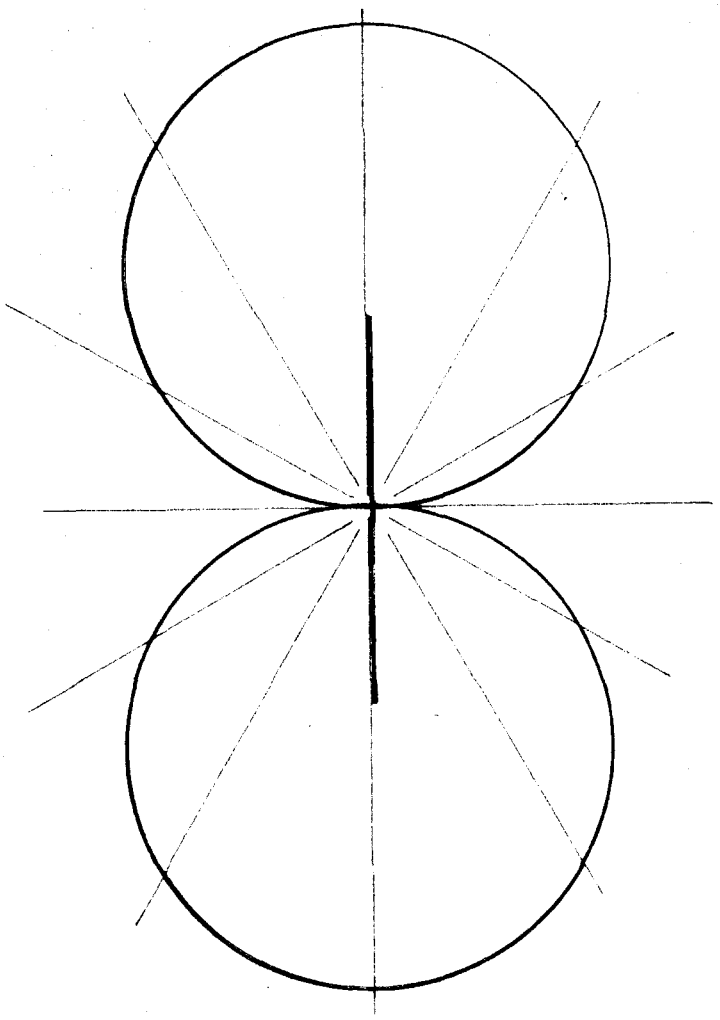

FIGURE 38 GROUND WAVE PATTERN OF A HORIZONTAL DIPOLE OVER THE EARTH

to the loop antenna for over-all S/N ratio.

The dipole and the loop are double-ended antennas which must be perfectly balanced if they are to have the theoretical characteristics. Essentially the ground waves are canceled in passing over the dipole leaving only the quadrupole effect. This balance is extremely critical for optimum operation of the dipole. The balance is a function of the length of the antenna and the distributed capacity to ground over the length of the dipole. It is also dependent upon the input stage of the receiver. Stanford University (Cf. pp. 8-15 of Ref. 10) used the horizontal dipole in work on the ionosphere at 100 kc/s and found that, by changing the angle of the dipole with respect to the horizon by only a few degrees, the antenna could effectively cancel out completely any one given ground wave.

The receiving dipole used was about 150 feet long; at 50 kc/s it is still an elementary dipole having a very highly capacitive reactance which is easily unbalanced. Two such antennas were placed at a right angle to each another so that one was along the line of sight to the receiver. Thus the relative polarization of the down-coming wave can be determined. In the case where the receiving site is at a right angle to the transmitting antenna, there is no interference from the 50-kc/s ground wave. However, in the over-all plan of the ionospheric research project, it was proposed that a receiving site be located off the end of the transmitting antenna; thus there would be a reasonably strong ground wave. Under such condition the receiving antenna normal to the line of sight would not be affected, but the dipole along the line of sight would pick up the ground wave. By manipulating the angle of the dipole slightly, the ground wave can be canceled out.

Cancellation can be obtained in another manner which was first conceived in an attempt to minimize the noise input to the receiver. This method involved the simulation of the dipole's quadrupole pattern in the horizontal plane. This simulation was done by using two modified ground-plane vertical antennas placed on a line parallel to the dipole (Cf. Fig. 36b) and fed by two equal lengths of coaxial cable. If V_1 is the voltage picked up by only one vertical antenna, the voltage V picked up by the combined vertical antenna is

$$V = V_1 (4\pi d/\lambda) \cos\alpha \qquad (42)$$

where d and α are defined in Figure 36b. The dipole pattern in the horizontal plane is also proportional to $\cos\alpha$. Therefore, if the ground-wave signal to the vertical antennas and to the dipole is mixed properly, the resultant voltages should tend to cancel. In the same manner, noise which comes into the antenna from all directions also tends to cancel. The noise cancellation is somewhat more difficult to achieve than is signal cancellation. This difficulty is discussed in Section III-B-4.

4. Receiver pre-amplifier. Almost all receivers designed for low and very low frequencies are single-ended, whereas the antennas used are double-ended. A pre-amplifier was built which consists of two double-ended to single-ended converters, one for the dipole and one for the two vertical antennas. The signal output of these two stages in turn can be subtracted in a third differential amplifier. As can be seen in Figure 39, the pre-amplifier consists of three identical amplifier sections.

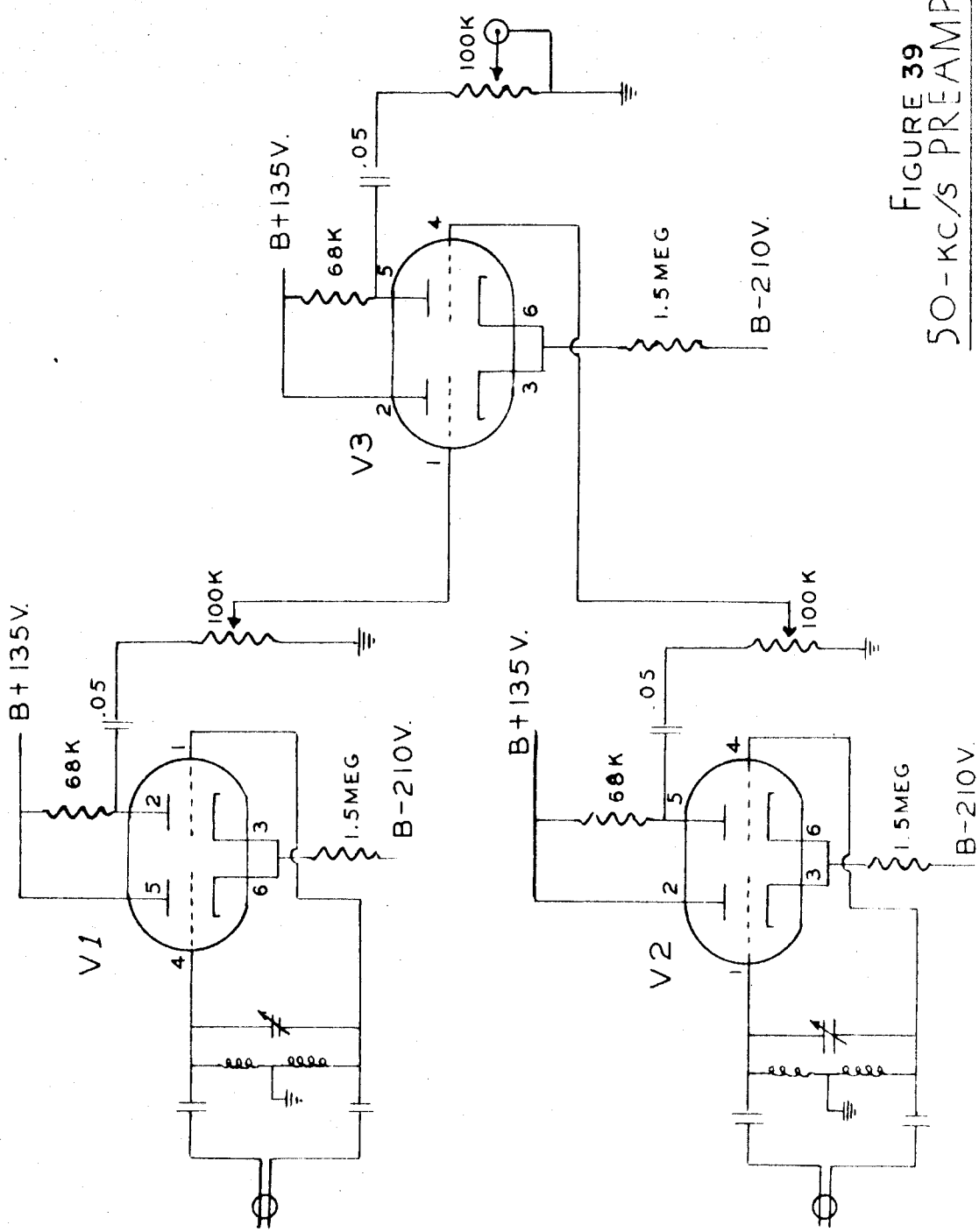

FIGURE 39
50-KC/S PREAMPLIFIER.

The differential amplifier actually subtracts the two voltages which appear at the grids of the two sections of the tube. One section operates as a cathode follower so that the cathode potential follows the grid voltage. The second section then amplifies the difference between the second grid and the cathode, which difference is the same as that between the second grid and the first grid. If these voltages are alike but 180° out of phase, the gain of the differential amplifier is approximately twice the gain of the amplifier stage.

The antenna system consisting of two vertical antennas and the dipole was set up so that each had maximum directivity toward a San Diego low-frequency station; it was found that by mixing the outputs of the two stages a reduction of 30 db in signal strength could be obtained. This is one way of nulling out an undesirable signal. However, the original idea of the antenna was to use it as a noise-cancelling device. It was found that the over-all noise could be reduced by a factor of 2 without affecting the level of the down-coming reflected wave. This fact verifies the assumption that a large portion of the noise entering the system with only the dipole used is part of the ground wave. The reduction by a factor of 2 in noise voltage is quite a sizable gain inasmuch as a gain of 2 in the S/N ratio at the receiver is equivalent to increasing the power output at the transmitter by a factor of 4. A still more valuable characteristic of the antenna (which is rather due to the nature of the noise) is that the pulses of noise which could cause the output voltage to fluctuate several hundred per cent are canceled out to the point where the output fluctuations are only 10 to 20 per cent.

It must be remembered that the peak output amplitude due to a received impulse is proportional to BW, whereas that due to received random noise is proportional to $\sqrt{BW}$. Also, as was pointed out in Section II-A, the duration of the response to the pulse is proportional to BW. Thus it is extremely desirable to reduce the magnitude and number of impulses that the receiver will have to handle. This final antenna system was not used in the actual measurement because it was not needed in the 50-kc/s system. The fact that the noise-cancelling system was successfully operated will probably allow future work to be carried on at lower frequencies where the atmospheric noise level is greatly increased.

The pre-amplifier was designed to operate in the field on batteries so that it could be placed at the antenna terminals. It serves to isolate the antenna from the rest of the system, has a gain of 40 db, and can be tuned from 15 to 100 kc/s with proper selection of toroids. The pre-amplifier has a Q of 50; thus at 50 kc/s it has an over-all bandwidth of about 1000 c/s.

5. Low-frequency double superheterodyne receiver. The importance of the receiver should not be underestimated, and its characteristics should be understood thoroughly. There are several factors which limit the usefulness of a receiver; for example, (1) the noise figure of the input stages, (2) the nature of the noise that enters the receiver, (3) the limitation of gain with a specified bandwidth, (4) limitations which involve the possibility of oscillation with a high gain, and (5) temperature stability required on L, C, and R components as well as on electron tubes, crystals, etc.

The noise figure of a receiver is a figure of merit. It is the ratio of the total noise power in the input stages per unit bandwidth

to the noise power of the resistance in the input network. The noise figure of the receiver is largely a function of the tube noise of the input stage; thus it is necessary to minimize this noise. Low plate voltage and plate current are the usual criteria in the design. If the gain of the first stage is sufficient, the noise contributed by the second is negligible. The noise voltage referred to the grid of the first stage for a BW of 100 c/s may be as high as 10 μvolts, but a properly designed input stage should have less than 1 μvolts of tube noise. In some receivers it is extremely important that the noise figures be kept as close to optimum as possible. For our purpose we find that, by lengthening the receiving antenna, the atmospheric noise overrides the receiver noise of a moderately well-designed first stage and thus becomes the limiting factor of the receiver.

Noise is the one factor that has been considered a necessary evil throughout the entire system. Essentially it is the one limitation that made the work on this project so very difficult. Noise forced the experimenters to maximize the power output of the transmitter and to limit the bandwidth of the receiving equipment to as small a value as possible. Noise in the low- and very-low frequency range is due largely to thunderstorms taking place all over the earth. The spectrum of a storm has a maximum value near 10 kc/s. This noise has the characterics of random noise with superimposed bursts occurring at rather close intervals. The noise level at any one time is dependent upon the number of thunderstorms going on in the world, the closest ones naturally having the greatest effect. Let us point out once more that the magnitude of disturbance at the output of the receiver is in proportion to $(BW)^{\frac{1}{2}}$ for random noise and to BW for impulse noise. Also for

impulse noise the length of the disturbance at the output of the receiver is proportional to Q. Here we have the equivalent of two opposing requirements. In order to reduce the magnitude of the impulse noise, the BW must be reduced; as a result the Q of the receiver must increase. But as Q increases, the duration of the disturbance due to pulses increases. This noise problem has already been discussed in Section III-B-3 and 4. First, the dipole discriminated somewhat against the ground-wave noise. Next, the noise-cancelling antenna system cut the impulse noise down and reduced the random-noise level. The reduction of the impulse noise was most important because of the difficulty involved in reducing its effect on the receiver output.

The atmospheric noise is considered as being composed of background noise whose average value is relatively constant and the impulse noise which occurs intermittently and has peak amplitude several times the amplitude of background noise. In order to function the receiver must first be able to detect the signal in the presence of the background noise. The signal we are trying to receive has a fixed frequency; thus its spectrum is a delta function at 50 kc/s. The spectrum of the noise may be considered uniformly distributed over the frequency range near 50 kc/s. It is found that, with a bandwidth of 350 c/s at 50 kc/s, the field strength of the noise picked up varies from 5 μvolts/meter or less in the winter to about 30 μvolts/meter in the summer nighttime. The question now arises as to what must be the field strength of the signal in order that the signal can be picked out of the noise. It is possible to detect the presence of a signal in the noise with S/N ratios down to -6db. Whether or not a signal exists cannot be determined if the field strength is less than half the magnitude of the atmospheric noise.

In general, if the spectra of the signal and of the noise are known, it is possible to design an optimum filter for the signal. This design would involve specifying a frequency response which (1) attenuates in that portion of the band where the S/N ratio is poor and (2) amplifies in the portion where the S/N ratio is good. For a complicated signal this is a complicated procedure. However, if there is signal power at only one frequency, the optimum filter is easily specified; namely, it must have infinite attenuation at all frequencies except 50 kc/s. This specification is not physically possible, but the filter should have a narrow enough band to obtain a reasonable S/N ratio. The 50-kc/s signal strength has no lower limit and may be as high at 75 μvolts/meter under optimum conditions. Therefore the receiver should be designed with as narrow a band as practical. For example, it is assumed that a receiver has a bandwidth of 360 c/s. To increase the S/N ratio by a factor of 6, the BW would have to be reduced to 10 c/s. To obtain the corresponding increase in S/N ratio by increasing the power transmitted would require 36 times the power. It is much simpler and less costly to improve the receiver than to increase the power output of the transmitter.

If one can reduce the BW as much as he pleases, a lower limit must be specified. So far as is known now, the type of disturbance that we want to detect would easily pass through a circuit whose bandwidth was 1/30 c/s. If this bandwidth could be obtained, then the S/N factor would be further reduced by a factor of 16 for a total of 100 reduction of the original S/N ratio at 350-c/s BW. Though this is speculation, it brings out the importance of noise and ways of discriminating against it.

The block diagram of Figure 40 shows the special-purpose receiver that was designed and built to operate at 50 kc/s. The receiver has two stages of superheterodyne in order to attain a final bandwidth of almost 30 c/s at the 1612 c/s second IF frequency. The 50-kc/s input is mixed with 40,322.58 c/s, which is the twenty-fifth harmonic of the 1612 c/s transmitted over the FM link. The resulting first IF frequency is 9,677.42 c/s. This frequency in turn is mixed with 11,290.32 c/s, which is the seventh harmonic of the 1612.90 c/s; the resulting IF frequency is 1612 c/s, which we note is the same frequency (as it must be) as that modulating the FM transmitter.

The converter can be considered as a device which multiplies its two input signals. Thus if f_o is the carrier frequency and f_1 is equivalent to the local oscillator frequency, their product is

$$\sin(2\pi f_o + \phi)\sin(2\pi f_1 + \alpha) \qquad (43)$$

It contains two frequency components, one the sum of f_o and f_1 and the other their difference. A filter is used to separate out the difference of the two frequencies. In this process the particular phase of each voltage is carried along (Cf. Appendix E), and since we desire to measure phase, this characteristic is very important. If f_o and f_1 are derived from independent sources, then as the source frequency varies, the measured phase varies also. It is desired that f_o and f_1 be derived from the same source, and for this reason it was necessary to transmit the reference signal to the receiving site in such a way that the frequency relationships could be determined.

One might ask why there are two stages of IF instead of one. In answer let us explain why a straight amplifier at 50 kc/s was not used.

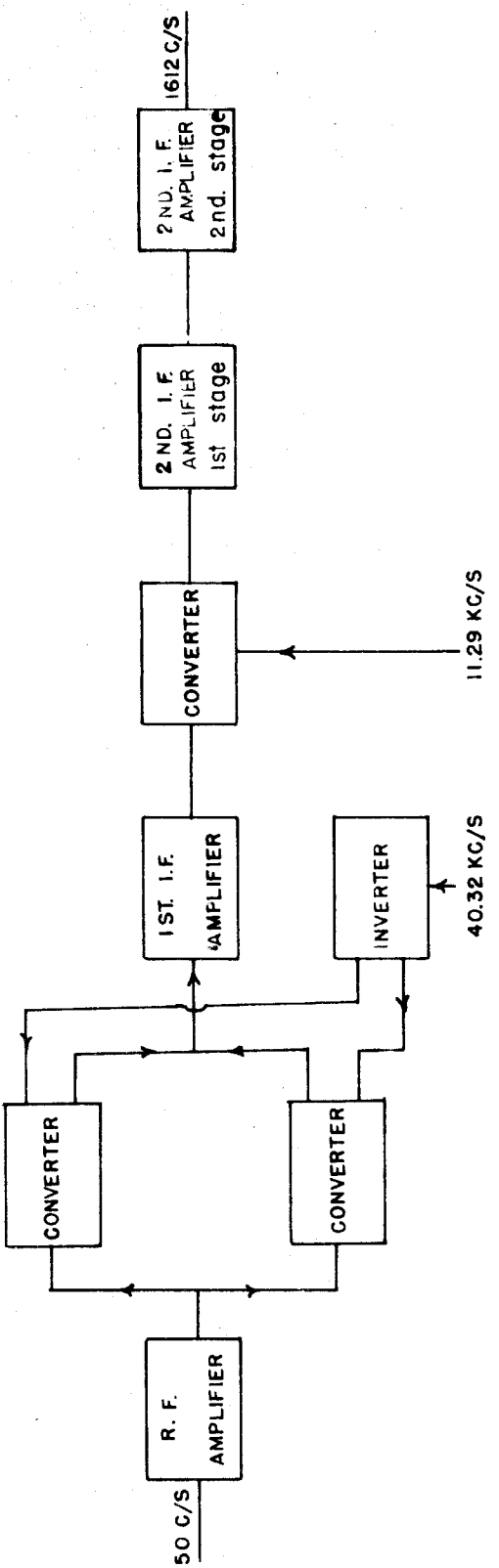

FIGURE 40 BLOCK DIAGRAM 50KC/S RECEIVER

If a straight amplifier were used, then at some point in the receiver the voltage level would be such that it would be almost impossible, without using very special shielding techniques, to prevent some of the signal from feeding back into the antenna. Also the reference signal for the phase measurement would be present at high level, and care would have to be taken to assure that it did not feed back into the antenna and appear as a signal at the output of the receiver. If the local oscillator frequency is chosen too close to the carrier, the input circuit may become overloaded by this voltage, and the converter may not function properly. The author used as the criterion that each IF frequency should be not less than one-tenth the previous IF or carrier frequency as the case might be.

The superheterodyne has other advantages, the main one being the virtual impossibility that it may oscillate since the amplification is accomplished in steps at the various frequencies. One characteristic of the frequency chosen that could cause trouble is that the second IF frequency and the reference signal are the same and could interfere with one another. However, not much gain is required in the receiver at 1600 c/s, and the input to the 1600 c/s amplifier is well shielded. In the frequency range of 1000 to 200,000 c/s it is quite easy to obtain toroids for use in tuned circuits which have Q values of over 100. Since the bandwidth of a circuit tuned to frequency f is f/Q, a bandwidth of 30 c/s is easier to obtain at 1600 c/s, where the effective Q need be only 50, than at 50 kc/s, where the effective Q would have to be 1600.

The circuit of the superheterodyne receiver (Cf. Fig. 41) is straightforward save for the first mixer section. An extension of a

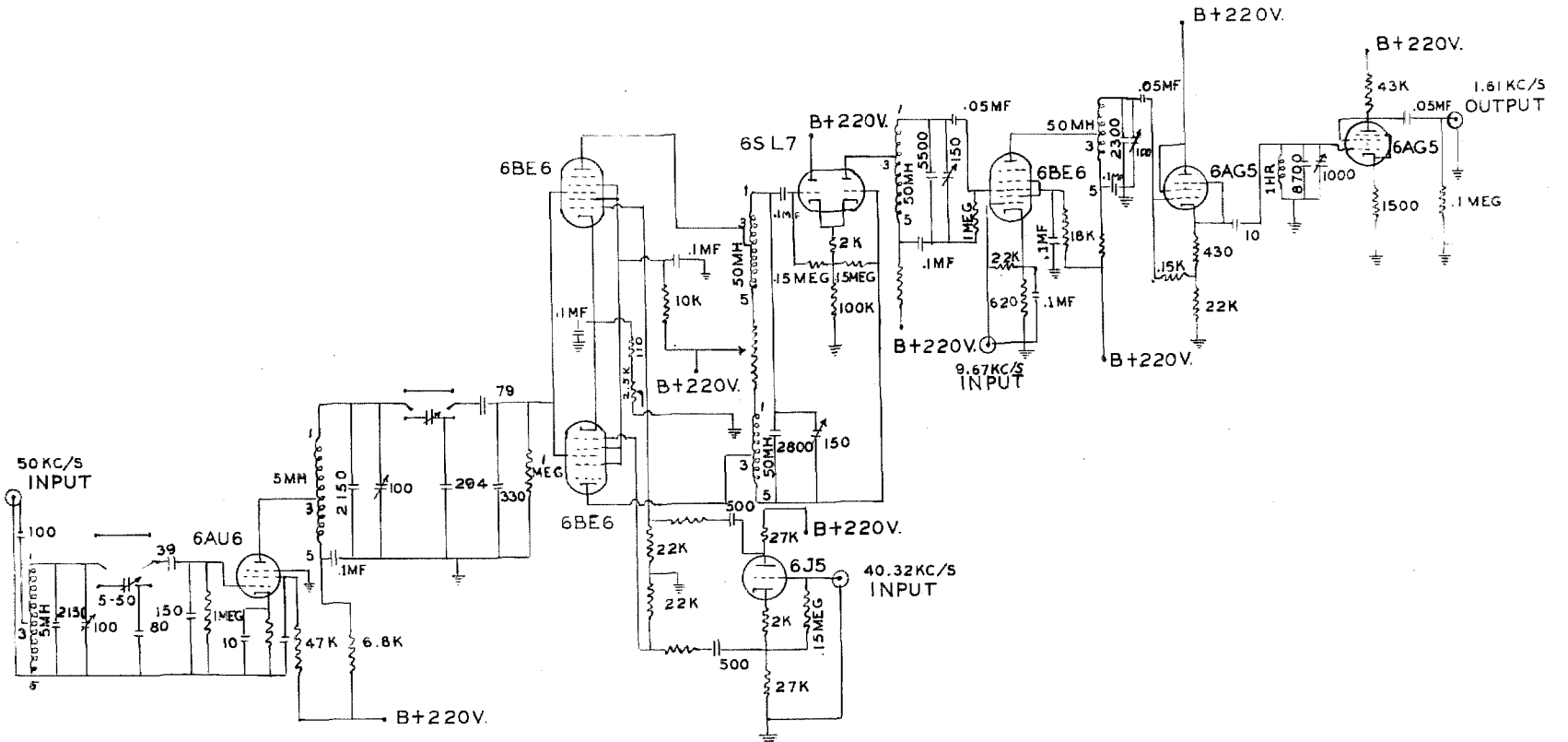

FIGURE 41

50-KC/S SUPERHETERODYNE RECEIVER.

technique used by Paul Thiene (Cf. Ref. 15) at D.C. frequencies is applied. The converter operates in a push-pull fashion. The signal grids are driven in phase with one another, and the local oscillator grids are driven 180° out of phase. The output is thus double-ended, and this output in turn is converted to single-ended by a differential amplifier. When a pulse of noise comes in, however, it is confronted with what looks like a push-push arrangement, and there is a tendency for the pulse to be cancelled in the circuit. This is an attempt to reduce further the effect of impulsive noise.

6. Phase-measuring equipment. The output of the receiver is 1612 c/s, and the output of the FM transmitter is likewise 1612 c/s. Since the phase of the receiver output varies exactly as the phase of the reflected wave, it is only necessary to compare the two signals and record the changes in phase angles between them. This comparison was made by using a phase meter (Type 320) made by Technology Instrument Corporation (Cf. Ref. 16). The inputs to the phase meter are labeled A and B. If the receiver output is put into A, the meter reads directly the number of degrees by which the receiver output leads the reference signal. Electronically the meter measures the time difference between the zero crossings of the signal A and the zero crossings of signal B, this difference being proportional to the phase difference. Signal A consists of the 1612-c/s signal plus noise. The position of the zero crossings varies at a rate of 30 c/s (the BW of the receiver), and the amplitude in degrees of this variation depends on the S/N ratio of the receiver output. The output of the phase meter can be, and is, filtered. But this filtering is good only so long as the phase meter does not become confused when operating near 0 or 360°; at that time the noise

causes large fluctuations in phase, and control is lost. There is a saving factor in that the phase meter can be switched so that 180° is added to the reference signal. This switching helps as long as the S/N ratio is not too poor coming out of the superheterodyne receiver.

The problems involved in filtering the phase meter output is not the conventional type. As long as the noise does not cause the phase meter to read 0° at one instant and -360° the next, filtering can be done by the conventional techniques, and very narrow bandwidth can be obtained. However, the S/N ratio determines how near to 0 or 360° the meter may be operated properly, and there will be values of S/N that will prevent use of the phase meter entirely. Under these conditions the receiver-output S/N ratio must be further improved.

The output of the phase meter provides for the use of a recorder. The recorder was an Esterline-Angus, 5-mil movement with a nominal 400-ohm impedance. The recorder circuit (Cf. Fig. 42) included a filter having a transfer function of $0.445/(1 + jf\ 0.755)$, which had a bandwidth of about 1.3 c/s (Cf. Fig. 43).

Thus we reach the finish of the discussion of the phase-measuring equipment that was used the nights of October 28 and 29, 1952, to record changes in the height of the reflecting layers as a function of time.

As early as September, 1951, a product detector very similar to that shown in Figure 44 was breadboarded and shown to be very satisfactory. The acquirement of the phase meter precluded the completion of a recordable product detector. This circuit, also known as a ring demodulator, operates on the same principle as the mixer in the superheterodyne receiver (Cf. Appendix E). The only difference is that the test signal and the reference signal are of the same frequency, and

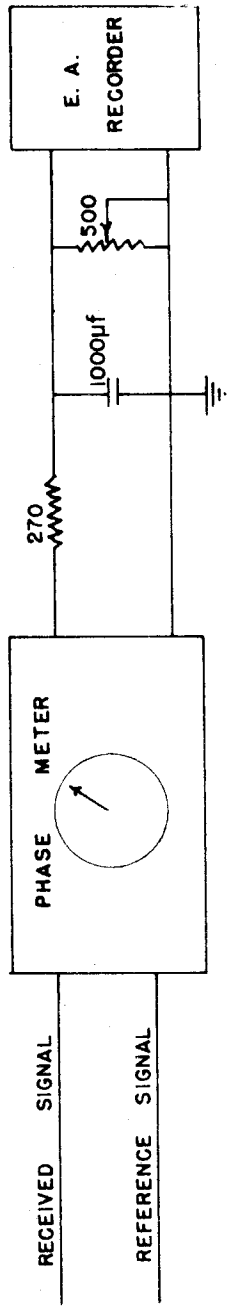

FIGURE 42 PHASE RECORDING CIRCUIT

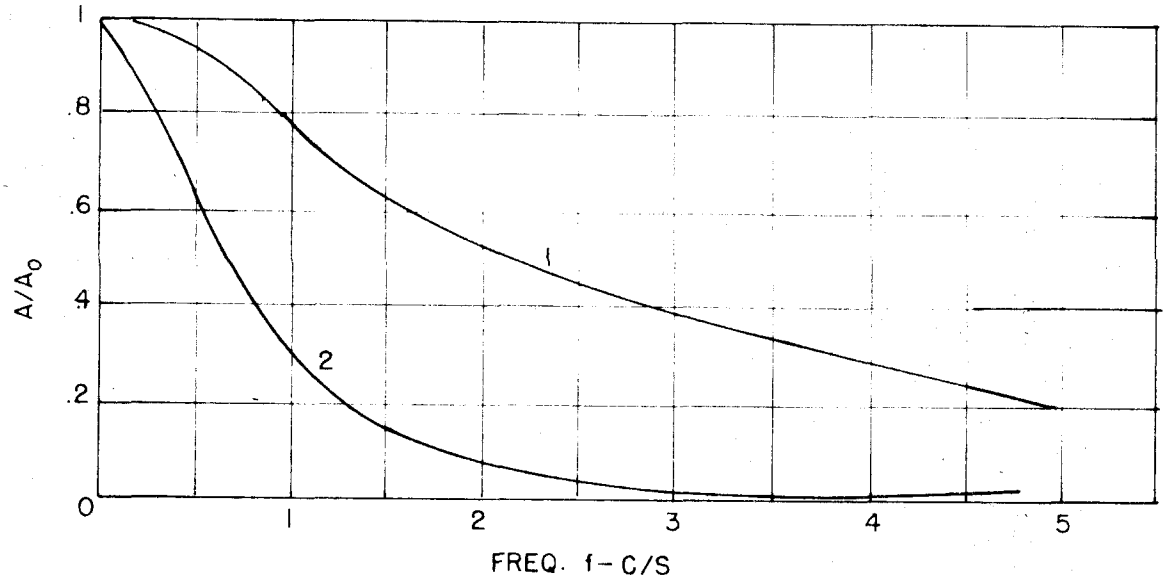

1) $Y(f) = .44S/(1+jf.755)$

2) $Y(f) = 5/(1-2.45f^2+j\,3.14f)$

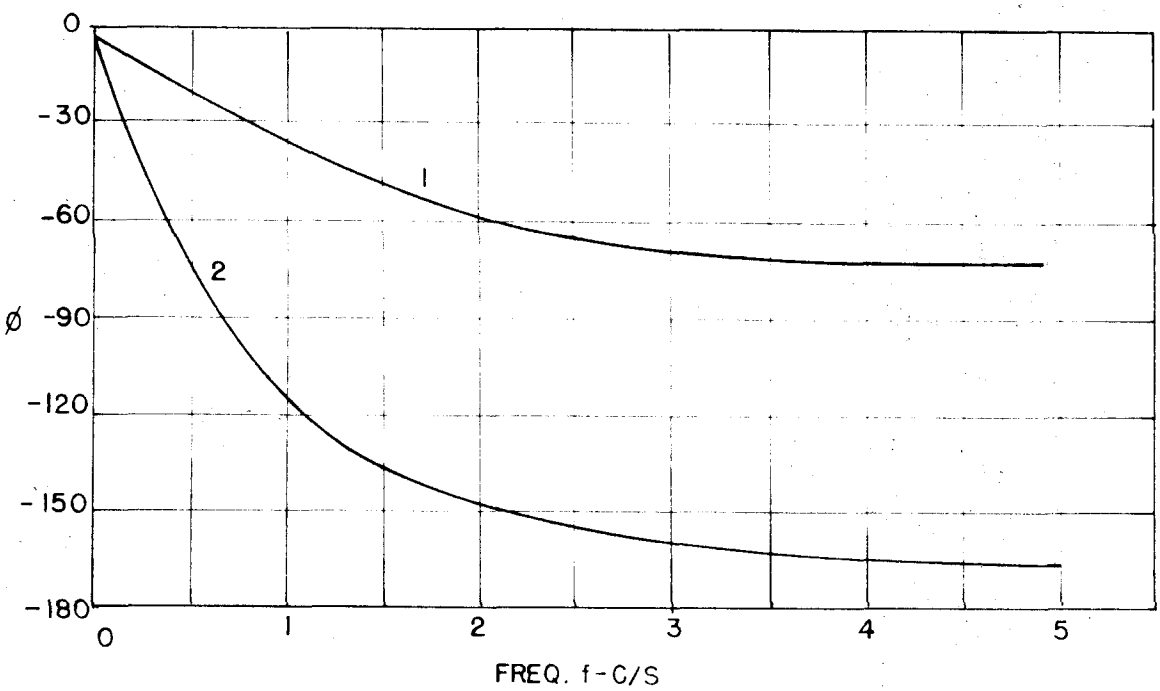

FIG. 43 PHASE AND AMPLITUDE RESPONSE OF LOW PASS FILTERS

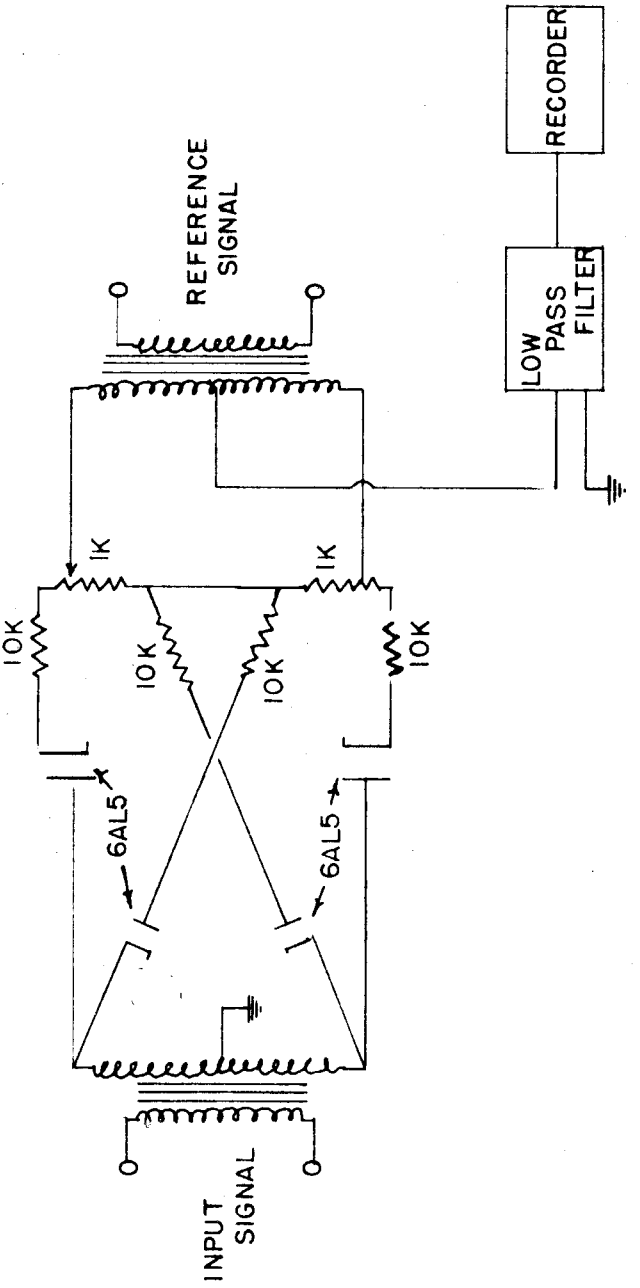

FIG. 44 RING DEMODULATOR

the difference is therefore zero or D.C. The magnitude of the D.C. voltage is proportional to the cosine of the difference in phase angle. The amplitude of the signal can be recorded by shifting the phase of the reference signal and feeding it into a second phase detector.

The advantage in using this technique is that the entire filtering can be done at the A.C. level; no requirements are specified concerning the S/N ratio of the signal going into the product detector. The block diagram of Figure 45 shows how this method can be used to record phase automatically. If the phase-shifting network is a resolver driven by a servo motor, the angle φ and α are always automatically separated by 90°. A potentiometer on the same shaft as the resolver may be used to record shaft position and hence phase.

7. Amplitude-measuring equipment. Through the Navy the project was able to obtain the use of the Stoddart (AN/URM-6) whose frequency range is 15 to 250 kc/s covered in four bands. The receiver was designed to be a field-strength meter as well as a communication receiver. The AN/URM-6 was used in much of the preliminary attempts to receive the signal from the transmitting dipole. There is not much doubt in the author's mind that the use of this receiver, which was much superior to any other receiver in this frequency range, shortened the work of the project by a period of 6 months to 1 year. The AN/URM-6 is a superheterodyne receiver with a bandwidth of 80 c/s at 16 kc/s, 100 c/s at 20 kc/s, and 350 c/s at 50 kc/s. The field-strength of the 50-kc/s signal was measured by the use of a calibrated loop antenna at the input of the receiver and recorded on an Esterline-Angus recorder.

8. D.C. amplifier for the Esterline-Angus recorder. A general-purpose recorder amplifier was built (Cf. Fig. 46) in order to drive the

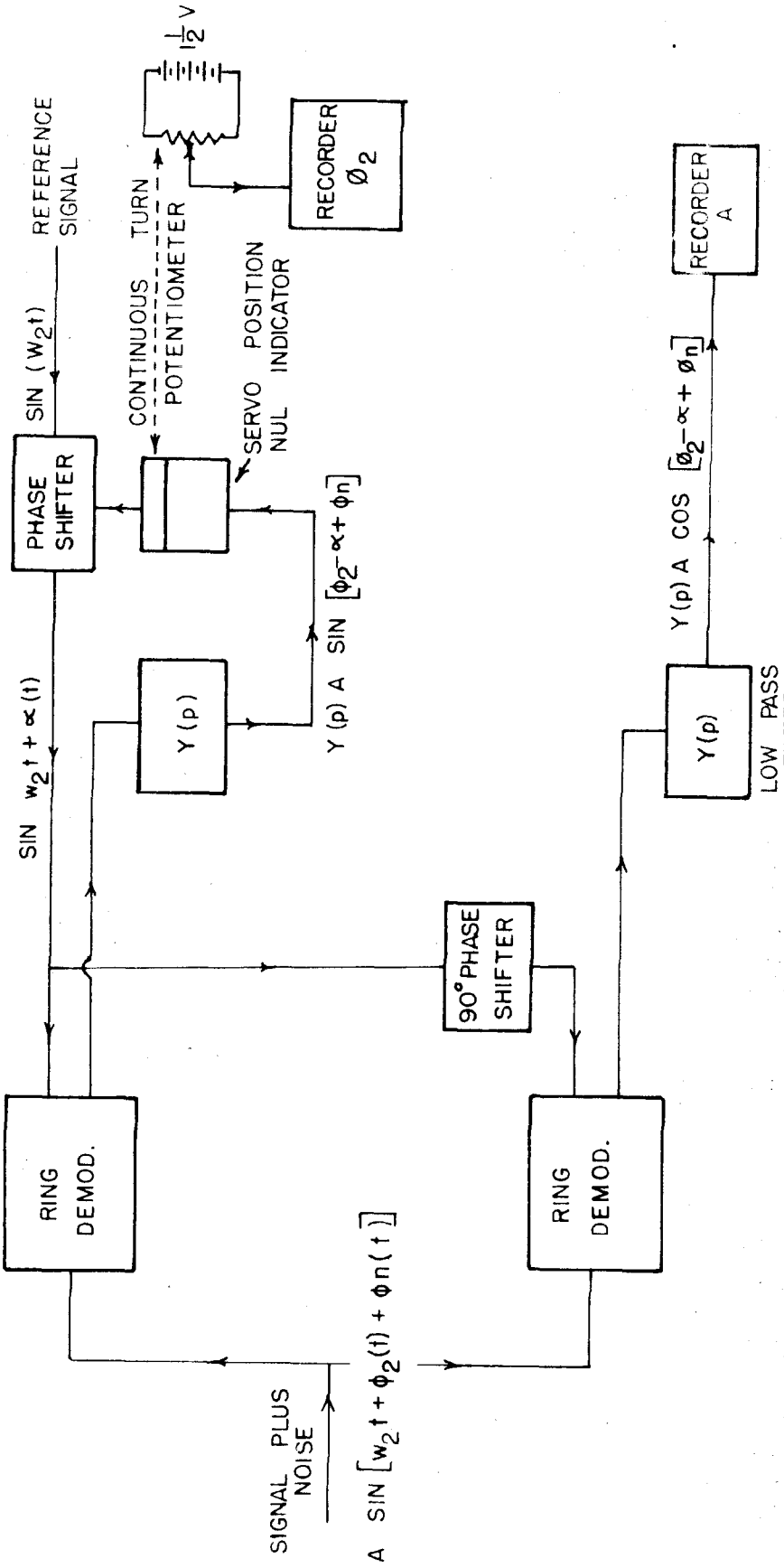

FIG. 45 PROPOSED AUTOMATIC RECORDING SYSTEM

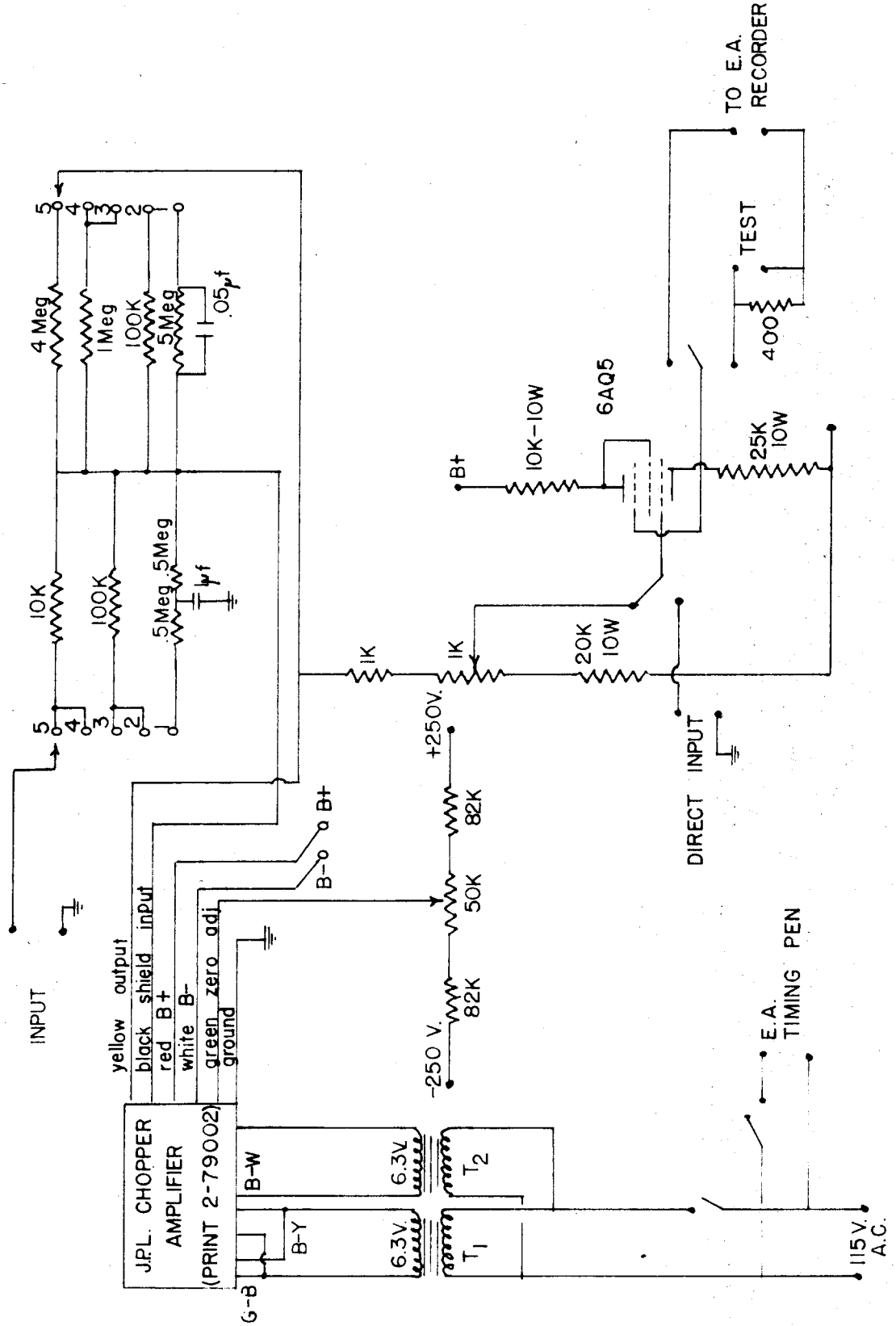

FIG. 46 D.C. AMPLIFIER FOR E.A. RECORDER

5-ma, Esterline-Angus recorder. A chopper-stabilized D.C. amplifier was used as an operational amplifier to obtain gains of 1, 10, 100, and 400. It was also operated as a filter having the characteristics shown in Figure 43. The transfer function of the filter was $5/\left[1 - (\omega^2/16) + j(\omega/2)\right]$, which has a BW of 0.4 c/s and a D.C. gain of 5. The main advantage of this type of filter is the 12-db per octave attenuation at the higher frequencies.

IV. CONCLUSIONS

On the nights of October 28 and 29, 1952, the system as described (Cf. Section III) was successfully operated. Recordings were taken which gave as a continuous function of time the phase and the amplitude of the reflected wave. Figure 47 shows the data in reduced form; the original appeared on Esterline-Angus recorder paper. The data are discussed by R. S. Macmillan in Reference 1. Over the period shown in Figure 47 the phase of the reflected wave changed about 1000°, which is equivalent to a change of height of almost 9 km (Cf. Fig. 17). Except when the S/N ratio was such that the phase meter was forced to read alternately 0 and 360°, the resolution of the system in phase was about 9°. The BW of the system was about 1 c/s. The 9° resolution is equivalent to about 0.1 km (or 330 ft) at a frequency of 50 kc/s. This resolution is ten times greater than that of any other system known to the author.

In Section II-A it was decided, in deriving the requirements for a pulse system, that a BW of 8.5 kc/s for a resolution of 1 km was sufficient. In order to make a fair comparison between the relative merits of the pulse system and the CW system, the specified BW of 8.5 kc/s must be increased to 85 kc/s.

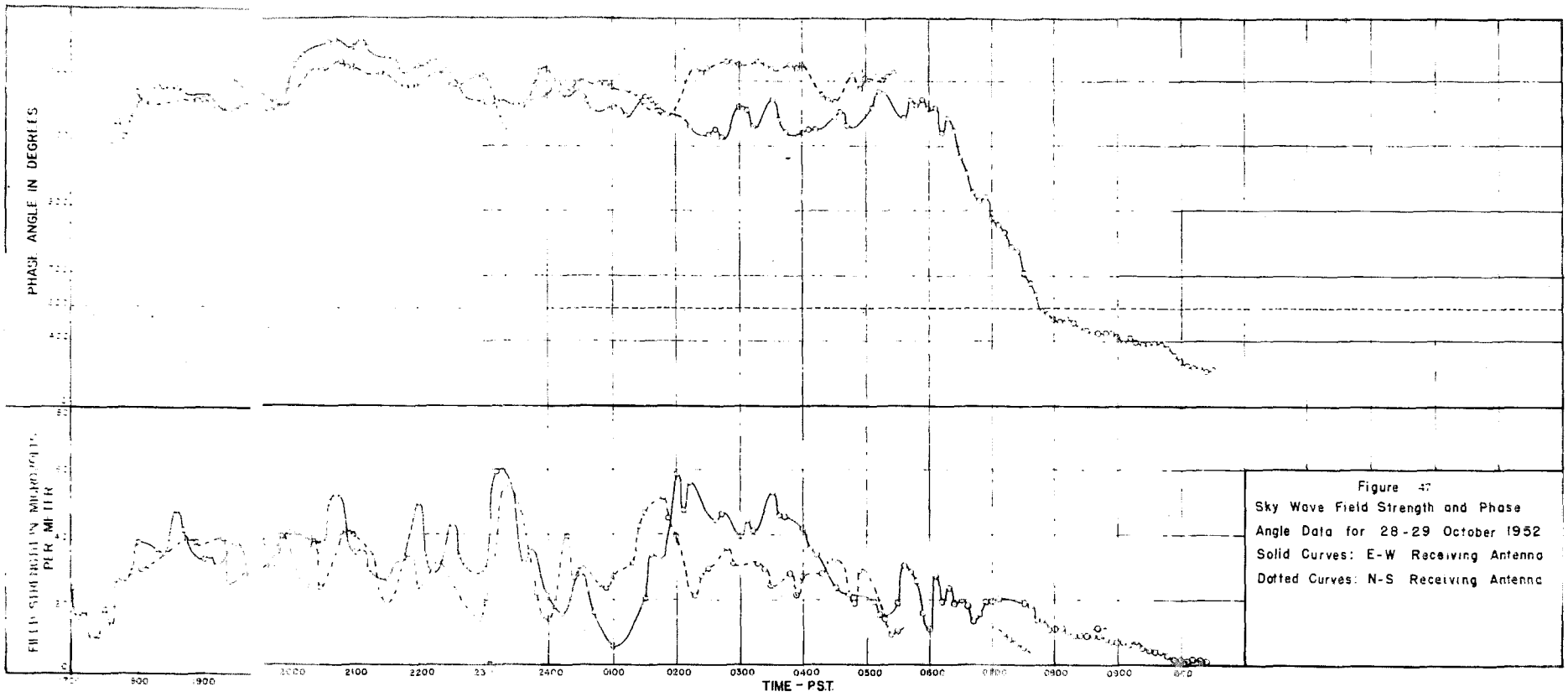

Figure 47
Sky Wave Field Strength and Phase Angle Data for 28-29 October 1952
Solid Curves: E-W Receiving Antenna
Dotted Curves: N-S Receiving Antenna

The amplitude-measuring equipment has a BW of 350 c/s at the point where the signal and noise are converted to D.C. for recording purposes. As well as obtaining a record of the amplitude of the reflected wave, this system provided a noise measurement once every 4 minutes when the 50-kc/s signal was off. The amplitude of the received signal had a maximum value of about 78 μvolts/meter and a minimum of something less than 5 μvolts/meter. Appendix A indicates that, if the dielectric constant of the earth at the receiving site is the same as that of the transmitting site, the maximum signal strength (for ${}_{\perp}R_{\perp} = 1$) expected would be 200 μvolts/meter. In comparing 78 μvolts/meter with 200 μvolts/meter, one sees that, by increasing the dielectric constant slightly (Cf. Appendix F) and assuming a value of 0.7 for ${}_{\perp}R_{\perp}$, the difference is explained.

The equipment of the transmitting system functioned very well during the 2 days of the data recording. The transmitter held to a steady 625-watt output, and the frequency sources of 50 kc/s and 1612 c/s as derived from the 100-kc/s crystal were very reliable. The VHF frequency-modulated transmitter also was held to a steady power output and thus gave no cause for concern. On the other hand, the motor generator furnishing the 60-c/s power was on the verge of a breakdown for the entire time, and only by the grace of God did the 2-day period pass without a failure in the power. It has been the experience of the author with every project requiring the use of motor generators that they are not reliable over extended periods of time. There is a real need for the production of better motor-generator sets.

Most of the trouble with the receiving system (Cf. Fig. 48) also came from the 60-c/s power source. The experimenters were very fortunate

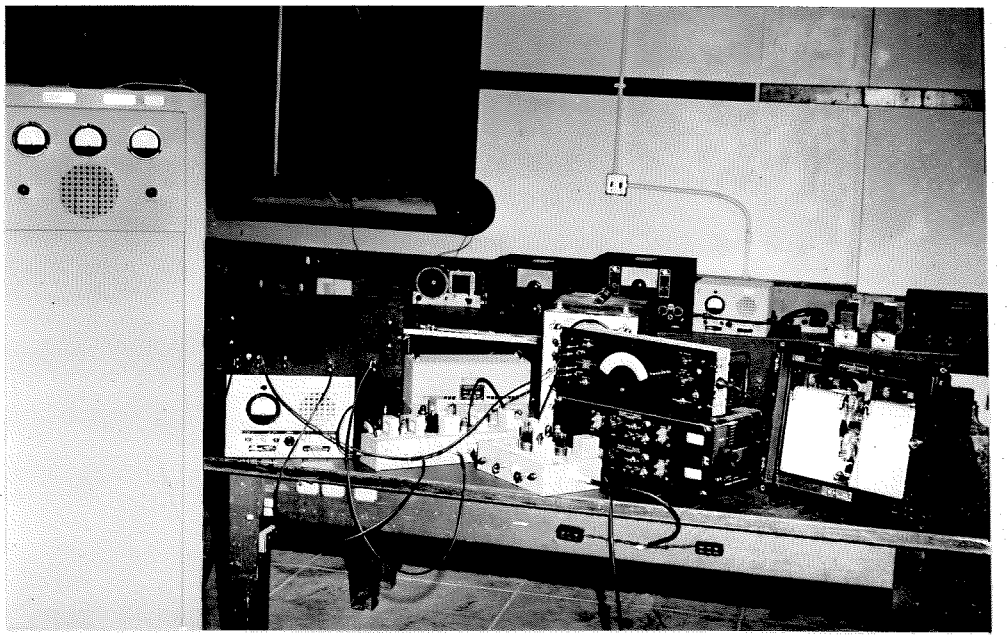

FIG. 48 EQUIPMENT USED AT THE RECEIVING STATION

in that the failure of the two available motor-generator sets did not take place until shortly after the successful completion of the experiment. For reasons discussed in Section III-B-3, the receiving antenna had to be balanced in order to give the best S/N ratio, and after this balance was obtained, extreme care had to be taken not to upset it. One other critical part of the system was the double superheterodyne receiver which, because of the very narrow BW of 30 c/s, was difficult to align. The remainder of the receiving equipment performed very reliably. Field tests were made on the receiver to check the phase stability, which was found to be well within the resolving power of the entire system.

The method of measuring the changes in height of the ionosphere as it now exists is probably better than any other now existing; with the successful operation of the first phase of the development, however, several possible improvements are apparent. Noise and frequency stability rise up as the limiting factors. The problem of achieving greater frequency stability is not an easy one although it is straightforward. Section III-A-3 specifies that the stability should be 2 parts in 1,000,000. Calibration procedures can be used to determine whether this specification is met.

In order to combat the noise problem three things can be done: (1) increase the transmitted power, (2) make the BW of the receiver narrower, and (3) increase the directivity of the antenna, thus cutting down on the noise input. In the present system the transmitted power is fixed, and its increase would involve a major installation. However, the BW of the receiving system can be greatly improved (as discussed in Section III-B-6) by replacing the phase meter with the circuit of

Figure 45. In the present system the nonlinearity of the phase meter near 0 and 360° is a severe limitation on the required BW of the superheterodyne receiver. By using the circuit of Figure 45 the BW of the receiver is not restricted, and yet the over-all BW of the system can be made to be less than 1 c/s.

By using the noise-cancelling antenna of Section III-B-3 it is possible to reduce both the background noise and the impulsive noise. Although this antenna system was not used during the recording period, it was found that the background noise can be reduced by a factor of 2 and that the impulsive noise can be reduced by a factor of 20 to 40. The noise-cancelling abilities of the push-pull converters used in the superheterodyne receiver (Cf. Section III-B-5) have not been fully exploited; thus it is possible that even more noise reduction may be obtained at this point in the receiver.

Although it has been impossible to investigate completely the characteristics of the dipole antenna above the earth at 50 kc/s, the experimental information obtained has yet to contradict the theory set forth in Appendix A. For example, the fact that the dipole excites the ground wave was verified. This ground wave has a maximum value directly off the end of the dipole and had the predicted null normal to the length of the dipole. The field strength of the reflected wave is very near to that which would be predicted at the receiving site; thus it is safe to assume that the field pattern directly over the antenna agrees with that derived in Appendix A.

The months of December and January constitute the rainy season in the Mojave desert area where the transmitting and receiving sites are located. How much an increased moisture content of the ground

would affect the transmitted and received signal could be determined only by actual experimentation. During the night of February 13-14, 1953, the NA/URM-6 receiver was used to record the signal strength (Cf. Fig. 49). For an input current to the transmitting antenna of 2.5 amperes, the maximum field strength recorded was 78 μvolts/meter. The maximum field strength recorded in October was 65 μvolts/meter. The measured input resistance was 104 ohms as against the October value of 100 ohms. These changes are not regarded as significant because of the limited accuracy of the measuring equipment; thus one can infer that the increased moisture content of the earth had no effect.

The field strength at a distance of 15 miles off both ends of the antenna was measured and found to be 140 μvolts/meter off the east end and 155 μvolts/meter off the west end for a transmitting antenna current of 2 amperes.

A major contribution to the field of low and very low frequency investigations of the ionosphere has possibly been marked by the completion of the first phase of the project. The nature of the transmitting antenna and the design of the receiving system (in that this design allows the use of a low-power transmitter) have made possible establishments of future ionospheric stations at a cost which is no longer prohibitive. The advantages of the over-all system are (1) no strong ground wave signal in the direction of the receiver, (2) a resistive input to the low-frequency transmitter, (3) a transmitting antenna which is readily tuned in the frequency range 18 to 100 kc/s, (4) a VHF frequency-modulation, line-of-sight communication link for the transmission of the reference signal, (5) a double-superheterodyne,

FIG. 49 FEBRUARY 1953 DATA

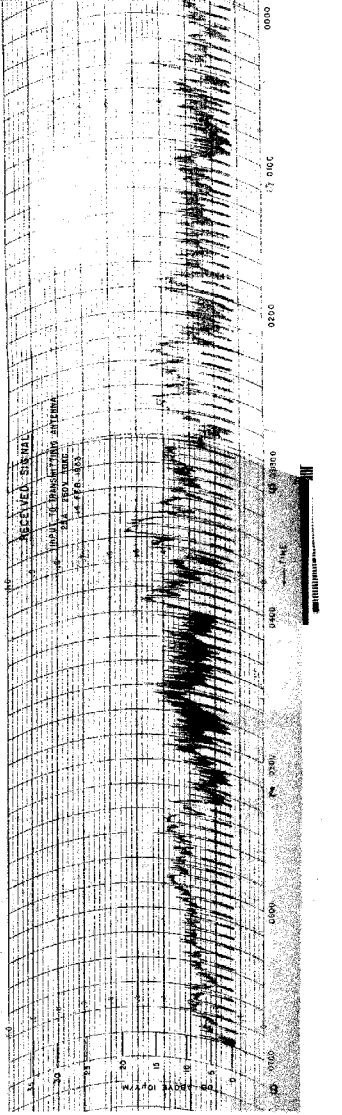

low-frequency receiver with a bandwidth of less that 30 c/s, (6) the means whereby to derive the intermediate frequencies for the receiver from the transmitted frequency, (7) the comparison of the output of the receiver with a subharmonic of the transmitted frequency, and (8) an over-all bandwidth for the receiving system of less than 1 c/s.

All of these factors permit the system to (1) resolve changes in height of the reflecting layer to less than 0.1 km, (2) measure the reflection coefficients down to 0.005, (3) measure the polarization of the downcoming wave, and (4) record all the information as a continuous function of time. The ionospheric research station at low frequencies is no longer restricted by the high cost of construction, for the California Institute of Technology has successfully operated a pilot-model, low-cost station with no sacrifices in the resolution of the final results.

APPENDIX A

A TRANSMITTING ANTENNA FOR INVESTIGATING THE IONOSPHERE AT LOW AND VERY LOW FREQUENCIES*

A research program is being started at the California Institute of Technology for the investigation of the D and E layers of the ionosphere at low and very low frequencies. Various frequencies in the range of 15 to 100 kc/s will be used. Conventional antenna systems were found to be undesirable because of the excessive cost which amounts to $1,000,000.00, on the average, for each 10 per cent of efficiency achieved. The cost of low-frequency antenna systems is high because they usually require tall towers, extensive ground systems, and either high-voltage tuning condensers or large tuning coils. Tuning coils or tuning condensers can be eliminated by using a resonant antenna such as a half-wave linear dipole, and it was with the idea of a resonant antenna in mind that an investigation of ground antennas was started. A ground antenna is, in this case, a half-wave linear dipole, or resonant loop, a full wavelength in circumference, placed directly on the ground or a very small fraction of a wavelength above the ground. A half-wave linear dipole at 15 kc/s would be 10 km (33,000 feet) long. The greater part of the material in this appendix deals directly with the dipole antenna; however, the theory is readily extended to the loop antenna.

---

* This appendix was written jointly by C. W. Bergman and R. S. Macmillan in March, 1952, at the conclusion of a study of radiation from a horizontal dipole over a dielectric earth.

1. Sommerfeld's Integral Equations

In order to determine whether or not it is practical to use such a ground antenna, we refer to the work of Arnold Sommerfeld (Cf. Refs. 17 and 18), who treated the problem of a horizontal Hertz dipole (Cf. Ref. 19) over an arbitrary plane earth. Sommerfeld has derived rigorous integral equations for the Hertz vector of such a dipole antenna. For completeness, his derivation is briefly outlined here.

The Hertz vector $\bar{\Pi}$ for the Hertz dipole of Figure A-1, which is located at (0,0,h), is

$$\bar{\Pi} = \hat{i}\,\Pi_x = \frac{\hat{i} I l}{4\pi\omega\epsilon}\, e^{j(kR-\omega t)} \qquad \text{(A-1)}$$

where k is the wave number $\sqrt{\omega^2\mu\epsilon - j\sigma\mu\omega}$ of the medium of dielectric constant ϵ, permeability μ, and conductivity σ; j is the usual imaginary notation, and

$$R^2 = x^2 + y^2 + (z-h)^2 = r^2 + (z-h)^2$$

The electric current in the dipole is i = I cosωt amperes. The Hertz vector satisfies the wave equation

$$\nabla^2 \bar{\Pi} = \mu\epsilon \frac{\partial^2 \bar{\Pi}}{\partial t^2} + \mu\sigma \frac{\partial \bar{\Pi}}{\partial t} \qquad \text{(A-2)}$$

as do the electromagnetic-field components. First of all, the time dependence can be removed, and the wave equation becomes

$$\nabla^2 \bar{\Pi} = -(\omega^2\mu\epsilon + j\sigma\mu\omega)\bar{\Pi} = -k^2\Pi \qquad \text{(A-2a)}$$

If the dipole is oriented in the x direction, the Hertz vector, at any point in space, has an x component only. In the plane z = 0, the magnitude of the Hertz vector is a function of r only.

The electric and magnetic intensity vectors $\bar{E}$ and $\bar{H}$ of the radiation field can be obtained from $\bar{\Pi}$ as follows:

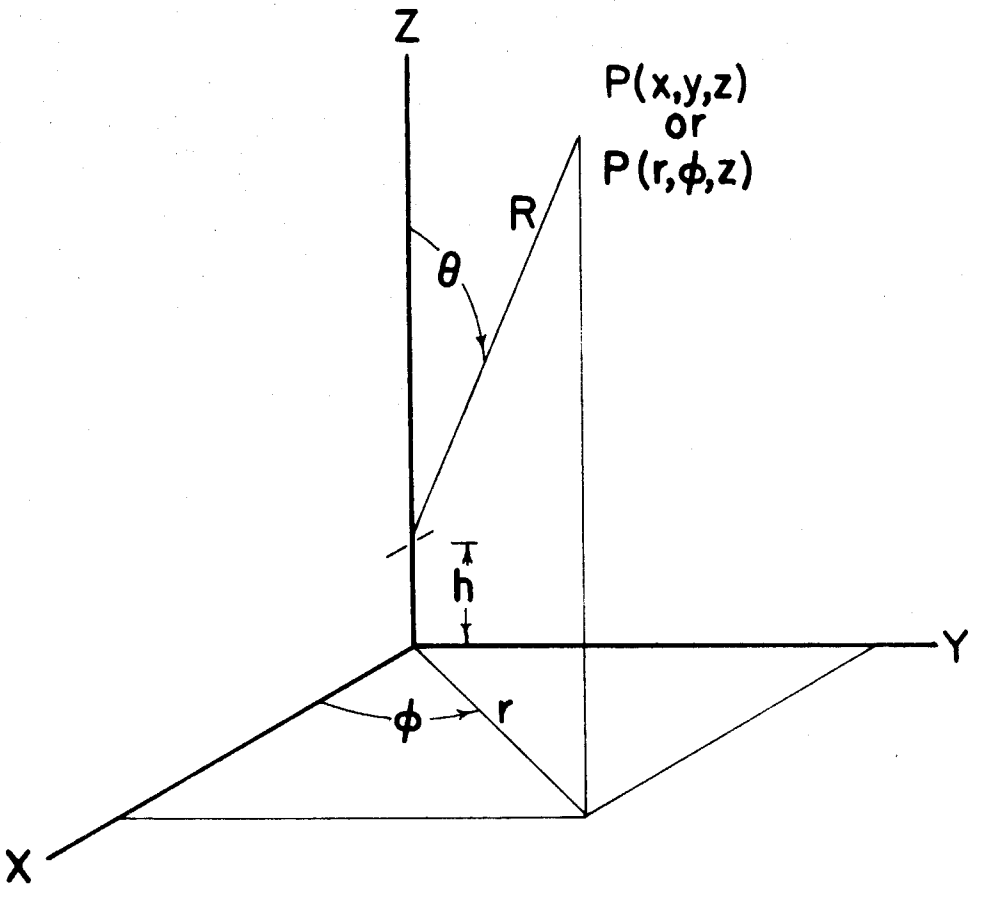

Figure A-1

Hertz dipole in free space

$$\bar{E} = k^2 \bar{\Pi} + \nabla(\nabla \cdot \bar{\Pi}) \tag{A-3}$$

$$\bar{H} = \frac{k^2}{j\omega\mu} \nabla \times \bar{\Pi} \tag{A-4}$$

Equations (A-3) and (A-4) may be derived from Maxwell's equations.

The horizontal dipole above a plane arbitrary earth, at z = 0, may be represented by the total Hertz vector $\bar{\Pi}_1$: $\bar{\Pi}_1$ is made up of a primary stimulation $\bar{\Pi}_{prim}$ due to the dipole only and a secondary stimulation $\bar{\Pi}_{sec}$ due to the perturbation effect of the plane earth. The Hertz vector in the earth $\bar{\Pi}_2$ is completely determined by the boundary conditions imposed upon Π by E and H. These boundary conditions for the three components of $\bar{\Pi}$, Π_x, Π_y, Π_z, are

$$\Pi_{x_1} = m^2 \Pi_{x_2} \tag{A-5}$$

$$\frac{\partial \Pi_{x_1}}{\partial z} = m^2 \frac{\partial \Pi_{x_1}}{\partial z} \tag{A-6}$$

$$\Pi_{z_1} = m^2 \Pi_{z_2} \tag{A-7}$$

$$\frac{\partial \Pi_{z_2}}{\partial z} - \frac{\partial \Pi_{z_1}}{\partial z} = \frac{\partial \Pi_{x_1}}{\partial x} - \frac{\partial \Pi_{x_2}}{\partial x} \tag{A-8}$$

where $n^2 = k_2^2/k_1^2$. The constants for the earth are $\epsilon_2, \mu_2, \sigma_2$, and the constants for air are $\epsilon_1 = \epsilon_0$, $\mu_1 = \mu_0$, $\sigma_1 = 0$.

In order to apply these boundary conditions, Equation (A-1) must be put in the form of a superposition of eigenfunctions. By making use of the Fourier-Bessel integral theorem, Equation (A-1) may be written in cylindrical coordinates as follows:

$$\bar{\Pi} = \bar{\Pi}_{prim} = \frac{\bar{i} I l}{4\pi\omega\epsilon_0} e^{jkR_1}$$
$$= \frac{\bar{i} I l}{4\pi\omega\epsilon_0} \int_0^\infty J_0(\lambda r) e^{-\mu(z-h)} \frac{\lambda \, d\lambda}{\mu} \tag{A-9}$$

where λ, the eigenvalue of the eigenfunction, has a continuous spectrum $0 \ll \lambda \ll \infty$, and where $\mu_n = \sqrt{\lambda^2 - k_n^2}$.

Sommerfeld's integral equations for Π_1 and Π_2 may now be written for the horizontal dipole at a height h above an arbitrary earth (Cf. Fig. A-2).

$$\Pi_{x_1} = \frac{Il}{4\pi\omega\epsilon_1}\int_0^\infty J_0(\lambda r)\frac{\lambda}{\mu}\left[e^{-\mu_1(z-h)} - e^{-\mu_1(z+h)}\left(1-\frac{2\mu_1}{\mu_1+\mu_2}\right)\right]$$

$$= \frac{Il}{4\pi\omega\epsilon_1}\left[\frac{e^{ikR}}{R} - \frac{e^{ikR'}}{R'} + 2\int_0^\infty J_0(\lambda r)e^{-\mu(z+h)}\frac{\lambda d\lambda}{\mu_1+\mu_2}\right] \qquad \text{(A-10)}$$

$$\Pi_{x_2} = \frac{Il}{4\pi\omega\epsilon_1}\frac{2}{m^2}\int_0^\infty J_0(\lambda r)\, e^{+\mu_2 z - \mu_1 h}\frac{\lambda d\lambda}{\mu_1+\mu_2} \qquad \text{(A-11)}$$

$$\Pi_{z_1} = \frac{Il}{4\pi\omega\epsilon_1}\frac{2\cos\varphi}{k_1^2}\frac{\partial}{\partial r}\int_0^\infty J_0(\lambda r)\, e^{-\mu_1(z+h)}\frac{\mu_1+\mu_2}{m^2\mu_1+\mu_2}\lambda d\lambda$$

$$= -\frac{Il}{4\pi\omega\epsilon_1}\frac{2\cos\varphi}{k_1^2}\int_0^\infty J_1(\lambda r)\, e^{-\mu_1(z+h)}\frac{\mu_1+\mu_2}{m^2\mu_1+\mu_2}\lambda^2 d\lambda \qquad \text{(A-12)}$$

$$\Pi_{z_2} = \frac{Il}{4\pi\omega\epsilon_1}\frac{2\cos\varphi}{k_2^2}\frac{\partial}{\partial r}\int_0^\infty J_0(\lambda r)\, e^{\mu_2 z - \mu_1 h}\frac{\mu_1+\mu_2}{m^2\mu_1+\mu_2}\lambda d\lambda$$

$$= -\frac{Il}{4\pi\omega\epsilon_1}\frac{2\cos\varphi}{k_2^2}\int_0^\infty J_1(\lambda r)\, e^{\mu_2 z - \mu_1 h}\frac{\mu_1+\mu_2}{m^2\mu_1+\mu_2}\lambda^2 d\lambda \qquad \text{(A-13)}$$

where $R^2 = x^2 + y^2 + (z-h)^2$ and $R'^2 = x^2 + y^2 + (z+h)^2$.

It is believed that Equations (A-10) through (A-13) are valid for the radiation field; however, the techniques that various people have used on these equations in order to find Poynting's vector or the electric

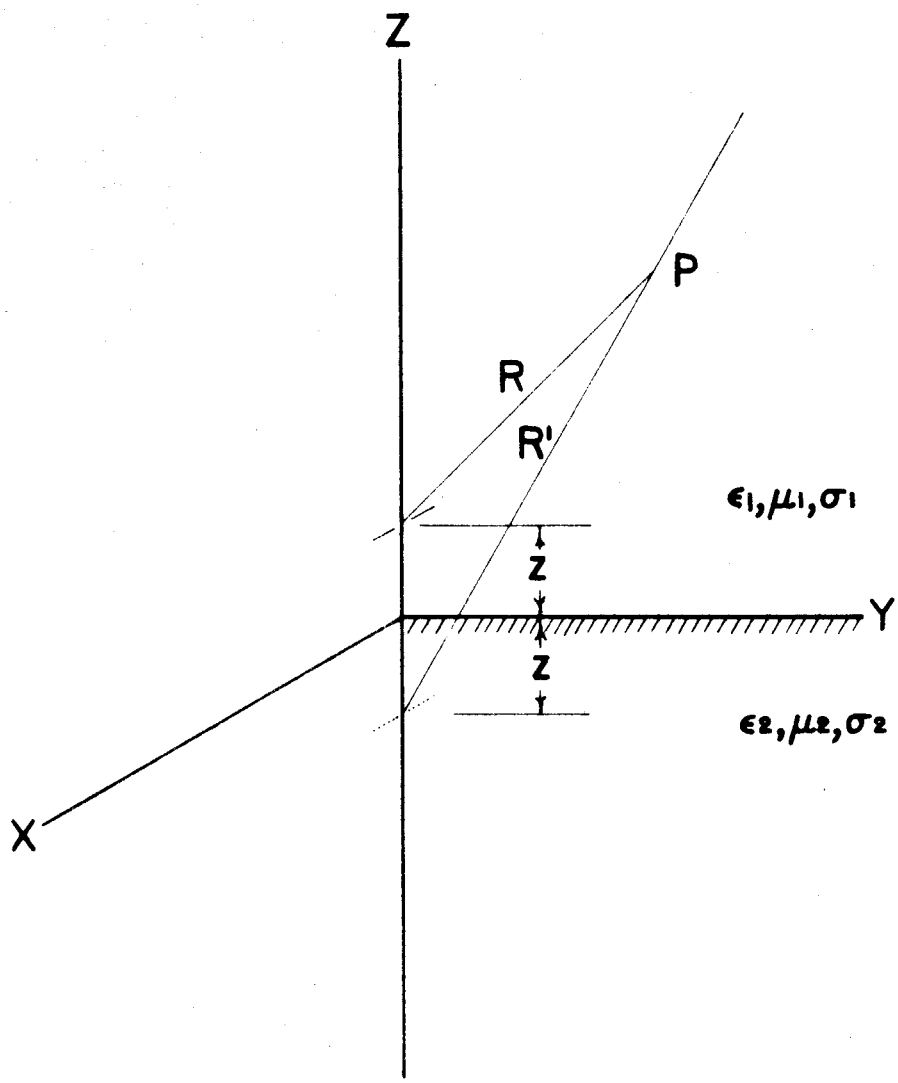

Figure A-2

Hertz dipole over a plane earth

and magnetic field strengths invariably involve approximations which are not valid for all values of k_2. It can be seen that the evaluation of these integrals involves integration of an equation having a Riemann surface of four sheets with branch points at $\lambda = k_1$ and $\lambda = k_2$. Care must be taken that the path of integration lies in the proper sheet. Equations (A-12) and (A-13) have an additional complexity of a pole at $\lambda = p$, where $1/p^2 = (1/k_1^2) + (1/k_2^2)$ because of the fact that $n^2\mu_1 + \mu_2$ is zero for $\lambda = p$. Sommerfeld places a significance upon the solution obtained by integration around this pole which is discussed in Section 5 of this appendix.

The appearance of a component of the Hertz vector in the z direction is worth noting, because the primary stimulation had no such component. The Π_z values of Equations (A-12) and (A-13) are brought about by the perturbation of the plane earth, and we see from Equation (A-3) that a vertically polarized wave results. This wave has a maximum value in the $\pm$ x direction and a zero value in the $\pm$ y direction. This property will be extremely important in the consideration of the antenna as an instrument for ionospheric research.

In Equation (A-10), we can see that the solution for Π_x is the sum of the solutions of two dipoles, one at z = h and another at z = -h, minus the expression

$$\frac{I\ell}{4\pi\omega\epsilon_1}\left[2\int_0^\infty J_0(\lambda r)\, e^{-\mu_1(z+h)}\, \frac{\lambda\, d\lambda}{\mu_1+\mu_2}\right.$$

We know from physical reasoning that for $k_2 = k_1$ this term must be equal to

$$\frac{I\ell}{4\pi\omega\epsilon_1}\, e^{jk_1R'}/R'$$

and that for $k_2 = \infty$ the term must equal zero. Furthermore, for finite

current I and with $k_2 = \infty$, then Π_{x_2}, Π_{z_1}, and Π_{z_2} must also be zero. In addition, Π_{z_1} and Π_{z_2} are, of course, zero for $k_2 = k_1$.

2. Ground Losses

Fortunately the determination of power output from Equations (A-10) through (A-13) is not unduly complicated. We will not go through the development which is available in References (17) and (18) but will merely write the expression for radiation resistance

$$R_{rad} = \frac{k_1^2 I^2}{4\pi}\sqrt{\frac{\mu_0}{\epsilon_0}}\left(\frac{2}{3} - \frac{\sin\zeta}{\zeta} + \frac{\sin\zeta - \zeta\cos\zeta}{\zeta^3} + L\right) \qquad \text{(A-14)}$$

where

$$L = \frac{1}{k_1^3}\,\mathrm{Re}\left(j\int_0^\infty e^{-2\mu_1 h}\,\frac{2\mu_1\mu_2 - \lambda^2}{n^2\mu_1 + \mu_2}\,\lambda\,d\lambda\right) \qquad \text{(A-15)}$$

and $\zeta = z k_1 h$. Thus R_{rad} is a function of the height h above the ground. L vanishes for $k_2 = \infty$. This special case is plotted in Figure A-3. The scale is changed so that the resistance of the antenna for infinite height is 70 ohms. If one wishes to evaluate L for finite values of k_2, again approximations must be made which are not valid in general. L is described as the term of Equation (A-15) which does not vanish for $h = 0$. The solution assumes an infinitesimal source, and at this source the fields must, of necessity, be infinite. Thus it seems plausible that, if h is allowed to approach zero, and if σ_2 is not zero, the radiation resistance R_{rad} will go toward an infinite value. It follows that an infinite field will cause infinite loss for a finite current in the antenna. This physical reasoning agrees with the result which Sommerfeld obtained on evaluating L for a partially conductive earth. It is important to note that the total resistance is infinite and is

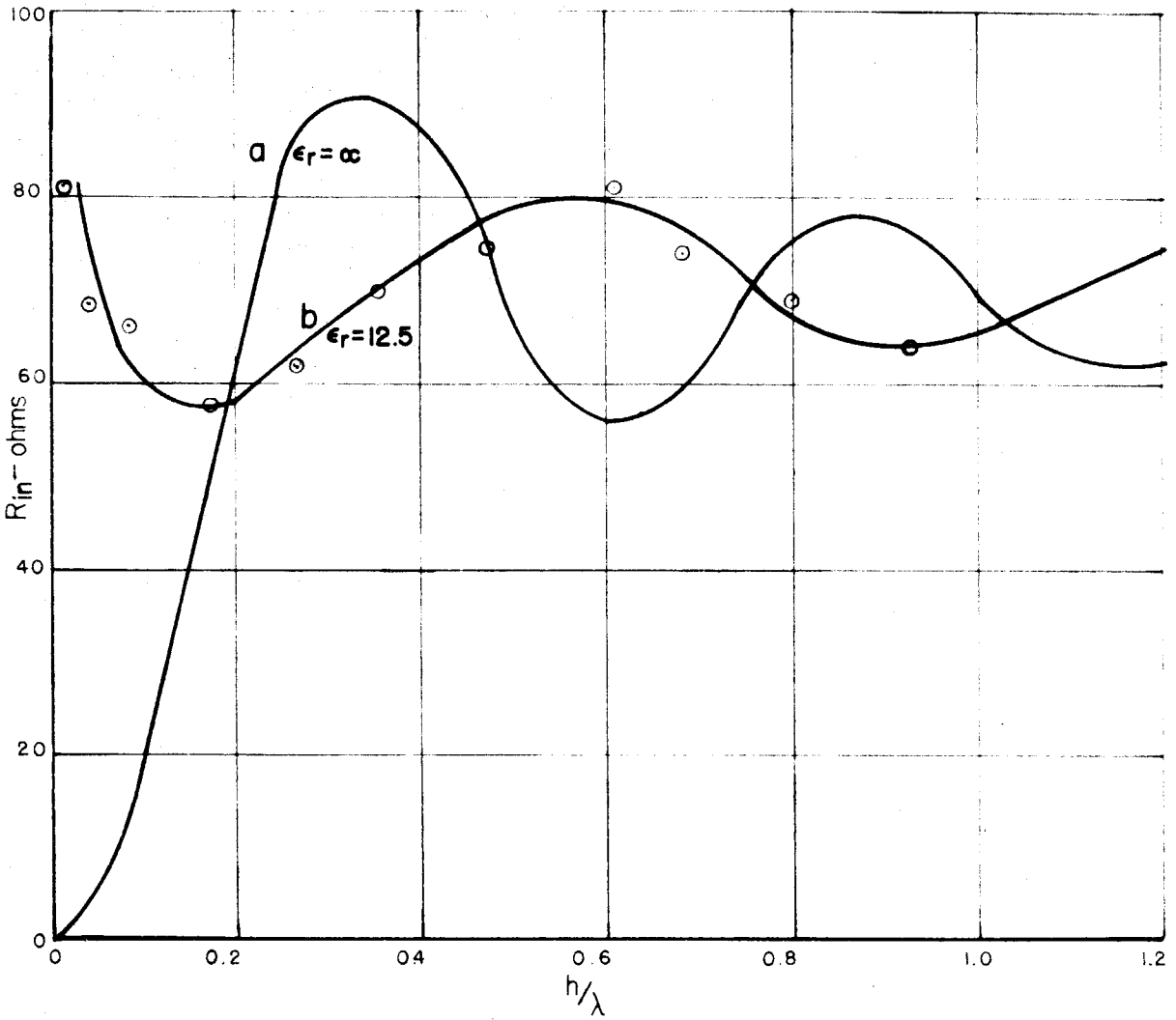

Figure A-3

Input resistance of a half wave dipole above a plane earth. a) Calculated for $\epsilon_r = \infty$ b) Experimental for $\epsilon_r = 12.5$

due entirely to absorption in the ground; only a finite amount of power is radiated into the air for a finite driving current. Therefore the efficiency of the dipole is zero.

If we consider an actual antenna, we find that, because of the finite dimensions of a physical antenna, infinite fields do not exist. The fields are high enough, however, to cause considerable losses if the antenna is actually laid on the ground. We are able to reduce the losses to a reasonable value by raising the antenna several feet above the ground. At low frequencies, it is apparent that the actual height above the ground is the determining factor for reducing losses, not the ratio h/λ.

3. Reflection Method

For an ionospheric-research antenna, one would be most interested in the field-strength pattern in two planes (the x-z plane and the y-z plane) for all angles of (Cf. Fig. A-2), for in these two planes the wave incident on the ionosphere is either polarized in the plane of incidence or normal to the plane of incidence. We can obtain this field pattern by developing a reflection method whose validity has been checked by experiment. In this method, we assume that the fields radiated directly from the antenna are related to the current flowing in the antenna and are independent of the presence of the earth. In order to find the field at a point P (Cf. A-4) due to a dipole an arbitrary distance h above the plane earth, the wave leaving the antenna at an angle θ is added to the reflected wave which left the antenna at an angle $180^\circ - \theta$. For this condition to be valid, ℓ_z/d must be much less than 1. A complex dielectric constant introduces a change in the phase of the reflected wave. However, this change need not be

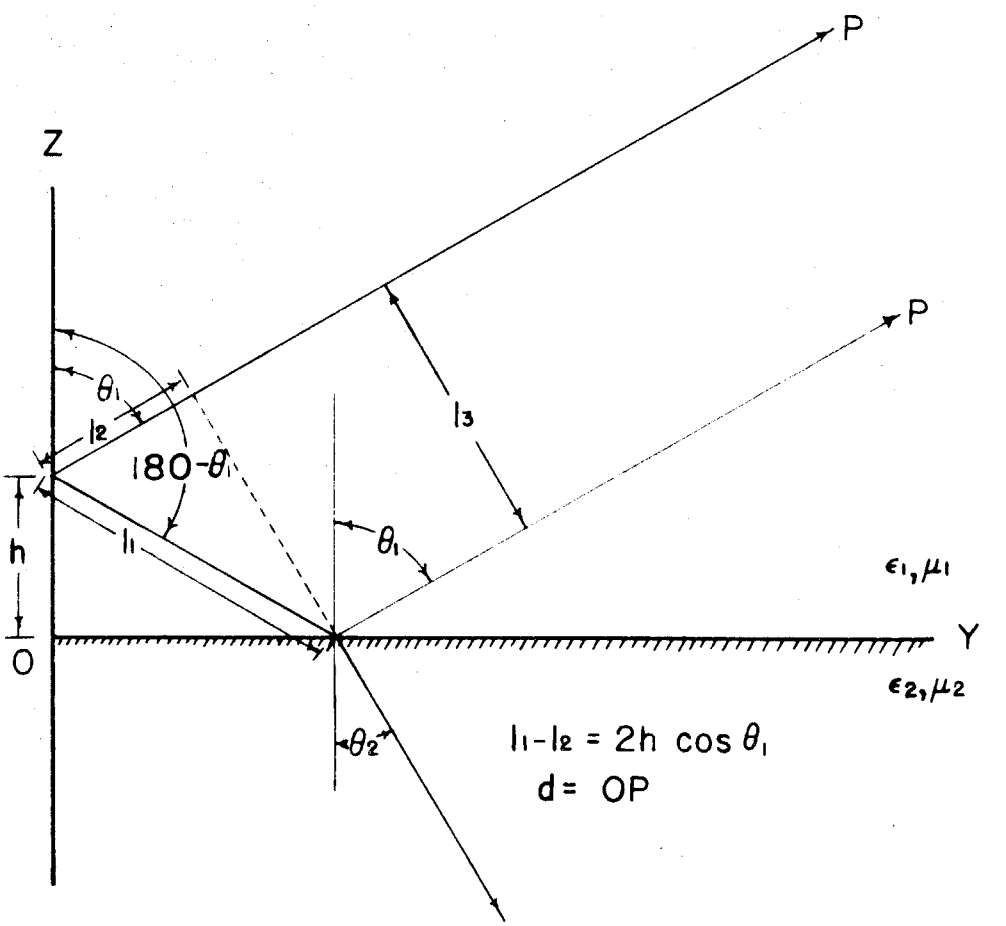

Figure A-4

Geometry of the reflection method

considered here, and the earth is assumed to be a perfect dielectric.

The reflection coefficient for an electromagnetic wave polarized perpendicular to the plane of incidence is

$$\rho_{\perp} = \frac{E_3}{E_1} = \frac{\cos\theta_1 - \sqrt{n^2 - \sin^2\theta_1}}{\cos\theta_1 + \sqrt{n^2 - \sin^2\theta_1}} \tag{A-16}$$

and for the wave polarized in the plane of incidence, it is

$$\rho_{\parallel} = \frac{E_3}{E_1} = \frac{\epsilon_2 \cos\theta_1 - \epsilon_1\sqrt{n^2 - \sin^2\theta_1}}{\epsilon_2 \cos\theta_1 + \epsilon_1\sqrt{n^2 - \sin^2\theta_1}} \tag{A-17}$$

Since the reflected wave travels a path which is longer by an amount $\ell = \ell_1 - \ell_2 = 2h \cos\theta_1$ (Cf. Fig. 4), it is delayed in phase by an angle

$$\delta = \frac{2h\cos\theta_1}{\lambda} 360^\circ \tag{A-18}$$

Thus, if the reflected field intensity is E_3, the total field at point P is

$$E_p = E_1 + E_3 e^{-j\delta} = E_1(1 + \rho e^{-j\delta}) \tag{A-19}$$

In the yz plane, for h = 0, Equation (A-19) becomes

$$E_p = \frac{2E_1\cos\theta_1}{\cos\theta_1 + n\sqrt{n^2 - \sin^2\theta}} \tag{A-19a}$$

Figure A-5 shows the result of such a computation, in the yz plane of Figure A-4, for various heights h with $\epsilon_2/\epsilon_1 = \epsilon_r = 10$. The antenna current in each case is held constant, and unity field strength is assumed for a dipole in free space. For this calculation $\rho_{\perp}$ was used, whereas $\rho_{\parallel}$ would be needed in order to find the fields in the xz plane. The pattern for the xz plane can be approximated for small

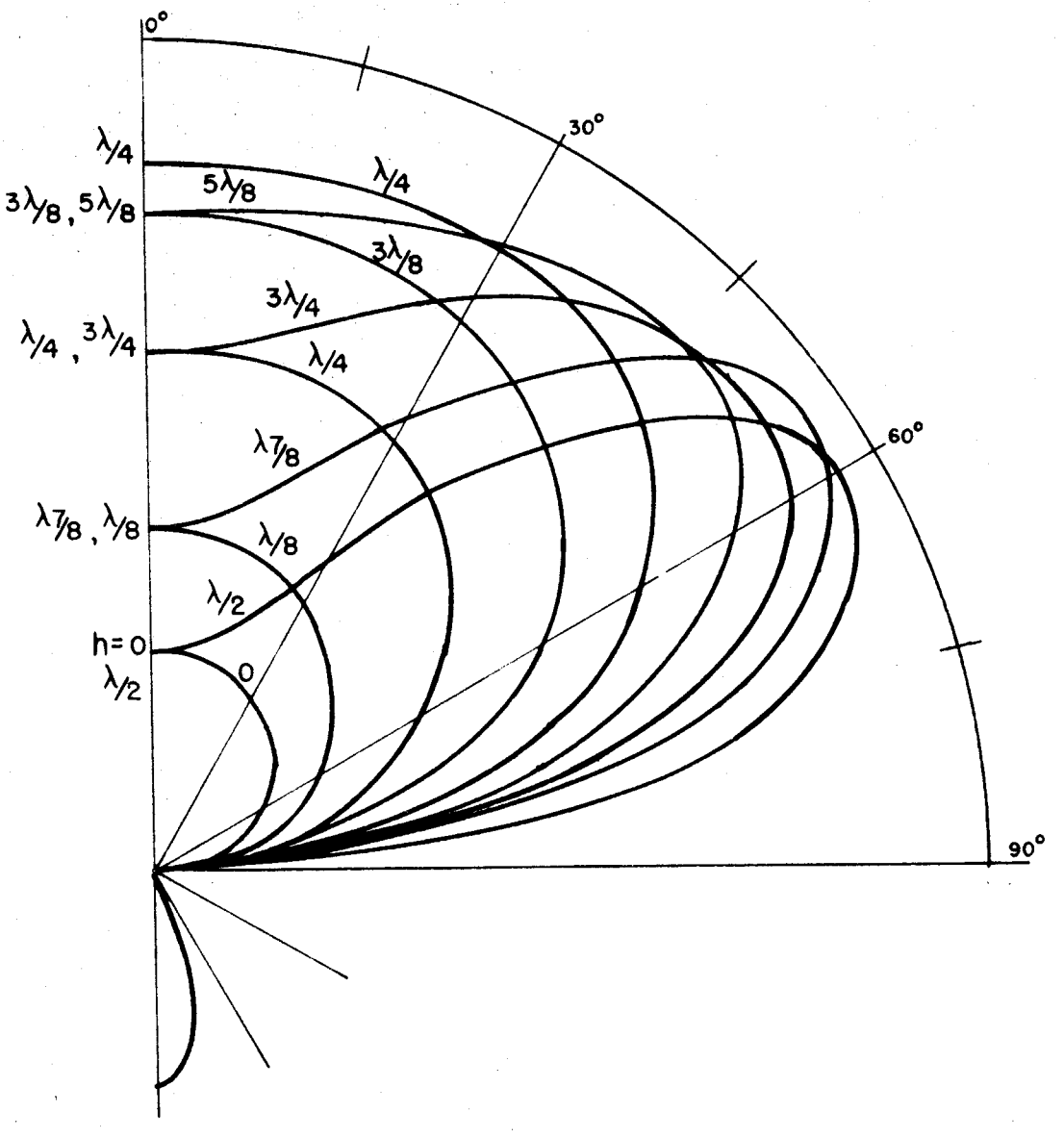

Figure A-5

Field pattern in y,z plane for a dipole at height h above the ground ($\epsilon_r = 10$).

angles of θ by multiplying the value in Figure A-5 by the directivity factor D_θ shown in Figure A-6.

$$D_\theta = \cos\theta \qquad \text{for the Hertz dipole} \qquad \text{(A-20)}$$

$$D_\theta = \frac{\cos(90\sin\theta)}{\cos\theta} \qquad \text{for the half-wave dipole} \qquad \text{(A-20a)}$$

For our low-frequency, ionospheric-research antenna, h/λ is essentially zero, but it is of interest to consider the radiation patterns for several heights above the ground. It is possible to see how the radiation resistance varies with height by noting the relative areas contained within each pattern of Figure A-5. Figure A-5 also shows the calculated pattern of the E field within the lossless dielectric. This pattern remains the same for various heights of the antenna above the ground. Note that, when h is equal to zero, the field has the same maximum value below the antenna as above. Moreover, in the dielectric, the entire pattern is confined to a cone of revolution whose central angle is

$$\alpha = \arcsin(k_1/k_2) = \arcsin(1/\sqrt{\epsilon_r}) \qquad \text{(A-21)}$$

where $\epsilon_r = \epsilon_2/\epsilon_1$.

Figure A-7 shows how the pattern for $h/\lambda = 0$ varies for different values of the dielectric constant, and we can observe how the radiation resistance decreases with increasing dielectric constant. As before, constant driving current is assumed. The pattern of the antenna has a maximum value in the $\theta = 0^\circ$ direction and has decreased by only 10 per cent at $\theta = 30^\circ$. Figure A-8 is a plot of the normalized maximum field as a function of ϵ_r. The fact that there is zero field strength in the $\theta = 90^\circ$ direction is useful, because the problem of separating

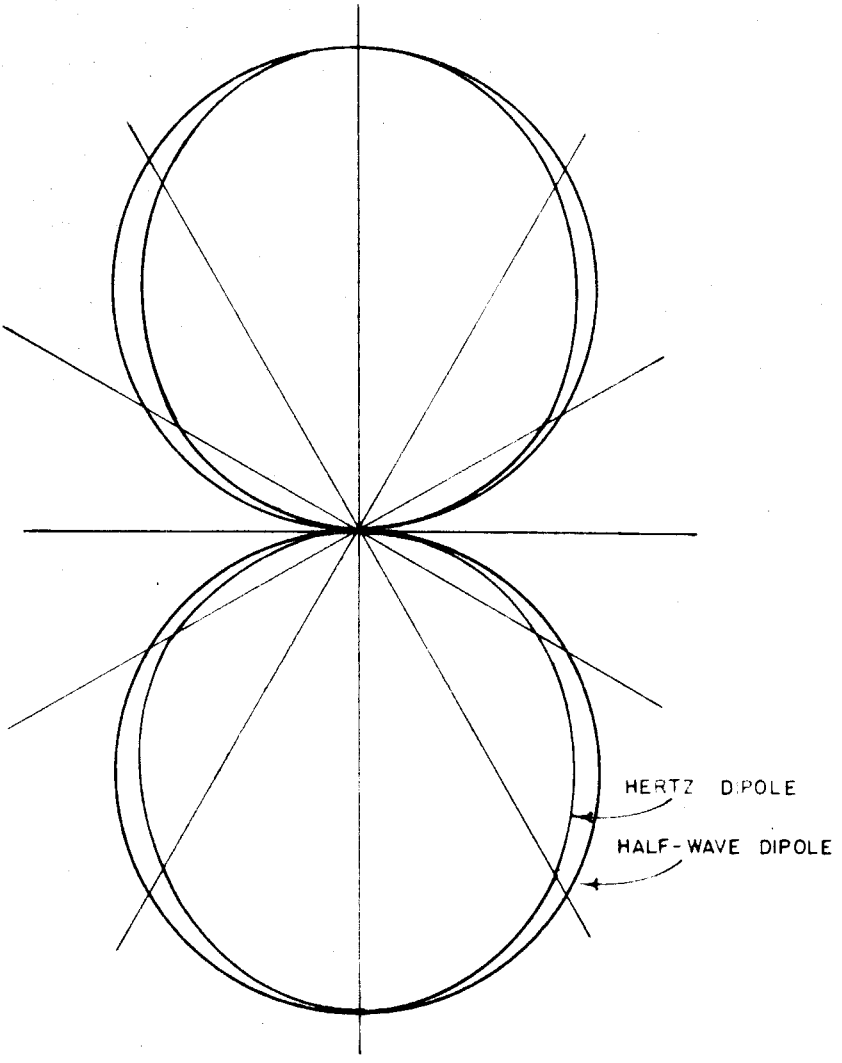

Figure A-6
Pattern in the x,z plane of a Hertz dipole and of a half-wave dipole.

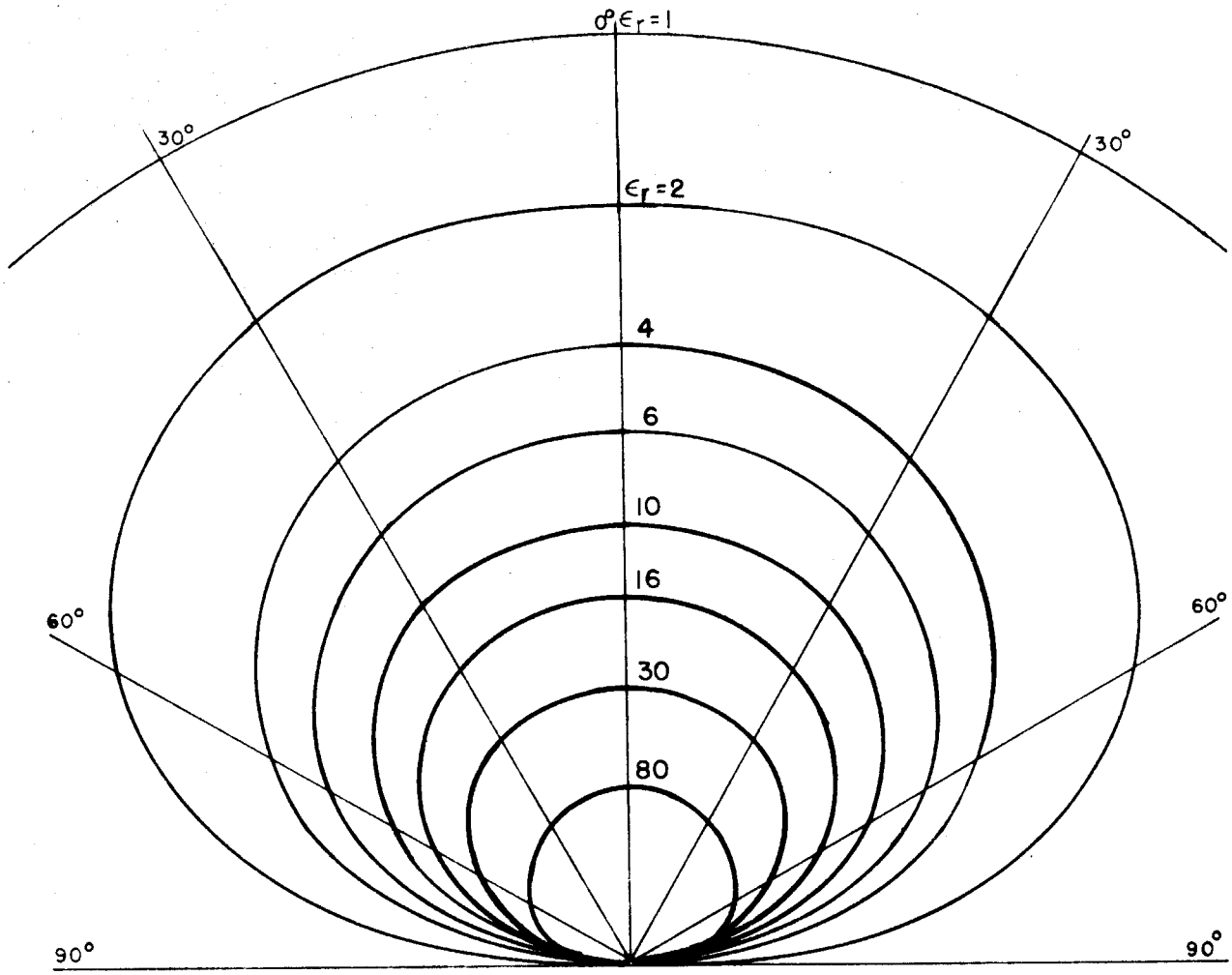

Figure A-7

Pattern in y,z plane of a dipole over a plane dielectric earth with h = 0.

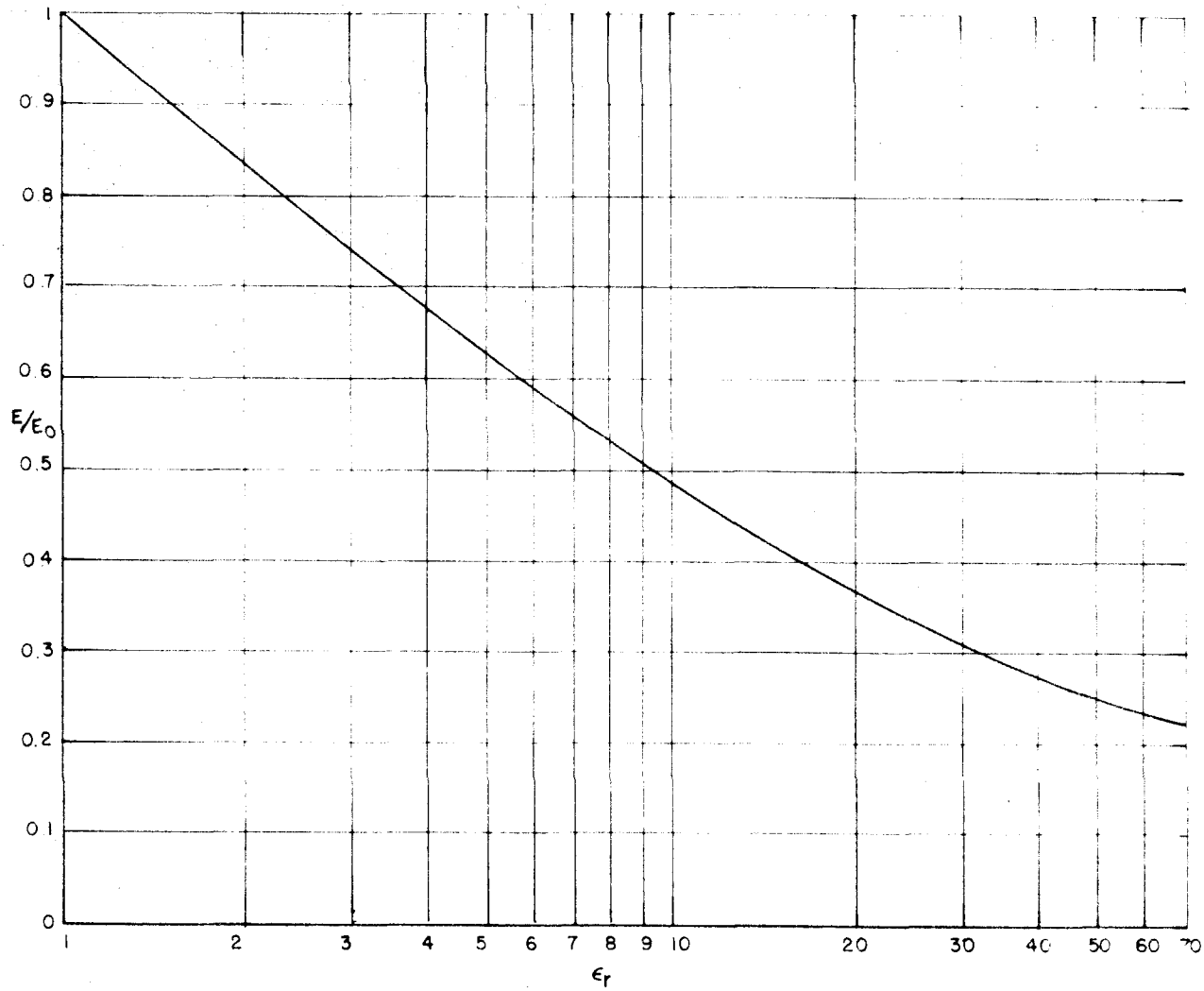

Figure A-8

Maximum field strength of a dipole over a plane dielectric earth ($h=0, \theta=0$) as a function of ϵ_r.

ground wave from sky wave is eliminated in the y or $\varphi = 90^\circ$ direction. The surface wave in the x or $\varphi = 0^\circ$ direction will be considered shortly.

It is possible to compare the results obtained by the reflection method for $h/\lambda = 0$ with Sommerfeld's results at a point directly above the antenna $\Theta = 0$ and at a point off the side of the antenna $\Theta = \pi$ and $\varphi = \pi/2$. For the latter case, $\Theta = \pi$ and $\varphi = \pi/2$, both methods give zero field strength (Cf. Ref. 18). At $\Theta = 0$, according to Equation (A-19a) the field strength is $2\sqrt{\epsilon}_1/(\sqrt{\epsilon}_1 + \sqrt{\epsilon}_2)$ times the field strength of an equivalent dipole in free space. At $\Theta = 0$ and $r = 0$, Equation (A-10) for Π_x becomes

$$\Pi_x|_{r=0} = \frac{Il}{4\pi\omega\epsilon_1}\left[\int_0^\infty \frac{e^{-\mu_1(z+h)}}{\mu_1+\mu_2}\lambda\, d\lambda + \frac{e^{jk_1(z-h)}}{z-h} - \frac{e^{jk_1(z+h)}}{z+h}\right] \quad \text{(A-22)}$$

The integral in this case can be evaluated for large values of z, and Π_x becomes

$$\Pi_x|_{r=0} = \frac{Il}{4\pi\omega\epsilon_1}\left[\frac{e^{jk_1(z-h)}}{z-h} - \frac{e^{jk_1(z+h)}}{z+h} + \frac{2\sqrt{\epsilon_1}}{\sqrt{\epsilon_1}+\sqrt{\epsilon_2}}\,\frac{e^{jk(z+h)}}{z+h}\right] \quad \text{(A-23)}$$

For $h = 0$, Π_x is $2\sqrt{\epsilon}_1/(\sqrt{\epsilon}_1 + \sqrt{\epsilon}_2)$ times the free-space value; thus the two methods give the same result.

4. Surface Wave

The radiation field of the horizontal dipole over an arbitrary earth consists of a horizontally polarized sky wave and a vertically polarized surface wave. The reflection method does not give rise to a solution corresponding to a vertically polarized surface wave. For the case of a horizontal dipole at the surface of a perfect dielectric

earth, the surface wave may be easily calculated from Sommerfeld's integral equation (Eq. A-12). This equation may be written in the form

$$\Pi_{z_1} = -\frac{Il}{4\pi\omega\epsilon_1}\frac{2\cos\varphi}{k_1^2}\int_0^\infty J_1(\lambda r)e^{-\mu_1 z}\frac{\mu_1+\mu_2}{m^2\mu_1+\mu_2}\lambda^2 d\lambda = P+Q \qquad \text{(A-12a)}$$

The integrand has branch points at $\lambda = k_1$ and $\lambda = k_2$ and a pole at $\lambda = p$, where p is given by the equation

$$m^2\sqrt{p^2-k_1^2} + \sqrt{p^2-k_2^2} = 0 \qquad \text{(A-24)}$$

or

$$p^2 = \frac{k_1^2 k_2^2}{k_1^2+k_2^2} \qquad \text{(A-24a)}$$

The term P of Equation (A-12a) is the contribution of the pole to the value of the integral. Sommerfeld has shown that this portion of the solution for Π_{z_1} gives rise to a surface wave. P may be calculated by applying the residue theorem of complex variable theory. The integral of Equation (A-12a) may be transformed into one involving the Hankel function H_1^1.

$$\Pi_z = -\frac{Il}{4\pi\omega\epsilon_1}\frac{\cos\varphi}{k_1^2}\int_{-\infty}^{+\infty} H_1'(\lambda r)e^{-\mu_1 z}\frac{\mu_1+\mu_2}{m^2\mu_1+\mu_2}\lambda^2 d\lambda \qquad \text{(A-12b)}$$

The residue of the integrand at the pole $\lambda = p$ is

$$R_{es} = -\frac{Il}{4\pi\omega\epsilon_1}\frac{\cos\varphi}{K}H_1'(pr)e^{-\sqrt{p^2-k_1^2}\,z}p\left(\sqrt{p^2-k_1^2}-\sqrt{p^2-k_2^2}\right) \qquad \text{(A-25)}$$

where $$K = \frac{k_2^2}{\sqrt{p^2-k_1^2}} + \frac{k_1^2}{\sqrt{p^2-k_2^2}}$$

Thus P is

$$P = j2\pi R_0 \tag{A-26}$$

For large r, the asymptotic expression for the Hankel function may be used, and P becomes

$$P = j\frac{I\ell\cos\phi}{2\omega\epsilon K}\rho\left(\sqrt{\rho^2-k_1^2}-\sqrt{\rho^2-k_2^2}\right)\sqrt{\frac{2}{\pi\rho r}}\,e^{j(\rho r-3\pi/4)}e^{-\sqrt{\rho^2-k_1^2}\,z} \tag{A-27}$$

The magnitude of P at $\phi = 0$ and $z = 0$ is

$$|P| = \frac{I\ell}{2\omega\epsilon}\sqrt{\frac{2\rho}{\pi r}}\,\frac{\sqrt{\rho^2-k_1^2}-\sqrt{\rho^2-k_2^2}}{K} \tag{A-27a}$$

5. Experimental Results

A half-wave antenna at 197 mc/s was used in order to investigate further the problem of a dipole over a dielectric earth. The field strength in the plane normal to the length of the antenna was measured, and the results are plotted in Figure A-9. The pattern of the antenna agrees very well with the calculated values.

If the field strength above the antenna is found for the two heights of the antenna h which give a maximum and a minimum value, it is possible to calculate the dielectric constant ϵ_r. We have from Equation (A-19)

$$E_{min} = \frac{2\sqrt{\epsilon_1}}{\sqrt{\epsilon_1}+\sqrt{\epsilon_2}}E_1 = \frac{2}{\sqrt{\epsilon_r}+1}E_1 \tag{A-28}$$

$$E_{max} = \frac{2\sqrt{\epsilon_r}}{\sqrt{\epsilon_r}+1}E_1 \tag{A-29}$$

The ratio of the two, E_{max}/E_{min}, is ϵ_r; ϵ_r was found to be 12.5.

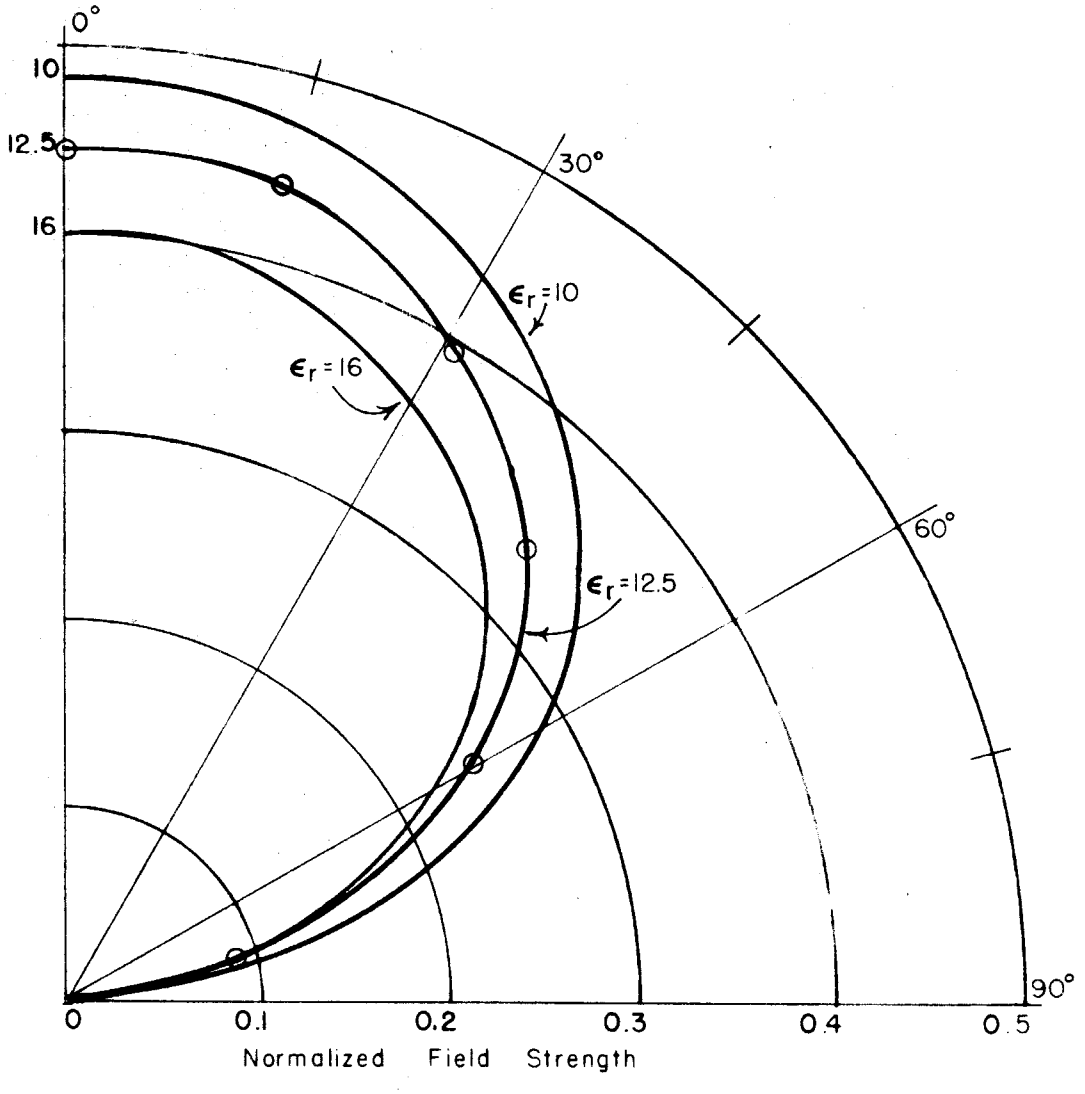

Figure A-9

Field pattern for a dipole over a plane earth h=o (calculated results for ϵ_r = 16,10 and measured values for ϵ_r = 12.5.)

We have not yet tried to determine the losses in the earth when the ratio h/λ_o is small. The 200-mc/s experiment provided a measurement of input resistance as a function of height, and the results are plotted in Figure A-3. Figure A-3 shows fluctuations about 70 ohms for h greater than $\lambda/4$, but as h approached zero, the input resistance increased instead of decreasing. This rise is attributed to higher field strengths in the dielectric that cause additional losses. With the antenna about 1.5 cm above the ground, the input resistance was found to be 80 ohms.

The resonant length of a half-wave dipole in this dielectric at 197 mc/s would be $\lambda_o/2\sqrt{\epsilon_r}$, or about 0.14 λ_o. As the antenna is brought near the earth, a change in the resonant length is observed; it is plotted in Figure A-10. When the field strength from a dipole, whose length is shortened, is calculated, the correction factor λ'/λ_o must be used, where λ' is twice the actual length of the dipole, and λ_o is the wavelength in free space. The pattern of a half-wave dipole with sinusoidal current distribution changes only in magnitude with decreasing antenna length.

A 60-kc/s antenna, approximately 2,000 meters long, was built over dry granite with a dielectric constant ϵ_r of about 6 or 7 and very low loss. This is a pilot model of a 20-kc/s antenna to be built later. The average height of the antenna above the earth is 1 meter, and the value of λ'/λ_o is 0.8. The input resistance of the dipole was 127 ohms, of which 39 ohms is attributed to copper losses. The remaining 88 ohms consists of radiation and absorption losses.

The maximum field of a half-wave dipole in free space is

$$E_{rms} = \frac{60 I_{rms}}{d} \text{ volts/meter} \qquad \text{(A-30)}$$

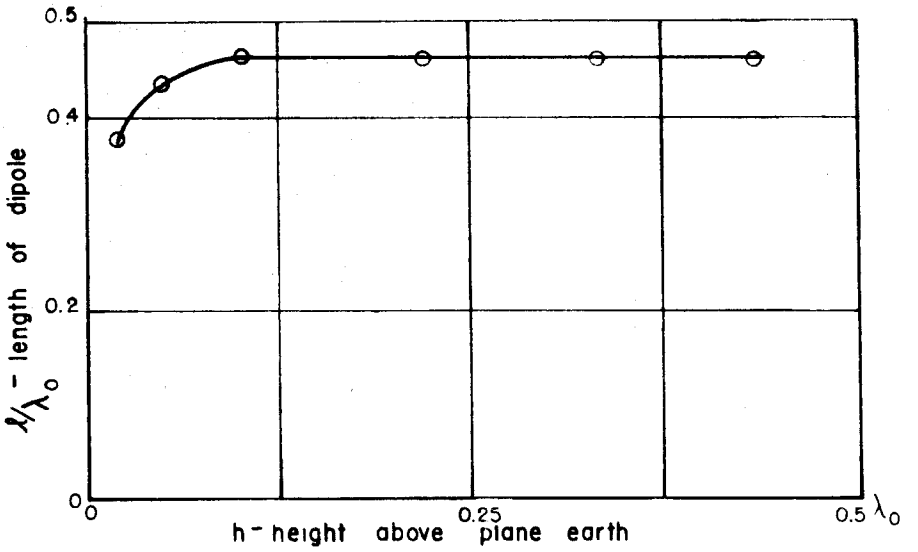

Figure A-10

The resonant length of a dipole as a function of height above the plane earth. $f_0 = 197$mc.

Therefore the field strength at a distance d directly above a ground dipole antenna is

$$E_{rms} = \frac{2}{1+\sqrt{\epsilon_r}} \frac{\lambda}{\lambda_0} \frac{60 I_{rms}}{d} \quad \text{volts/meter} \qquad \text{(A-31)}$$

which we see depends upon dielectric constant and current. If we use $\epsilon_r = 6$ for the 60-kc/s antenna, we obtain

$$E_{rms} = 0.46 \frac{60 I_{rms}}{d} \quad \text{volts/meter} \qquad \text{(A-32)}$$

The effective efficiency may be obtained from Equations (A-30) and (A-31)

$$\mathcal{E}_{eff} = \left(\frac{2}{1+\sqrt{\epsilon_r}} \frac{\lambda'}{\lambda_0}\right)^2 \frac{72}{R} \times 100\% \qquad \text{(A-33)}$$

where R is the input resistance of the ground antenna. Neglecting the copper losses, the 60-kc/s antenna has an effective efficiency of 17 per cent. When the effective efficiency is defined as the ratio of the power required to set up a unity field strength at the height h_o over the earth to the power required to set up the same unity field strength at the height h_o over the dipole in free space.

In order to find the order of magnitude of a signal that can be expected at the receiver site, let us assume that d in the reflection from the D layer is 180 km and that the reflection coefficient is about 0.1. Equation (A-32) gives the result of 15 μvolts/meter for each ampere of current in the antenna.

A receiving site was set up about 64 km from the transmitter, and the signal came in quite clearly. Except for the fact that the receiving antenna need not be resonant, it has the identical characteristics of

the transmitting antenna. In addition to being able to separate the normal and abnormal component of the reflected wave, it also improves the S/N ratio by virtue of its discrimination against vertically polarized waves.

Experimentation was also carried out with a resonant loop. The radiated signal from this antenna was received at a distance of 160 km from the transmitting site. This antenna has zero field strength above it and a maximum field at low angles of elevation. With this antenna we found that, by raising the wire off the ground by about 1/2 meter, the resonant frequency is increased by a factor of 1.7, and the loss is reduced by a factor of 2. The loop antenna was abandoned temporarily in favor of the dipole which had the desired properties necessary for ionospheric research at small angles of incidence. The cost of either antenna is small, and of course, this fact is a prime factor in determining whether or not it is possible to carry on the proposed program of research.

APPENDIX B

THE SPECTRAL DISTRIBUTION OF A PULSE

The spectral distribution $|G(\omega)|$ of a sine-wave pulse, n cycles long, is by definition the Fourier transform of the function of time g(t) describing the pulse.

$$G(\omega) = \int_{-\infty}^{+\infty} g(t)\, e^{-j\omega t}\, dt \tag{B-1}$$

$$g(t) = \sin \omega_0 t \qquad 0 < t < \tau$$

$$= 0 \qquad t < 0;\ t > \tau$$

where $\tau = 2\pi n/\omega_0$.

Let $$F(\omega) = \int_{-\infty}^{+\infty} f(t)\, e^{-j\omega t}\, dt$$

where $$f(t) = 1 \qquad 0 < t < \tau$$

$$= 0 \qquad t < 0;\ t > \tau$$

Then $$F(\omega) = \int_0^{\tau} e^{-j\omega t}\, dt = \frac{1}{j\omega}\left(1 - e^{-j\omega t}\right)$$

and $$g(t) = f(t) \sin \omega_0 t = f(t)\, \frac{e^{j\omega_0 t} - e^{-j\omega_0 t}}{2j}$$

Substituting this expression in Equation (B-1), we get

$$G(\omega) = \int_{-\infty}^{+\infty} f(t)\, \frac{e^{j\omega_0 t} - e^{-j\omega_0 t}}{2j}\, dt = \frac{1}{2j}\left[F(\omega - \omega_0) - F(\omega + \omega_0)\right]$$

$$= -\frac{1}{2}\, \frac{2\omega_0}{\omega^2 - \omega_0^2}\left(1 - \cos \omega\tau + j \sin \omega\tau\right)$$

$$|G(\omega)| = \frac{2\omega_0}{\omega^2 - \omega_0^2} \sin \frac{\omega\tau}{2} = \frac{2\omega_0}{\omega^2 - \omega_0^2} \sin \frac{\omega}{\omega_0}\pi n \tag{B-2}$$

The value of $|G(\omega)|$ for $\omega = \omega_0$ is $\tau/2 = \pi n/\omega_0$.

A plot of $|G(\omega)|\,\omega_o/\pi n$ for n = 4 is given in Figure 12. An inspection of Equation (B-2) shows $G(\omega) = 0$ for values of

$$\frac{\omega}{\omega_o} = \frac{1}{n}, \frac{2}{n}, \cdots \frac{n-1}{n}, \frac{n+1}{n}, \frac{n+2}{n}, \cdots$$

APPENDIX C

THE RESPONSE OF A TUNED CIRCUIT TO A PULSE

To obtain the response of a series-tuned circuit with an initial charge on the condenser, the voltage source E(t) is shorted out E(t) = 0 :

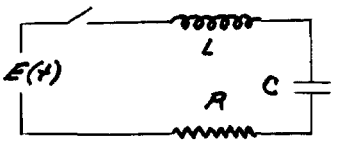

Solution of the differential equation using Laplace transform:

$$L\frac{di}{dt} + Ri + \int \frac{i\,dt}{C} = 0 \qquad \text{(C-1)}$$

The initial conditions are

$$i(0+) = 0$$
$$v_c(0+) = V$$

The transform of Equation (C-1) is

$$I(s)\left(Ls + R + \frac{1}{Cs}\right) = \frac{V}{s}$$
$$I(s) = VC\omega_o^2 \Big/ \left(s^2 + \frac{\omega_o s}{Q} + 1\right) \qquad \text{(C-2)}$$

where $Q = \omega_o L/R$ and $\omega_o^2 = 1/LC$.

Using the relationship

$$\mathcal{L}\left[e^{-\alpha t}\sin\beta t\right] = \frac{\beta}{s^2 + (\omega_o/Q)s + 1}$$

let

$$\alpha = \omega_o/2Q$$
$$\beta = \omega_o^2\left[1 - (1/4Q^2)\right]$$

Therefore i(t) is of the form

$$i(t) = \frac{Vc\omega_o}{1-(1/4Q^2)}\, e^{-(\omega_o/2Q)t} \sin \omega_o\left[1 - (1/4Q^2)\right]t$$

The time required for i(t) to die out to a value of 1/e of the initial value is $2Q/\omega_o$ seconds, or Q/π cycles of the frequency f_o.

APPENDIX D

ANALYSIS OF A SQUARE

The Fourier expansion of the following waveform is

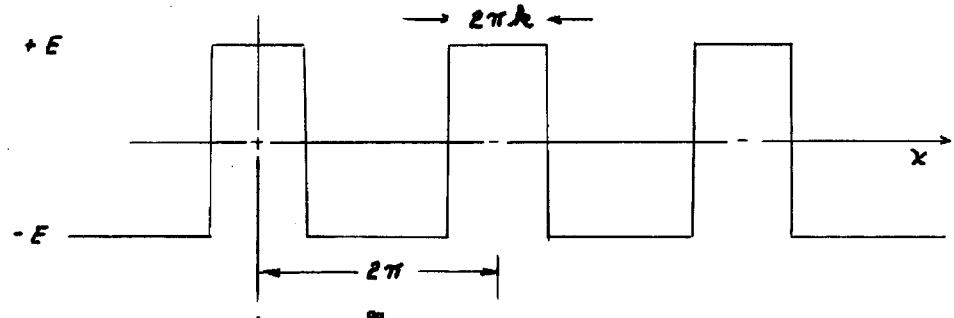

$$y = \frac{4}{\pi} E\left[\frac{(2k+1)}{4}\pi + \sum_{n=1}^{\infty} \frac{1}{n} \sin n k\pi \cos nx\right] \qquad \text{(D-1)}$$

Note that, to make the nth harmonic zero, $\sin(nk\pi)$ must be zero. If $k = 1/2$, Equation (D-1) becomes

$$y = \frac{4}{\pi} E \sum_{m=1}^{\infty} (-1)^{m+1} \frac{2}{m+1} \cos \frac{m+1}{2} x \quad ; \quad m = 2n+1$$

which is the expansion of a square wave. The energy in each harmonic is proportional to the term $(1/n)^2$. Since

$$\sum \frac{1}{n^2} = 1.232$$

we find that 81.2 per cent of the total energy is contained in the first harmonic.

APPENDIX E

PRODUCT DETECTION

If two signals, $\sin[\omega_1 t + \alpha(t)]$ and $\sin[\omega_2 t + \varphi(t)]$, are multiplied, the result is

$$\tfrac{1}{2}\cos[(\omega_1-\omega_2)t + \alpha(t) - \varphi(t)] - \tfrac{1}{2}\cos[(\omega_1+\omega_2)t + \alpha(t) + \varphi(t)]$$

where ω_1 and ω_2 are frequencies and α and φ are time-variant phase angles. In general, the sum of the frequencies is filtered out, leaving only the difference

$$\tfrac{1}{2}\cos[(\omega_1-\omega_2)t + \alpha(t) - \varphi(t)] \qquad \text{(E-1)}$$

The important thing to note is that, if φ is a constant, the phase angle α remains intact. Thus, if the phase of the difference of frequencies is measured, changes in $\alpha(t)$ are directly recorded.

A special case of this discussion results if $\omega_1 = \omega_2$, in which case Equation (E-1) becomes

$$\tfrac{1}{2}\cos[\alpha(t) - \varphi(t)]$$

APPENDIX F

CALCULATION OF RECEIVED FIELD STRENGTH

The field strength E_r at the receiver site is given by (Cf. Eq. A-31)

$$E_r = {}_{\perp}R_{\perp}\left(\frac{2}{\sqrt{\hat{\epsilon}_n}+1}\right)^2 \frac{\lambda'}{\lambda_o} \frac{60\, I_{rms}}{2h \cos(x/\lambda')360^\circ} \qquad \text{(F-1)}$$

where ${}_{\perp}R_{\perp}$ is the reflection coefficient

$\hat{\epsilon}_n = \epsilon / \epsilon_o - j\frac{\sigma}{\omega\epsilon_o}$ is the complex dielectric constant of the earth

$\lambda'/2$ is the length of the transmitting antenna

λ_o is the free-space wavelength of the transmitted frequency f_o

h is the height of the reflecting layer

I_{rms} is the input current to the transmitting antenna

x is the distance of the feed-point of the transmitting antenna the center

The experimental values are

$\lambda' = 17{,}200$ ft

$f_o = 50$ kc/s

$I_{rms} = 2.5$ amperes

$x = 1{,}700$ ft

Equation (F-1) can now be written

$$E_r = \frac{{}_{\perp}R_{\perp}}{h}\left(\frac{2}{\sqrt{\epsilon_n}+1}\right)^2 \cdot 80.5$$

If we assume $R = 0.7$ and $h = 10^5$ meters, this equation reduces to

$$E_r = 56.4 \times 10^{-6}\left(\frac{2}{\sqrt{\epsilon_n}+1}\right)^2 \quad \text{volts/meter}$$

By further assuming $\sigma = 5\times10^{-5}$ mhos/meter and $\epsilon_r = 6$, we find

$$E_r = 83.4 \ \mu\text{volts/meter}$$

This value is not far from the maximum received value of signal strength of 78 μvolts/meter.

Careful inspection of these results establishes the fact that σ must indeed be of the order of 5×10^{-5} mhos/meter. (And if this be the case, we can expect a signal strength of 32 μvolts/meter when operating in the frequency range near 20 kc/s.)

The skin depth $\delta = 1/\sqrt{\pi f \mu \sigma}$ at 50 kc/s for $\sigma = 5 \times 10^{-5}$ mhos/meter is 318 meters (1050 feet).

REFERENCES

1. Macmillan, R. S. Thesis for partial fulfillment of the requirements for the degree of Doctor of Philosophy at California Institute of Technology, (1953).

2. Bracewell, R. N. The Proceedings of the Institutions of Electrical Engineers, Part III (1951), Vol. 98, pp. 215-236.

3. Hobart, T. D. Electronics (1952), Vol. 25 (No. 12), pp. 98-101.

4. Mitra, S. K. The Upper Atmosphere (2nd ed. The Asiatic Society, Calcutta, 1952).

5. Choudhury, D. C. Physical Review (1952), Vol. 2, pp. 405-8.

6. Mitra, A. P. Journal of Geophysical Review (1951), Vol. 56 (No. 3), pp. 373-402.

7. Gardener, F. F. Philosophical Magazine (1950), Vol. 41, pp. 1259-69.

8. Bracewell, R. N. Monthly Notices of the Royal Astronomical Society (1949), Vol. 109(No. 1), pp. 28-45.

9. Goldman, S. Frequency Analysis, Modulation and Noise (1st ed., McGraw-Hill, 1947).

10. Helliwell, R. A. Electronics Research Laboratory, Stanford University, California, Report for period July, 1948, to June 30, 1949, under Bureau of Standards Contract CST-8966.

11. Railroad Commission of the State of California, Rules for Overhead Electric Line Construction General Order No. 95.

12. Electronic Training Staff of the Cruft Laboratory, Harvard University, Electronic Circuits and Tubes (McGraw-Hill, 1947).

13. Department of the Army, Technical Manual TM 11-5506.

14. Department of the Army, Technical Manual TM 11-5023.

15. Thiene, P. G., Jr. Thesis for partial fulfillment of the requirements for the degree of Doctor of Philosophy at California Institute of Technology (1952).

16. Technology Instrument Corps. Instruction Book for Phase Meter type 320 AB.

17. Sommerfeld, A. and Renner F. Annalen der Physik (1942), Vol. 41 (No. 1), pp. 1-36.

REFERENCES (Cont'd.)

18. Sommerfeld, A. Partial Differential Equations in Physics (Academic Press Inc., 1949).

19. Hertz. Die Krafte elektrischer Schwingungen, Collected Works, Vol. 11, p. 147.